Characterizing Resilience of LEO Satellite Networks Against Disasters

E.G. Chen

Technische Universiteit Delft

TU Delft

Characterizing Resilience of LEO Satellite Networks Against Disasters

by

E.G. Chen

to obtain the degree of Master of Science

at the Delft University of Technology,

to be defended publicly on January 23rd, 2026 at 14:00.

Project duration:	Dec, 2024 – Jan, 2026	
Thesis committee:	Prof. Dr. K.G. Langendoen,	TU Delft, advisor & chair
	Dr. G. Iosifidis,	TU Delft, chair
	Dr. A. Asadi PhD,	TU Delft, supervisor
	Dr. N. Mohan PhD,	TU Delft, supervisor
	Dr. T. Shreedhar,	TU Delft, external advisor

An electronic version of this thesis is available at `http://repository.tudelft.nl/`.
Cover image adapted from [1].

TU Delft

Preface

When I was looking for a possible thesis topic, I wanted to combine both my interests and my previous academic experience. After getting a Bachelor's degree in Aerospace Engineering, I decided to pivot to electronics and software, and enrolled in the Computer and Embedded Systems Engineering masters with a focus on communication systems and networking. As such, a potential thesis topic exploring aspects of the new satellite internet constellations caught my interest, since it combined networking, space engineering, and communication technologies. Things were a bit bumpy during the process of writing the thesis, and I often struggled with balancing the research tasks while also serving as part of the board of the Delft Aerospace Rocket Engineering student group. I am thus thankful of the support from my main supervisors and advisors, Arash, Nitinder, and Tanya. Everybody were kind and helpful when I had uncertainties and questions, and always gave valuable feedback and new perspectives. Additionally, I was also lucky to be supported by my friends who helped cheer me up when I was feeling uncertain in the past year. This really helped me keep going.

This thesis documents my research into the interdisciplinary intersection between networks, orbital mechanics, simulations, and natural disasters. I personally find satellite communications to be interesting, having previously experimented with reception of satellite signals using amateur equipment. This thesis gave me an opportunity to explore the various complex aspects of modern satellite constellations, while gaining insight into the challenges and opportunities associated with the technology. I hope you enjoy reading about this research.

E.G. Chen
Delft, January 2026

Abstract

Low Earth orbit satellite internet networks such as Starlink, OneWeb, and Amazon LEO (formerly known as Project Kuiper) have in recent years emerged as a new way to access the internet. These systems offer the possibility of high-speed and low-latency connectivity in remote regions, but have also been introduced as potential options for use in emergency situations. As these technologies become more commonly used for critical applications, it is important to analyze how resilient these networks are, and how they may be vulnerable to various threats.

LEO satellite internet is enabled by a network of ground stations, satellites, and user terminals. Since the ground stations are terrestrial, they can be vulnerable to threats such as natural disasters or power outages. As a result, analyzing the effect of terrestrial disruptions on the performance of satellite networks provides insight into how the service can be adversely affected. Using simulated models of Starlink, OneWeb, and Amazon LEO combined with case studies based on the 2025 Iberian Peninsula power outage and the 1960 Valdivia earthquake, it was found that optical inter-satellite links (ISL) significantly contribute to the resilience against terrestrial disasters. ISL-enabled networks such as Starlink and Amazon LEO enable alternative connections to more distant ground stations, thus avoiding a loss of regional coverage. This rerouting results in an increased link latency within the region.

Simulated disasters in space were also analyzed. A distributed attack on satellites based on their betweenness centrality revealed that constellations with a larger quantity of satellites degraded more slowly. Additionally, an analysis of regional satellite outages revealed that a damaged satellite cluster can propagate to different regions, causing a local decrease in the satellite density. By analyzing the motion of the satellite constellation after a 3000 km radius disruption, it was found that constellations containing different orbital altitudes experienced a passive redistribution of satellites over time, stabilizing after 2-4 days. Additionally, deliberate maneuvering restored the density in approximately 4 days for Starlink and OneWeb, with the lower-thrust Amazon LEO satellites taking approximately 7 days.

This work aims to provide insight into an often overlooked aspect of the emerging satellite networks, by showing that the resilience of these networks is affected by many distinct factors such as inter-satellite connectivity, ground stations, orbital mechanics, and more.

Contents

Acronyms

ATTR Average Two-Terminal Reliability.

ESA European Space Agency.

FANET Flying Ad-Hoc Network.

GEID Global Earthquake Impact Database.

GS Ground Station.

HEO High Earth Orbit.

ISL Inter-Satellite Link.

IXP Internet Exchange Point.

LEO Low Earth Orbit.

MANET Mobile Ad-Hoc Network.

MEO Medium Earth Orbit.

MTTR Mean Time to Recovery.

PoP Point of Presence.

RIM Reachability Impact Metric.

TBC Temoiral Betweenness Centrality.

TIM Traffic Impact Metric.

TLE Two-Line Element Set.

UAV Unmanned Aerial Vehicle.

UT User Terminal.

WANET Wireless Ad-Hoc Network.

1 Introduction

The global availability of the internet allows for near-instant communication and access to information across the world. Towards the end of the 2010s, satellite internet constellations emerged as a new and unique approach to global internet connectivity. Initiatives such as SpaceX's Starlink, OneWeb, and Amazon LEO (formerly known as Project Kuiper) each seek to deploy hundreds or thousands of low Earth orbit (LEO) satellites in coordinated constellations [2, 3]. These networks are supported by a global network of ground stations and provide internet access to specialized user terminals, thus promising low-latency, high-throughput connectivity that is competitive with terrestrial broadband internet. This technology is especially valuable in isolated or developing regions, where traditional fiber or cellular infrastructures are unavailable or unreliable. Satellite internet has also been deployed in regions following natural disasters or network outages [4, 5], and has been explored as a potential technology for handling emergency connectivity [6]. As of the start of 2026, Starlink has the largest market share, with approximately 8 million subscribers [7]. Amazon LEO is still in the process of building up its new constellation, aiming to compete with the service provided by Starlink.

Satellite networks are often seen as a resilient alternative to terrestrial networks. However, the growing reliance on space-based internet infrastructure introduces new challenges and research questions related to resilience, especially as these systems are used for critical tasks. Although these systems offer a wide area of coverage due to the number of orbiting satellites, they remain dependent on key terrestrial and orbital infrastructure elements. Centralized ground stations (GS), points of presence (PoPs), and inter-satellite communication links (ISLs) are key components that constitute potential points of failure. Natural disasters, technical faults, or even intentional threats can significantly degrade or interrupt the service. The latter is especially important in the context of geopolitical conflicts, where satellite internet providers have, in recent years, played a significant role by providing internet access in active conflict regions [8].

As global internet access and satellite internet networks become increasingly critical, understanding and improving the resilience of satellite internet networks is essential. This is further amplified by climate- and space-related risks that may impact infrastructure in both the terrestrial and orbital elements. Understanding potential risk factors and their resulting effects will provide insight into how suitable the satellite networks are as a tolerant alternative to terrestrial internet services.

1.1. Threats to LEO Networks

LEO satellite internet networks can be threatened in three main ways: by terrestrial events, by orbital disruptions, or by deliberate hostile action. Terrestrial disruption scenarios can be a result of a natural

disaster or attacks affecting ground stations [9], or it can also be the result of outages to the supporting terrestrial infrastructure, such as an electrical blackout or disruptions to the internet backbone [10]. In the past, such unpredictable disasters have led to widespread outages in terrestrial communication services, making it difficult for both emergency services and regional residents to contact each other [11]. These scenarios can disrupt the functioning of ground stations supporting satellite networks. As an example, data from the 2025 Iberian Peninsula power outage indicates that regional Starlink traffic was redirected to alternative ground stations in other countries due to the loss of power [5]. Redirecting internet traffic to more distant ground stations may require satellite-to-satellite connections, which is not a capability supported by all satellite networks. This can result in regional service disruptions near the affected region.

While terrestrial infrastructure can be vulnerable to natural disasters, the orbital segment faces its own challenges. Orbiting satellites are isolated from most terrestrial disruptions, but they are almost impossible to physically access for maintenance. Satellites operate in the harsh environment of space, where they are susceptible to extreme conditions caused by solar storms and other space weather events [12, 13]. These unpredictable events can result in satellite outages due to the impact of high-energy particles, and cause unpredictable changes in the atmospheric drag for LEO satellites. In 2022, this increased density led to the unexpected reentry of 38 newly launched Starlink satellites [14]. Another threat facing satellites is the risk of collisions. This risk is rising as the density of LEO objects continues to increase each year. ESA estimates that over a million objects greater than 1 cm are in various orbits around Earth [15]. In the upcoming years, thousands of additional LEO satellites are scheduled to be deployed by existing and emerging satellite constellations. Although active satellites use maneuvering to minimize collision risks, the debris from such a collision could lead to a disastrous cascading failure of other satellites in nearby orbits. Such a scenario is known as 'Kessler Syndrome', which can make it difficult to deploy new satellites into orbit due to the high collision risk [16].

Threats to satellite networks can also be deliberate. In the past, China, India, Russia, and the United States have successfully demonstrated the ability to target and shoot down decommissioned satellites, generating significant amounts of orbital debris [16]. Although these weapons have not been used offensively, their existence pose a threat by directly or indirectly affecting orbital satellites if they are ever used offensively. Additionally, satellite networks can face cyberattacks [9], or experience temporary non-deliberate outages. Such outages occasionally occur to all major internet providers, and have occurred to Starlink and OneWeb in the past. This raises the question of how the resilience of these LEO networks can be analyzed, while also considering the similarities and differences compared to traditional internet infrastructure.

1.2. Internet Resilience

Existing work on internet resilience has primarily focused on the terrestrial infrastructure and outages [10]. Previous research has investigated how critical elements of the terrestrial internet backbone, including internet exchange points and submarine cables, may be susceptible to damage as a result of terrestrial disasters or extreme space weather events. The largest recorded solar storm was the 1859 Carrington Event, and research has indicated that a similar event may be capable of disconnecting parts of the internet by inducing currents in long submarine cables [17].

Some existing studies have investigated the resilience of satellite networks, however, these focus primarily on the networking elements rather than threats posed by physical disruption scenarios. Some studies have investigated how different types of packet routing through satellite networks can influence the resilience against targeted satellite attacks [18], while other studies have identified the importance of critical satellites [19]. By comparison, the terrestrial side of satellite networks has seen limited resilience analysis. In particular, the effect of ground station disruptions on the network performance is important when considering resilience against natural disasters, and this has not seen extensive academic analysis. This constitutes a research gap which will be investigated in this thesis. Such an investigation can paint a clearer picture of how suitable different types of satellite networks are at

providing service in a region following a natural disaster.

An additional topic with limited research is the effect of satellite motion and maneuvering on the resilience and recovery of a network. Existing satellite mega-constellation analysis tools such as Starrynet primarily focus on constructing a virtual network that can be used for packet-level simulations [20]. Although these simulation tools are useful for analysis of packet routing within the network, they do not paint the full picture of how a satellite network is capable of reacting after an orbital disruption scenario using maneuvering. Previous work investigated how maneuvering within a single orbital plane affects the resilience of inter-satellite links [21], but have not considered how the motion of satellites in a full constellation may be able to recover following a disaster event. As such, there exists a research gap in investigating how maneuvering at the scale of a full mega-constellation can affect the post-disaster recovery process. In addition to deliberate maneuvering, some mega-constellations contain multiple orbital shells which can lead to a natural redistribution of satellites over time. This has seen limited research in the context of resilience, and as such, will also be considered in this thesis.

By analyzing the resilience of satellite networks, more insight can be gained into the advantages and disadvantages of satellite networks as an alternative to their terrestrial counterparts. Additionally, comparing different satellite constellations to each other can help identify the important parameters affecting the resilience. This knowledge can aid end users who require highly resilient networking options, but also provide a starting point for further research into a resilience analysis model for satellites, which can aid both academic research and the development of future satellite constellations.

One unique aspect of satellite networks compared to terrestrial networks is the highly dynamic behavior of the network nodes. For instance, a Starlink satellite makes an entire orbit in approximately 95 minutes. During this period, the satellite covers a wide global area around the world. As a result, a single satellite can have a large influence on geographically distinct areas of the world. Additionally, maneuvering satellites have parallels to dynamically changing terrestrial ad-hoc networks. Although the orbital mobility of satellites is limited due to the amount of propellant. The orbital mobility will be investigated based on the resilience triangle framework, in which a disruption and subsequent recovery of the operational performance provides an indication of the overall resilience.

1.3. Thesis Overview

Based on the limited research on satellite resilience against physical threats, the primary goal of this thesis is to expand on this knowledge and investigate the resilience of internet mega-constellations when exposed to various types of physical disruption scenarios. With the main research question in mind, ”How resilient are LEO satellite internet services to terrestrial and space-based disruptions?”, this thesis aims to:

- Analyze how LEO satellite networks depend on critical ground infrastructure.
- Simulate historical and hypothetical disaster scenarios to assess their impact on network availability and performance.
- Evaluate the structural vulnerabilities of satellite constellations to terrestrial and space-based outages.
- Compare the resilience of different satellite network providers when exposed to outage scenarios.
- Investigate how satellite maneuvering may be used to recover from an outage.

As of the start of 2026, multiple LEO broadband satellite internet providers are either in the process of building a constellation, or have a functioning network with active users. This thesis will focus on Starlink, OneWeb, and Amazon LEO, which represent three service providers with different technologies and levels of deployment. Each of these satellite constellations has key differences in the number of ground stations and satellites. Starlink is the network with the highest degree of deployment, with over 9,000 active satellites and a wide global network of ground stations. Starlink is continuously deploying

new satellites to their network, with a goal of around 12,000 operational satellites. OneWeb operates an active network with 648 satellites, while Amazon LEO is in the process of deploying the initial phase of their constellation, targeting a full constellation with thousands of satellites. Additionally, the satellites themselves have different capabilities, with OneWeb satellites lacking the optical inter-satellite links found in Starlink and Amazon LEO satellites. These differences have implications on the resilience aspects against physical disaster scenarios, which will be investigated by comparing the competing service providers.

By combining a review of currently deployed satellite internet architectures with simulation-based modeling of disruption scenarios, this thesis aims to explore how real-world constellations can be impacted. The simulations are informed by real-world case studies, such as the impact of a historical earthquake, in addition to artificial disruption scenarios based on space disruptions. Two simulated terrestrial case studies are applied to the different satellite networks: The 2025 Iberian Peninsula blackout, and the 1960 Chile Earthquake. This aims to model the effect of various failures on resilience and service metrics and compare how different satellite networks are affected. These two scenarios each represent a distinct geographic region with different number of ground stations. Chile represents a region with a low number of ground stations, while the Iberian Peninsula is located in a region with both a higher user density and a higher ground station density. Additionally, both of these scenarios have available data which can be used to guide the modeling process. The space-based disasters are based on a simulated wide-area outage, which may be the effect of a powerful space weather event. The considered constellations are primarily modeled using tracking data, with the additional use of a Walker-Delta constellation model to simulate different deployment stages of Amazon LEO. The simulations of the case studies are based on a orbital models combined with a coverage and latency model. At each snapshot in time, the constellation is evaluated in order to compute the resilience measures, including coverage and latency.

The simulated maneuvering is based on tracking data of how satellites modify their orbit. If satellites become non-operational, the remaining satellites across the entire constellation can shift their positions in order to repair holes in the orbit. Additionally, satellites located at different altitudes have different orbital periods. This means that a local disruption may disperse over time, thus reducing the impact. This is analyzed by computing the local density of satellites over time, following a satellite disruption event. The densities are evaluated using the resilience triangle for disaster recovery, thus allowing for resilience comparisons between different networks.

1.4. Scope and Thesis Structure

One of the limitations of the scenarios is the lack of consideration of resilience associated with digital threats, these include cyberattacks or network congestion. These are excluded since they necessarily require additional information about how the network operates, such as the operational vulnerabilities and the routing algorithm employed. By focusing on the structural aspects and physical constraints, the performance of different constellations can be directly compared with each other.

Additionally, although the use of case studies can provide insight into the impact of specific scenarios, they are only valid for a specific scenario and locality. This means that they may not generalize to threats across the world, where parameters such as the local user density, the regional ground stations, and the overhead satellite density are different. Additionally, many factors are unknown due to the proprietary nature of existing satellite internet networks. This requires assumptions and simplifications in the modeling process. These include assuming a shortest-path approach to routing between satellites for latency estimation, which may not reflect how data is routed in the actual network. The proprietary aspects also limit how much their real-world performance can be generalized in an analysis model that considers multiple network operators.

Since the resilience is investigated from primarily a structural and performance perspective, the resilience impact of the companies operating the networks are not considered. These include factors

such as the different sizes of the companies, differences in market share, and how they may be able to respond to a disaster differently based on their available resources.

The thesis is structured into chapters containing background information, the modeling and simulation, and the results. Chapter 2 covers some background regarding satellite internet networks. It starts by discussing the architecture of satellite networks, including orbital constellations, network components, communication links, and maneuvering. Additionally, the chapter gives an overview of ways satellite networks can be disrupted by external factors.
Chapter 3 covers the resilience aspects of satellite and related networks. It starts by providing an overview of relevant resilience metrics and how they may apply to satellite networks. This is followed by an investigation into related work about network resilience and satellite simulation tools.
Chapter 4 goes into detail about the development of the simulation tool for analysis of satellite resilience. This chapter explains the assumptions and methods used for modeling the satellite network, and how the data was gathered for the various satellite network operators. Additionally, it explains how different disruption scenarios are computed for the resilience analysis.
Chapter 5 presents and discusses the key results found through the simulation process. Using a series of case studies, the results of simulated ground disruptions to critical infrastructure are discussed. Additionally, the results of space disruptions are presented along with a simulation of how compromised satellite networks can be repaired through maneuvering.
Chapter 6 discusses some of the limitations with the work and other aspects that warrant further study, and also contains the conclusion with the main findings of the thesis.

2

Background and Related Work

Satellite internet networks have been developed and analyzed from both practical and theoretical perspectives. Since the mid-2010s, the concept of large-scale satellite constellations has gained renewed interest, with several commercial entities aiming to provide broadband internet access to a geographically diverse and often underserved global population. These systems leverage advances in satellite manufacturing, launch economics, and communications technology to offer scalable, low-latency connectivity from low Earth orbit (LEO).

In this chapter, relevant literature and prior work regarding the design and operation of satellite networks are reviewed. Special attention is given to system architectures, deployment models, and the technologies and main characteristics of operational satellite networks. Additionally, possible disruption scenarios and mechanisms of action are discussed. This forms the basis for the simulation model and resilience analysis presented later in this thesis.

Section 2.1 introduces the key technologies and network architectures used in satellite internet systems. Section 2.2 provides an overview of major active satellite internet operators and the structure of their respective networks. Section 2.3 focuses on vulnerabilities of terrestrial infrastructure components, while section 2.4 discusses potential disruptions affecting the space segment of the network.

2.1. Network Architecture

A broadband satellite network consists of many components and technologies working together. This section gives an overview of the main components involved with such a network, types of orbital constellations, types of connectivity, and how satellites maneuver. Although the primary focus is placed on the systems used with LEO satellite internet constellations, some related technologies are discussed in order to provide context. This serves as foundational background knowledge for further analysis.

2.1.1. Network Components

A satellite internet network consists of multiple interconnected elements that work together to facilitate data transmission. These can broadly be divided into three domains: the user domain, the space segment, and the ground segment. An overview of the components is shown in Figure 2.1.

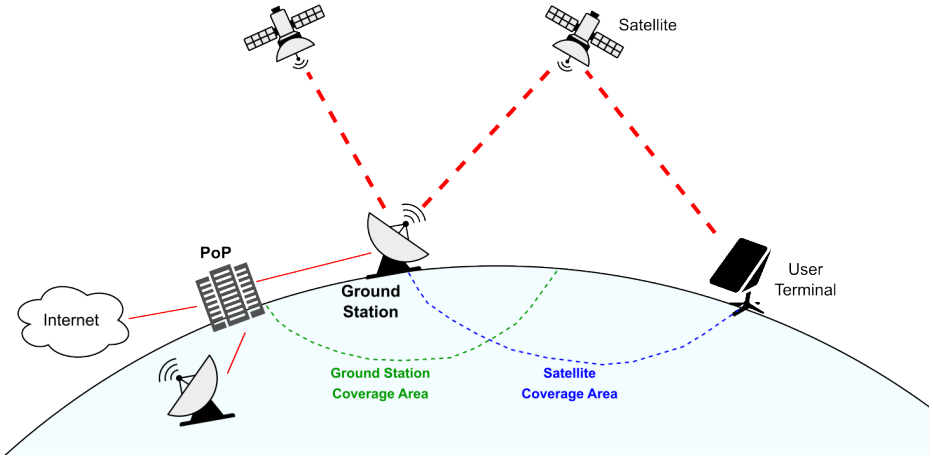

Figure 2.1: Overview of the main components in a satellite internet network

A user terminal (UT) is the ground-based elements that a customer uses in order to access a satellite network. User terminals use antennas ranging from portable electronically steered phase array devices to larger mechanically steered parabolic antennas. Parabolic dish antennas have been extensively used historically for satellite communications, offering good performance and low cost for tracking a single satellite. The disadvantages are slow tracking speeds, large sizes, and the potential of mechanical issues over time. Modern user terminals employ phased array antennas, which allow for a lower profile, faster steering, and multi-beam capability. These use electronic beamforming in order to generate the desired radiation pattern with fewer or no moving parts. Manufacturers often offer multiple user terminal options depending on the customers requirements for data rate and portability [22].

Satellites are launched by space launch vehicles into an orbit where they are subsequently deployed. Common for most communication satellites is the use of solar panels and batteries for power, actuators for attitude control, thrusters for maneuvering, onboard electronics for control, and antennas for communication to and from the ground. Similar to ground stations, internet satellites often use directional parabolic antennas or phased array antennas for high-speed connectivity. Low-gain antennas may also be present in order to receive commands from the ground or provide telemetry data. Broadband satellites generally use the Ku-band (12-18 GHz) or Ka-band (27–40 GHz) [23], which allows for larger bandwidths compared to lower frequency bands.

Ground stations (GS), or gateways, are fixed terrestrial installations capable of contacting orbiting satellites. This can be for commanding and controlling the satellites themselves, or handling of traffic to and from the satellites. Multiple ground stations located around the world can work together to serve a single satellite network. Such a ground station network is critical for the proper functioning of a satellite internet network, since it must be capable of handling the traffic of all active network users. This necessitates high-throughput connections, with each ground station location often using multiple parabolic dish antennas tracking the movements of overhead satellites.

In order to connect a satellite network to the wider internet, ground stations need access to the internet backbone. These interface points are points of presence (PoPs), which are often data centers or internet exchange points [24]. For the users of of a satellite network, their traffic will appear to originate from these locations, making it possible to identify which PoPs are used by a network. These have been used in order to create crowd-sourced datasets of the infrastructure surrounding satellite networks [25, 24].

Similar to terrestrial broadband, customers generally pay a subscription fee to gain access to the net-

work [3]. When the network is fully operational, these key components work together in order to give a user seamless access to high-speed low-latency internet without the use of cellular networks or terrestrial broadband.

2.1.2. Orbital Satellite Constellation

A communication satellite moves in a regular orbit around the Earth. The orbit of a single communications satellite is characterized by a number of key parameters, namely the orbital altitude (related to semi-major axis), inclination, orbital period, and eccentricity.

Different satellite orbital altitudes are classified in groups. Low Earth orbit (LEO) are orbits with an altitude below 2000 km, medium Earth orbit (MEO) are orbits between 2000 and 35 786 km, and high Earth orbits (HEO) are orbits above 35 786 km. The orbital period of point masses can be computed using Kepler's third law,

$$T = 2\pi \sqrt{\frac{a^3}{GM}}, \tag{2.1}$$

where a is the semi-major axis, G is the gravitational constant, and M is the mass of the larger body. For satellites in orbit around Earth, factors such as flattening, different densities, and the influence of other terrestrial bodies result in minor discrepancies [26]. Satellites located in higher orbits have longer orbital periods. At an altitude of 35 786 km, the orbital period matches the rotation of Earth. When orbiting near the equatorial plane, the satellites appear either stationary in the sky (geostationary) or within the same region (geosynchronous). This is favored for some communication and television satellites, since a fixed satellite dish can be installed. However, this distance results in a worse link budget and in a round trip delay of over 200 ms, making it unsuitable for many low-latency applications. In contrast, LEO satellites make an entire orbital revolution approximately every 90 minutes. This allows for lower latencies, but limits the contact period and generally requiring active tracking. Additionally, the lower altitude limits the possible coverage area due to visibility and angle constraints, requiring a greater number of satellites in order to achieve global coverage.

Due to the high number of required LEO satellites, it is generally advantageous to distribute them in a regular grid-like pattern. This is achieved by dividing all the satellites up into groups with similar motion characteristics. A set of satellites placed in the same spatial orbit constitutes an orbital plane. The satellites located in the same plane have temporal offsets in order to distribute them. A shell consists of multiple such planes with coordinated spacing and phasing. Orbits within a shell have the same orbital altitude, and often similar inclinations to form regular orbit patterns. A full satellite internet constellation may include multiple shells to improve the global coverage area. A common design pattern is the Walker-Delta constellation, which arranges satellites in uniform phase across multiple planes. This allows for efficient coverage, simplified handoff management, and predictable behavior for routing algorithms [27]. Examples of satellite constellation patterns are shown in Figure 2.2

Modern constellations may consist of thousands of satellites, with some configurations such as Starlink targeting over 12,000 active satellites in their final design. These span several orbital shells and inclinations, thus providing a high degree of coverage tailored to the target service areas and user densities.

2.1.3. Bent-pipe and Inter-satellite Links

Satellite-based communication has the goal of forming a communication link between two points on Earth. The simplest approach is using a direct bent-pipe connection. A direct bent-pipe satellite architecture is one in which satellites do not have direct connections between each other. Instead, they relay data between a user terminal and a ground station. In the most basic form of a bent-pipe connection, a signal received at a specific frequency is amplified and transmitted back at a shifted frequency. This

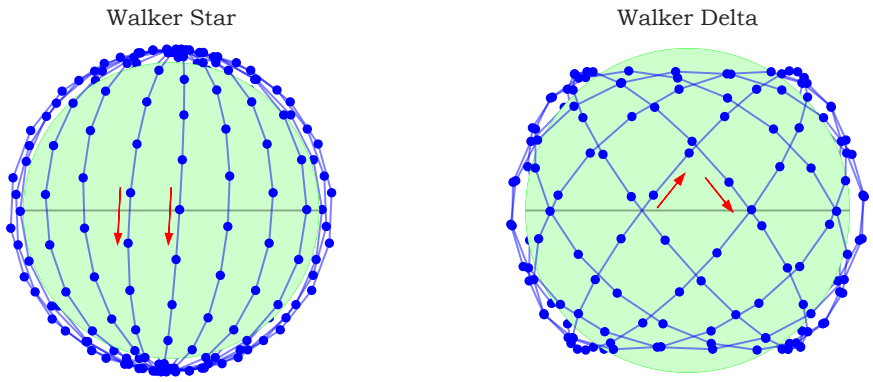

Figure 2.2: Illustrations of basic satellite constellation geometries. The red arrows indicate the direction of motion within the satellite planes.

approach has limitations, since each transponder can only handle one data stream, but is still widely used for amateur radio satellites and some communication satellites. In the context of satellite internet networks, one satellite still needs to perform some onboard processing in order to handle traffic from multiple users, with the bent pipe terminology referring to the networking structure.

Due to the nature of the direct bent-pipe connection, the satellite must simultaneously be in view of both the user terminal and a suitable ground station to allow for a successful connection. This limits the coverage area of a ground station, and requires terrestrial deployments that cover the entire service region. Since each satellite only communicates with hardware on the ground, no data is directly routed between the orbiting satellites. This approach has limitations in terms of global reach and network resilience. If no ground stations are visible, the satellite cannot forward data, even if other satellites are in view. As such, the coverage area is dependent on the global distribution of ground stations. The example in Figure 2.1 shows a direct bent-pipe connection between the user and the ground station.

Since orbiting satellites are in view of each other, a natural solution is to communicate between orbiting satellites. Such connections are referred to as inter-satellite links (ISLs), and are direct communication links formed without an intermediary ground station. These connections make it possible for satellites, which would otherwise not be within the coverage area of a ground station, to have an indirect connection through one or more satellites acting as relays [24]. ISLs allow for a ground station to serve users much farther away than what is possible with a direct bent-pipe connection, an architecture sometimes referred to as ”extended bent-pipe”. A satellite has limited amounts of transceivers for inter-satellite connections, which limits the ways in which data packets can be routed through the network. Consequently, one approach for forming an interconnected constellation is to use the regular pattern of the constellation (e.g. Walker-Delta constellation) for scheduling inter-plane and intra-plane connections, which results in predictable and regular inter-satellite connections [28].

The range and performance of inter-satellite links are limited by hardware and physical constraints. Since satellites operate outside the dense atmosphere of Earth, they can use optical laser systems which are not attenuated in the vacuum of space. These offer a lower power consumption, reduced scattering, and smaller footprint compared to radio systems. Additionally, optical communications are not restricted by the limited radio frequency spectrum and radio regulations, which are advantageous for satellite operators [29]. The lasers are heavily attenuated by Earth’s atmosphere and require an unobstructed line of sight, which places a limit on the maximum distance. Additionally, the power, optics, pointing accuracy, and sensitivity of the optical communication equipment limit the maximum possible range of these systems. Starlink claims that the lasers used on the satellites can achieve data rates up to 200 Gbps, with the Starlink Mini satellites having a reported maximum range of 4000 km with link speeds of 25 Gbps [30].

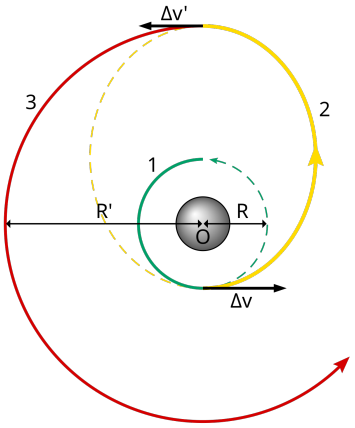

Figure 2.3: Illustrative example of a transfer orbit [34].

2.1.4. Satellite Deployment and Maneuvering

One important aspect of satellite constellations is the deployment and maneuvering capabilities of the satellites. During launch, satellites are securely located in a launch vehicle. Once the correct orbit has been reached, satellites are deployed from the launch vehicle, often as a group. The initial parking orbit is generally lower than the operational orbit, and satellites are subsequently raised to their operational orbits using the onboard thrusters once they are confirmed to be operational. The available onboard propellant of a satellite determines the total amount of maneuvering it is capable of over its operational lifetime, while the thrust of the propulsion system affects how quickly it is able to perform maneuvers. Additionally, the efficiency of the propulsion system affects the propellant consumption. Electric thrusters such as hall-effect thrusters are highly efficient, but exhibit low thrust compared to chemical propulsion systems [31]. Due to their high efficiency, electric propulsion systems are being used in many newly deployed satellites and mega-constellations [32].

Once deployed to a target orbital plane and inclination, large changes the plane and inclination consume a significant amount of propellant [26]. Satellites thus generally maneuver by raising or lowering their orbits while staying within the same inclination and plane. If out-of-plane are performed, it is generally for station-keeping or for making small corrections to the plane.

In-plane orbital maneuvers are used for multiple purposes. During the initial orbit-raising phase, in-plane thrust is used to raise the orbits. By combining orbit-raising and orbit-lowering, the relative phase of satellites within an orbital plane can be controlled, which is used in order to distribute satellites to their target positions following their initial grouped launch. Additionally, in-plane maneuvers are used for station-keeping in order to counter the effect of atmospheric drag. Finally, maneuvers are used in order to temporarily change the altitude or phase of a satellite to avoid other satellites or orbital debris [33]. One basic type of orbital maneuvering is the Hohmann transfer orbit, shown on Figure 2.3, which can be used to transfer between two different circular orbits. The classical Hohmann transfer orbit uses instantaneous momentum changes, which is not possible for the low-thrust propulsion systems used in many LEO satellites. Instead, a longer burn results in a spiral trajectory as the satellite maneuvers. As explain in subsection 2.1.2, lower orbits have lower orbital periods. By timing when and how satellites are raised to their target orbit, a desired satellite distribution can be achieved. The perpetuance from the non-spherical shape of Earth can also be exploited to induce indirect orbital changes using fuel-efficient low-thrust maneuvers [31]. Once a satellite has reached its end-of-life, it is generally de-orbited using the remaining propellant [32]. The satellite subsequently burns up during reentry into Earth's atmosphere, which reduces the amount of inactive space junk.

2.2. Satellite Network Operators

Multiple companies have proposed or created designs for large-scale satellite internet networks. In this section, Starlink, Amazon LEO, and OneWeb are introduced with their overall network characteristics. A summary of their main characteristics can be found in Table 2.1.

	Starlink	**OneWeb**	**Amazon LEO**
Operator	SpaceX	OneWeb (Eutelsat)	Amazon
Satellites Planned	∼12000	∼648	∼3236
Satellites Operational	>9000	656	182
Orbit Altitude [km]	340–550	1200	590–630
ISLs	Yes	No	Yes

Table 2.1: Comparison of Starlink, OneWeb, and Amazon LEO as of January 2026 [35]

Starlink is the satellite internet network with the largest amount of satellites. As of the start of 2026, the Starlink network consists of over 9000 satellites in multiple different orbital shells in LEO, operating at altitudes of around 550 km [36]. 12000 satellites are currently planned to be deployed in the full constellation. This may change in the future as the constellation evolves. The satellites are deployed into different orbital shells and inclinations in order to provide global coverage, with the proposed satellite inclinations including 42°, 48°, 53°, 70°, 74°, and 81° [37]. The Starlink network is operated by SpaceX, and is supported by a global network of dedicated ground stations. Starlink satellites utilize optical inter-satellite links (ISLs) in order to extend the connectivity to areas without nearby ground stations. Additionally, since this network is operated by a space launch company, they can launch with a high cadence compared to other satellite internet operators [3]. This network is unique compared to the other considered satellite networks, since it is the only fully operational consumer-targeted broadband satellite internet service as of the start of 2026. Customers can purchase and use small phased-array user terminals (Dishy) with a broadband subscription in order to access the network. Starlink has over 9 million subscribers, which constitutes the largest market share in the consumer market [38].

OneWeb, operated by the French Eutelsat group, is another satellite internet provider aiming to provide internet access across the world. Compared to Starlink, OneWeb is primarily business-focused with fewer operational satellites (with just over 600 satellites as of 2025). OneWeb satellites are stationed in polar low Earth orbits at an altitude of approximately 1200 km, forming a Walker-Star constellation [3]. This constellation consists of a single shell with every satellite orbiting at the same altitude and pattern. Additionally, OneWeb has a network of ground stations distributed across the world, serving users through a direct bent-pipe connection without inter-satellite links. In order to access this network, customers deploy user terminals varying from large parabolic antenna solutions to compact phased array terminals.

Amazon LEO, a subsidiary of Amazon, aims to create a large-scale satellite internet network comparable to Starlink. 3236 satellites are planned to be stationed in orbital shells at altitudes between 590 and 630 km, with 27 initial production satellites launched in April 2025 [39] and 182 operational satellites as of January 2026 [40]. Many of the proposed elements of Amazon LEO are similar to Starlink, with network planning to use high-capacity optical inter-satellite links. Additionally, the existing Amazon Web Services ground station network serves as a starting point for the initial deployment. Internet access through Amazon LEO is not yet publicly available as of the start of 2026, meaning that operational performance characteristics are unknown.

These three constellations have the goal of providing high-speed broadband internet access using a LEO satellite network. There are, however, other examples of operational satellite constellations supporting low-speed communications and limited internet access. These include Globalstar, Iridium, Orbcomm. Additionally, Viasat is an example of an internet provider using geostationary satellites. Other mega-constellations are currently being deployed or planned. One example is the Chinese Guowang, targetting a full constellation with approximately 13 000 satellites. One estimate indicates that there may be approximately 80 000 LEO satellites if all planned constellations are fully deployed [41].

2.3. Terrestrial Disruptions

The terrestrial elements of a satellite internet network, such as the ground stations or the PoPs, can be susceptible to disruptions or damage. In this section, some background information and existing studies are considered in order to identify ways in which the terrestrial elements can be damaged or disrupted.

Natural disasters: Terrestrial communication infrastructure can be affected by natural disasters, either through direct damage or indirect effects, such as electrical failures and power loss. These natural disasters are often unpredictable, with some trends indicating that the risk of these disasters are rising over time. Examples of natural disasters are earthquakes, hurricanes, tsunamis, wildfires, and volcanic eruptions [42]. The risk carried by these disasters depends on both the geography and the level of preparedness of the local infrastructure. The impact of earthquakes has also been investigated using case studies, which have shown that the failure of communication systems due to earthquakes can cause significant disruptions to personal life and disrupt economic activities [43].

The 2011 Japan earthquake resulted in disruptions to telecommunication systems and submarine cables, with the affected region losing almost all terrestrial communication services. Disaster response teams relied on the cellular network when available, but also used satellite phones and other communication options, which were often plagued by poor reception and quality [11]. A hurricane is another example of a natural disaster with high damage potential to telecommunications. Tens of hurricanes occur yearly that result in power outages and communication disruptions. An extreme example is hurricane Katrina in 2005, which disrupted cellular and emergency communications, making it difficult for first responders to coordinate rescue operations [44].

When it comes to satellite networks, earthquakes and other natural disasters can impact the operation of PoP locations, the satellite ground stations, or other network infrastructure serving these nodes. Earthquakes are unpredictable events, so the analysis of earthquakes is often focused on seismic risk based on historical data, with The Global Seismic Hazard Assessment Program (GSHAP) [45] and the OpenQuake software [46] being common tools used for risk assessments.

Power outages: Both the ground stations and the internet backbone require electricity for operation. In the event of a power outage, these sites can be disrupted. Power outages are a common effect of natural disasters due to damage to key grid components, but they can also occur due to human errors or faults in the electrical grid. Modern electrical power grids contain many safety systems designed to prevent blackouts, but the failure of these systems can lead to devastating cascading failures affecting a wide area. A survey of recent power outages indicate that thousands of power outages occur on a yearly basis in the USA alone. Additionally, the survey analyzed global blackouts between 2011 and 2019, finding that 50% were due to weather or trees, 31.8% were due to equipment or human error, 10.6% were due to vehicles or accidents, 6.1% were due to over demand, and 1.5% were due to animals [47].

As a recent example, in April of 2025, a large-scale power outage occurred, impacting almost the entire Iberian Peninsula. This blackout resulted in telecommunications and internet access being unavailable for most people in the region. Internet data from Starlink users in the region indicated that their data was routed to alternative ground stations following the blackout. This indicates that Starlink ground stations in the area were taken offline, but that the network was able to rapidly adapt and use the ISL connections to reroute the data [5].

Attacks: Disruptions to the ground infrastructure can also occur as a result of deliberate attacks. One possibility is cyberattacks aimed at disrupting the operation of key internet infrastructure or the ground stations [48]. Physical attacks targeting the infrastructure are also a possibility. In the past, there have been significant disruptions to submarine fiber optic cables, attributed to either accidental or deliberate actions [49]. Additionally, there have been disruptions to land-based fiber optic cables as a result of sabotage.

One study investigated ways in which satellite ground infrastructure can be attacked [9]. It highlights how hostile actors can gain access to critical satellite infrastructure through hacking with examples of previous attacks. Some of these attacks were disruptive in nature, while others sought to gain sensitive data.

2.4. Space Disruptions

Although satellites in orbit around Earth are generally not physically affected by terrestrial disaster events, they operate in a harsh environment where physical repairs are almost impossible. This section presents some of the challenges facing the space segment of a satellite internet network, and how this can lead to damage or disruptions to the satellites.

2.4.1. Space Weather Events

Extreme space weather events such as solar super storms can have a disruptive effect on orbiting satellites. The increased amount of radiation can be damaging to the onboard electronics, and the solar storm can have indirect disruptive effects on satellites [50].

Satellites exposed to solar storms can experience signal degradation, signal loss, or radio blackouts due to disturbances in the ionosphere. Additionally, the thermal effects of the solar storm can lead to swelling of the atmosphere and increased drag in low orbits [50]. This has the highest impact on newly launched satellites which are still positioned in lower orbits before orbit-raising maneuvers.

The radiation from solar storms includes energetic charged particles, which can induce charges and faults within the onboard electronics of satellites, such as bit flips or bit errors, collectively known as single-event upsets. Charged particles from the solar wind are captured by the Earth's magnetic field, with the highest concentrations found within the Van Allen belt. These high-radiation regions extend down to 200 km at the South Atlantic Anomaly, where the magnetic field is weakest. This is also the region where the highest number of single-event upsets occur within LEO satellites [51]. Sustained exposure to high-energy particles also result in degradation of equipment over time, such as reduced solar cell efficiency and damage to materials [50].

In March 1989, a geomagnetic storm resulted in multiple satellites experiencing electrical faults and malfunctions, with weather and communication satellites experiencing temporary loss of control [52]. The same solar storm caused some power grid disruptions on the ground. In January of 1994, the Anik-E1 and E2 geosynchronous communication failed due to the effects of a solar storm. This led to disruptions in television, data, and telephone services in regions of Canada [13]. Anik-E1 was restored to operation after seven hours, while Anik-E2 was only restored to operation after five months due to failures in the backup systems. Investigations attributed the failures of these satellites to high-energy electrons disrupting onboard electronics.

In a more recent example, a 2022 solar super-storm increased atmospheric density, leading to the early de-orbit and loss of 38 recently launched Starlink satellites [14]. Another large-scale geomagnetic storm occurred in May 2024, resulting in increased LEO atmospheric drag. Analysis of satellite tracking data show that thousands of satellites, predominantly Starlink satellites, performed orbital maneuvers in response to the altitude loss following the geomagnetic storm [53]. Additionally, a study investigated the effects of recent solar storm activity on satellite internet services during 2024 and 2025, finding a measurable decrease in throughput during periods of high solar activity. Network performance tests conducted using the LEOScope testbed indicated that intense solar storms can lead to a 20% decrease in throughput, a 10% increase in latency, and a doubling in packet losses with the Starlink network [12].

The effect of solar storms have been considered from an operational readiness perspective. In 2025, ESA organized a campaign simulating the effect of the 1859 Carrington event, the strongest recorded

geomagnetic storm, on launch operations of a satellite. This revealed major challenges due to the possibility of communication blackouts, instrumentation failure, and unpredictable changes to atmospheric drag [54].

2.4.2. Satellite Damage and Lifespan

Although physical anti-satellite attacks are rare, anti-satellite weapons have been successfully demonstrated by the United States, China, India, and Russia. These tests have resulted in extensive debris fields, some of which are still in orbit around Earth. One example was a Russian test of an anti-satellite missile in 2021, which destroyed the Kosmos 1408 intelligence satellite. The remains of the satellite posed a collision threat to the International Space Station and other LEO satellites. A nation-state actor thus has the capability of directly destroying target satellites, which can also result in a wider disruption due to the resultant orbital debris [16].

Similar to the ground systems, satellites can be targeted through indirect attacks, such as jamming or hacking attempts. This is exemplified in the 2007 and 2008 disruptions of two NASA satellites, in which hackers gained unauthorized access through a ground station, with an official report stating that such interference has the possibility of damaging or destroying satellites [55].

Physical destruction of satellites can also occur due to collisions with space debris. Over time, both the amount of space debris and the number of functional satellites have significantly increased. 2025 estimates from ESA indicate that there are approximately 54 000 objects greater than 10 cm, and over a million greater than 1 cm in orbit around Earth [15]. In extreme scenarios, a few destroyed satellites can result in the so-called Kessler syndrome, where space debris destroys other satellites in a cascading manner, creating a dense debris field, and making it difficult to deploy additional satellites in the region. This is a risk that continues to increase with the deployment and expansion of LEO mega-constellations like Starlink [56].

Satellites must withstand the harsh conditions in space, which cause natural degradation over time. Satellite faults can also be due to design issues, electrical problems, or mechanical failures [57]. Satellites which are no longer operational can be taken out of the networks by lowering their orbit to intentionally de-orbit them. In mid-2025, estimates show that approximately one or two Starlink satellites are de-orbited per day [58]. Satellites can also be de-orbited once they reach the end of their operational lifespan. The number of de-orbited Starlink satellites is expected to increase with the size of the constellation. It is estimated that up to five satellites will be de-orbited daily once full constellations are deployed in the future [59, 37]. Intentional de-orbiting of retired satellites differs from unexpected satellite disruptions, since the latter can occur without warning or replacement plans. Satellites can be deliberately retired as satellites with improved capabilities are deployed, or because their onboard propellants are close to being depleted. As an example, Starlink satellites have an estimated lifespan of 5 years, leading to a high rate of retirement across a fully populated constellation [37].

3

Resilience

Network resilience considers how robust and tolerant a network is against disruptions. In this chapter, resilience of various relevant networks are discussed in order to identify ways in which a satellite network can be analyzed. Additionally, literature relevant to satellite resilience is discussed.

Section 3.1 provides an overview of metrics commonly used for resilience analysis. Section 3.2 discusses how related work about resilience are applicable to satellite networks. Based on this, section 3.3 discusses gaps in the existing research and ways in which this thesis can contribute.

3.1. Resilience and Metrics

Resilience as a concept can cover many different fields. On a fundamental level, resilience refers to the capability of resisting difficulties and recovering after adverse events. This can be applied to many different systems and fields of research, such as biology, sociology, engineering, computer science, and healthcare. The importance of resilience analysis lies in understanding ways a system may be vulnerable, and often finding ways to lessen these vulnerabilities. An important aspect of this analysis involves being able to quantify the resilience in order to allow representative comparisons between related systems. Due to the diverse nature of resilience, different fields of study have adapted various relevant metrics [60]. In order to identify possible analysis approaches for a satellite network, multiple types of resilience analysis and metrics have been identified.

One example of resilience analysis is found in network theory. Many real-world systems can be modeled as a network or graph, which makes network theory a powerful tool capable of generalizing to different scenarios. There are many ways to quantify the resilience of a generic network. In graph theory, the concept of the largest connected component is commonly used as a purely structural measure for resilience [61]. In a sparse network, this indicates how many of the total number of nodes are inter-connected. A similar structural metric is the average two-terminal reliability (ATTR), which is a measure of the impact of a disaster event. It is the ratio between the number of connected node pairs and the total number of node pairs in the network [62]. The purpose of this metric is to quantify how disconnected a network is, rather than the amount of redundancy available. Although these measures are effective in indicating the level of connectivity within a network, they are primarily applicable when the nodes serve similar purposes and transfer information between each other. For a satellite network, ground stations, satellites, and users each represent different distinct systems. Due to this asymmetry, the largest connected component or ATTR do not give useful indications of resilience. Additionally, networks without ISLs make it difficult to define how the largest connected component is computed.

Since the graph-based metrics are less suitable for analyzing the performance of a satellite internet network, performance-based metrics can be considered. Here, both the structure and the performance of the network must be evaluated, which can change as a result of an external disruption [61]. These performance characteristics include the following:

Coverage: The coverage metric indicates the terrestrial coverage area of the network. This can either be normalized by the population density to estimate the user availability, or evaluated as-is to quantify the available coverage area. The latter gives an indication of how well the satellite network covers the entire world. The difference in coverage before and after the event provides a numerical metric for quantifying the overall impact, either on the number of users, or the geographical coverage area.

Service capacity: This is an estimation of the number of users the network is capable of serving at a baseline performance. Reductions in service capacity are indicators of how severely degraded the system is.

Latency: This is the propagation time for a packet through the network. The latency depends both on the position of the user, and the path the packet takes through the network to reach its destination, such as a ground station.

Recovery time: Mean time to recovery (MTTR) is a metric that indicates the recovery rate of a device or service in response to a fault. In the context of a satellite network, it can be used to quantify how quickly a fault can be repaired, and the network returns to its full capacity. This is related to service downtime [21]. Estimating the MTTR requires modeling or measuring how quickly a network recovers from faults, which can be challenging for proprietary systems with limited data.

These metrics are influenced when a system performance is degraded, either by natural or artificial means. A generic comparative framework can be constructed by combining these service metrics with a way to target the system.

Figure 3.1: Illustrative example of a resilience triangle

When assessing the resilience of a system, the recovery phase after a disruption is important. One approach is to evaluate a performance metric to reveal how it is impacted and returns to the baseline over time. This forms a triangle, known as the disaster resilience triangle. An illustrative example is shown in Figure 3.1. The area of the triangle gives an indication of how resilient the system is against the given disruption scenario. This area is affected by both the impact of the disaster and how quickly the performance metric partially or fully recovers [63].

With the resilience triangle, the loss of resilience is defined as the cumulative impact on the performance,

$$R = \int_{t_0}^{t_1} [1 - Q(t)], dt \tag{3.1}$$

where Q is the evaluation function indicating the performance or quality of an infrastructure. One disadvantage of the resilience triangle is the reduction of two measures, impact and recovery time into one. A larger impact with a faster recovery time can thus result in the same calculated resilience as a smaller impact with a longer recovery. Additionally, the ending time, t_1, is the time when the performance measure recovers to the original value [64]. In some cases, it may not return to the original measure, or it may recover to a higher-than-initial value. In these cases, t_1 can be defined as the time the infrastructure reaches a new steady state, representing the restored performance. Additional metrics can be derived from the resilience triangle [65]. The residual performance is the lowest normalized performance during the disruption, with its complement being the depth of impact. The restored performance is the normalized performance once it reaches a new steady state. The disruption duration is the period of degraded performance. The failure and recovery rates describe the slope of the performance curve during the failure and recovery phases. Additionally, the cumulative performance is the complement of the cumulative performance loss defined in Equation 3.1.

3.2. Related Work

Resilience of networks, especially critical terrestrial networks, has been extensively analyzed for various fault conditions. Additionally, research into resilience aspects of satellite networks has been investigated to a certain extent. The purpose of this section is to provide an overview of the relevant existing literature related to satellite network resilience, which can serve as a baseline for additional research in this thesis.

3.2.1. Satellite Constellation Analysis

Due to the opaque nature of many commercial satellite internet deployments, direct knowledge of the inner workings and routing of satellite networks is generally unavailable. Using publicly available information in combination with dedicated measurements, researchers have gained insight into the performance characteristics of Starlink, and how it handles bandwidth- or latency-critical tasks [24]. Other studies have attempted to gain knowledge about the physical characteristics of satellite constellations by making use of direct RF measurements [23], thus providing insight into the deployed physical layer. Companies planning to operate satellite constellations must operate under regulations imposed by agencies such as the FCC. Public regulatory documents have been analyzed in order to derive information about the planned satellite networks. These provide additional insight into LEO constellations, primarily related to constellation shape and radio frequency allocations. A 2021 study conducted a detailed comparison between Starlink, Amazon LEO, Telesat, and OneWeb using data from FCC filings [2].

The unknown elements are still subject to academic interest. One area of research include the exploration of different routing methods in a LEO network. The challenge lies in the dynamic nature, making many traditional routing algorithms unsuitable. A related topic is the investigation of how different routing algorithms affects network performance when under heavy load conditions [66]. Inter-satellite links and constellation topologies also represent an interesting topic for research. Prior to the deployment of active mega-constellations, the research investigated how network structures and ISL configurations affect the performance in LEO constellations [67]. In recent years, such research is often considered in the context of real-world mega-constellations like Starlink, including investigations into theoretical performance characteristics of networks based on the limited ISL connections deployed by Starlink [68].

Although LEO satellite networks are generally consumer-oriented, research has investigated whether orbital infrastructure can be used to compliment submarine fiber cables as part of the internet backbone. The highly variable latency was found to be one factor making it challenging to directly replace terrestrial backbone infrastructure [69]. Additionally, the existing networks have been investigated from a risk management perspective. A 2025 study investigated whether LEO networks can be used as an emergency backup network during a large-scale outage, finding that only 14.7% of lost submarine cable capacity can be restored at most [6].

Some research have investigated the negative aspects of satellite networks. The increasing number of LEO satellites have given rise to concerns about space junk and the impact of reflective satellites affecting astronomical observations. A higher density of satellites can also negatively affect radio astronomy due to unintended radiation. These concerns have led to astronomical parties proposing regulations to limit the impact on astronomy [41].

3.2.2. Resilience of Ad-hoc Networks

One unique aspect of satellite networks is the dynamically evolving topology, which has similarities to ad-hoc networks. These are decentralized networks in which the network nodes work together to handle the traffic, with examples being the wireless ad-hoc network (WANET) or mobile ad-hoc network (MANET). The decentralized nature requires the nodes to discover and construct links to each other, which draws parallels to inter-satellite connections. Exploring the approaches applied to ad-hoc networks can thus provide insight into how a dynamic time-evolving network can be analyzed.

The measure of resilience is relevant in the context of a decentralized network due to the impact on reliability. Some types of ad-hoc networks are used in support of military or disaster response applications, where a highly reliable decentralized system is desired. Connections between the nodes can appear or disappear as the network changes over time, making it difficult to predict the future topology [61]. Survivability in the context of network resilience can be applied to ad-hoc networks, where network resilience is measured in terms of how the service handles operational disruptions.

One example of an ad-hoc network with many similarities to a satellite network is the flying ad-hoc network (FANET), in which multiple UAVs communicate to form a decentralized network. Similar to a satellite network, a FANET exhibits spatial and temporal changes in the nodes forming the network, with the possibility of rapid changes in the network structure. Additionally, the individual nodes can communicate with each other similar to inter-satellite communication links. One study introduced a resilience analysis method for FANETs. This is on the basis of using the performance loss as a metric for the system resilience. Additionally, it incorporates the ability of UAVs forming a FANET to dynamically respond to an outage event in their resilience analysis and use a case study to evaluate the methods, which forms the basis of a resilience triangle as discussed in section 3.1. The results indicate that the network performance decreased as nodes are attacked. Additionally, the performance of the FANET was found to be dependent on the range and number of nodes [70]. The use of case studies and the reactive reconfiguration of the network are methods that can be applied to satellite networks. There are, however, key differences between ad-hoc networks and satellite networks. Although satellite networks are highly dynamic, they generally operate in a grid-like predictable topology, which makes it possible to plan the connectivity in advance. Additionally, the motion of satellites are limited due to the maneuvering capabilities as explained in subsection 2.1.4, which limits how much the constellation can be modified.

Wireless mesh networks are related to ad-hoc networks. The mesh network topology employs connections between individual nodes, which are often decentralized. Many decentralized ad-hoc networks as themselves constructed as a mesh network, but meshes can also be deployed in a deliberately planned structure. Wireless mesh networks have been considered as a potential candidate for expanding cellular connectivity with a lower deployment cost compared to traditional infrastructure. One example is WiBACK, a technology developed to extend cellular communications infrastructure in under-served areas using a wireless mesh instead of wired connections. Although the technology handles dynamic network reconfiguration, management, and healing, it is primarily designed to operate using stationary

node installations [71]. The resilience of these networks are also subject to research. One study investigated how weather-induced attenuation can affect the performance of a mesh network based on fixed router installations. It found it advantageous to use weather forecasts to proactively plan the future topology [72]. This draws a parallel to the effect of space weather events, the effects of which can be predicted using short-term forecasts based on observational data. These forecasts are published by the Space Weather Prediction Center [73].

3.2.3. Internet Resilience

Researchers have investigated the causes and impacts of historical internet outages. A 2018 paper identified and classified the outages into different categories: natural or human, accidental or intentional, physical or logical. The study also explored evaluation metrics used in prior research, which are relevant when analyzing the impact of internet outage scenarios. These include non-formalized metrics, user-centric metrics, and network-centric metrics [10].

One user-centric metric estimates the number of affected users by combining population density data with outage information [74], but does not take into account the effect on network performance. It does, however, give a quantitative estimation of the impact of an event, which was used to analyze a hurricane case study.

Network-centric approaches have also been used. The authors of one publication [75] defined Reachability Impact Metrics (RIMs), which quantify the number of disconnected network paths, and Traffic Impact Metrics (TIMs), indicating how alternative paths are impacted. These metrics can be used to assess how widespread a disruption is. When outages occur in an information network with multiple paths, the resultant load redistribution can lead to bottlenecks or congestion elsewhere in the network, an effect known as cascaded failures.

The risk of specific disaster events impacting internet connectivity has also been examined. The most intense solar storm recorded was the Carrington event in 1859, which led to widespread electrical outages. A 2021 study investigated the potential impact of a similar solar super-storm on the present-day internet infrastructure, finding that damage is likely to occur. It was found that long submarine internet cables are particularly vulnerable due to the high currents induced during a solar storm. Additionally, it proposed potential defenses against wide-scale disconnections [17]. One of the main challenges in predicting the impact of solar super storms on the modern day infrastructure is the rarity of these events. Predictions estimate that a Carrington scale event may occur again with a 1.6% to 12% probability per decade [17]. Smaller coronal mass ejection have affected both terrestrial and satellite systems in the past, but these were weak compared to the Carrington event.

Internet connectivity can also be impacted by earthquakes, with different regions of the world exposed to varying levels of seismic risk. A 2022 study investigated the risk of earthquakes to internet exchange points (IXPs) using global seismic hazard models, finding that 50% of IXPs have a greater than 2% probability of potentially damaging seismic activity over a period of 50 years [76].

The global internet is supported by a network of submarine cables connecting key infrastructure around the world. Cuts or malfunctions in these cables can result in disruptions in the internet traffic. This complex network has been extensively analyzed academically. As an example, a 2023 study introduced Nautilus, a framework for mapping submarine cables [77]. This framework formed the basis of the Xaminer tool, which was used to analyze the impact of natural disasters and solar storms on internet connectivity.[78]. These tools showed that the resilience of the internet is affected by how susceptible the physical elements are to damage.

3.2.4. Satellite Resilience

Although some research has analyzed the use of satellite internet to enhance the resilience of the internet following a disaster [79], recent studies have also analyzed resilience aspects of large satellite constellations themselves.

One study [18] analyzed the robustness of a hypothetical satellite constellation when exposed to random or targeted satellite failures. It examined how different routing methods can impact the robustness and found that selectively attacking specific high-load satellites results in the fastest network collapse. Additional research has investigated the resilience of ISL-enabled Starlink and Amazon LEO satellites when exposed to satellite damage, but did not consider the currently deployed ground station locations or the effect of terrestrial damage [80]. Many other studies have been published investigating routing algorithms, including their effect on network performance and resilience against disruption scenarios and adversarial attacks. These generally consider packet-level performance metrics such as packet delivery rate, packet latency, and jitter [81].

The use of satellite maneuvering have been studied to some extent. A 2022 study investigated how low-thrust maneuvers can be used to reconfigure a LEO constellation, investigating different strategies. By treating satellite reconfiguration as an optimization problem with the goal of minimizing the maneuvering cost, a genetic algorithm was used to find maneuvering options [82]. One study investigated how maneuvering is used within the Starlink network based on tracking data [19]. A 2024 study introduced an availability model for LEO satellite constellations to estimate the expected downtime resulting from satellite faults, considering both service gaps and satellite redistribution using maneuvering [21]. However, this preliminary model only considers a single orbital plane, and does not consider the overlap of other satellites within a full network. Research is thus limited relating these capabilities to resilience for a mega-constellation.

Direct data showing how the onboard electronics of commercial LEO internet satellite systems are affected by solar events is unknown, since this depends highly on how hardened the onboard systems are against the environment. The vice president of the Renesas, a semi-conductor supplier, indicated that these LEO satellites use a combination of radiation-tolerant and off-the-shelf parts. This lowers the production costs of the satellites compared to using fully radiation hardened components [83]. The impact of space weather also depends on the exact orbits of the satellites. Data showing the occurrence of single-event upsets for other satellites existing [51], which are expected to be comparable for internet satellites.

The effects of real disaster scenarios on deployed satellite networks have been analyzed to a limited extent. A 2024 paper used RIPE Atlas measurements in order to gain insight into how Starlink satellites reacted to the May 2024 solar super-storm [14]. It identified a small impact on packet losses, followed by slight increases in packet latencies. Although some satellite networks have found widespread adoption, the technology and deployment is still relatively new. This means that there are only a limited number of studies investigating the use of satellite internet technologies following a natural disaster. Reports have indicated successful use of Starlink following the 2024 Noto Earthquake [4] and the 2025 Iberian Peninsula power outage [5], Additionally, Starlink has previously provided free service following the 2022 volcano eruption in Tonga and following Hurricane Helene in the United States. Despite these reports, the effect of the natural disasters from a networking perspective has not been investigated in depth.

3.2.5. Centrality Measures

When assessing the resilience of a graph, the relative importance of nodes within the graph can be used to determine critical nodes to target in a simulated attack. One common metric is centrality, for which multiple variants exist [60].

The betweenness centrality is often used when assessing the importance of a node as a mediator

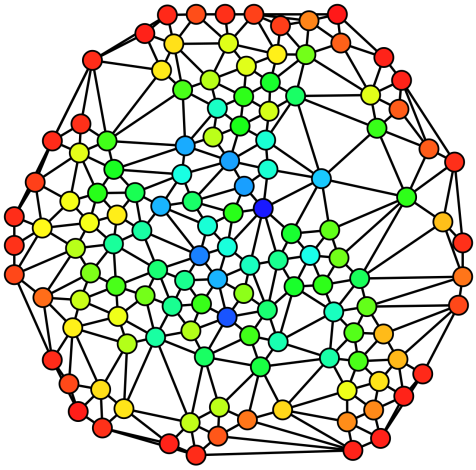

Figure 3.2: Illustration of betweenness centrality. The nodes with the highest centrality are blue [84].

of transfer across the graph. The betweenness centrality measures the number or proportion of all shortest paths passing through a specific node, while a variant, the L-betweenness centrality only considers paths below a maximum length. A simple example is illustrated in Figure 3.2. In the context of a satellite ISL network, the betweenness centrality provides an indication of the relative importance of satellites based on the network structure. The general application of betweenness centrality is applicable for static graphs, but studies have generalized the shortest path to also include a time component, where information can be transferred to a node in one timestep and away in another timestep, giving the Shortest-Fastest Path. This is then combined across multiple snapshots by summation to assess the Temporal Betweenness Centrality (TBC) [85]. Combining centrality measures across snapshots through averaging has also been investigated in comparison to TBC, with the results being comparable if the temporal component is less significant during routing.

In the context of resilience analysis, the betweenness centrality in combination with a network metric (such as the largest connected component) is often used to determine the impact of an attack on the degradation of the graph [60]. Differently connected networks degrade in distinct ways, with some degrading slowly, and other collapsing. Using other indicators of the network state, this approach is applicable to other types of resilience analysis.

3.2.6. Satellite Simulation Tools

Various simulation tools have previously been developed to analyze different aspects of satellite networks. Hypatia [86] is a LEO satellite modeling and simulation tool designed to model the orbital constellation and the data flow within a satellite network. Celestial [87] and StarryNet [20] are additional LEO simulation tools, with Celestial focusing on satellite edge computing, and StarryNet providing broader simulation capabilities for full LEO networks. Recent work on χeoverse [88] gave rise to a full mega-constellation simulation with improved runtime performance capable of real-time simulations. These tools predominantly focus on simulating or emulating satellite network characteristics, with limited built-in capabilities for analyzing complex terrestrial disruptions or satellite failures. Additionally, existing tools for mega-constellations primarily focus on creating a regular constellation layout without considering the ability for satellites within the network to maneuver and respond to disruptions in the constellation.

A separate group of satellite simulation tools focus on the mission-planning aspects of a space mission. Examples are the open-source General Mission Analysis Tool (GMAT), developed by NASA, and the proprietary Systems Tool Kit (STK), developed by Ansys. These are general purpose programs that can be used to plan and simulate an entire space mission. These programs can be used to simulate orbital trajectories, but are generally used for a relatively small number of satellites compared to a full

mega-constellation. They can, however, be used with scripting as orbital propagation solvers. Similar to the network-oriented simulation programs, these programs have limited built-in capability for resilience analysis.

Although the existing tools can be adapted for resilience analysis purposes, the primary challenge lies in the modeling of the disruptions and computing the relevant metrics. The other aspect is the computation of the orbital characteristics of the network and the ability for satellites to maneuver in response to a disruption. In order to allow for flexibility in generating artificial datasets and propagating existing orbital data, it was decided to implement a standalone simulation program specifically to perform the resilience analysis of mega-constellations.

3.3. Research Gaps

When reviewing the literature on the resilience of terrestrial and satellite networks, it becomes evident that, due to the relatively new deployments of large-scale internet mega-constellations, studies analyzing the resilience while considering terrestrial infrastructure and maneuvering are limited. Existing studies of satellite network resilience primarily focus on satellite damage and routing, mostly in the context of proposed or hypothetical architectures, as opposed to currently deployed architectures. Additionally, existing studies cover the routing and networking aspects, but to a lesser extent the physical events resulting in the disruptions.

Existing work on satellite resilience has predominantly focused on the orbiting satellites, but there has been less focus on the importance of critical ground infrastructure. Ground stations or points of presence are still susceptible to terrestrial disruptions and are essential for the performance of the entire network. As such, this thesis aims to investigate how a network can be affected by both terrestrial and space-based faults. Additionally, existing work on the effect of satellite maneuvering on resilience is limited. Some studies have explored reconfiguration strategies, but the ways a full satellite constellation can use maneuvering in order to respond to a disruption scenario represents a knowledge gap which will be investigated. Investigating this topic will provide further insight into how quickly baseline operation can be recovered, and how the performance of a compromised constellation changes over time.

These aspects will be explored in the remaining part of this thesis, with the goal of comparing satellite networks to each other and the terrestrial counterparts in terms of resilience. The goal is thus to analyze how the various emerging satellite networks may fare when exposed to system disruptions, including both ground station and satellite outages, and approaches to recovering the system performance.

4

Simulating a Satellite Internet Network

In order to perform the resilience analyses discussed in the previous chapter, it is necessary to simulate aspects of a satellite network. Developing a simulation requires both the underlying model, and a set of assumptions and parameters. These will be explained and discussed in this chapter.

The primary goal of the simulation tool is to provide a framework for satellite network disaster resilience analysis, with a primary focus on the Starlink, OneWeb, and Amazon LEO. Relevant metrics are derived from analyses of defined case studies, which reveal how the different constellation designs respond to challenges or outages.

Section 4.1 gives an overview of the simulation model and assumptions, section 4.2 describes how the input data and parameters were selected for the various networks, including ground station locations and constellation data, finally, section 4.3 describes how the various terrestrial and space disruptions modeled in the simulation in order to simulate disaster scenarios.

4.1. Model overview and assumptions

This section provides an overview of the structure of the simulation model. The model and simulator are designed with flexibility in mind. Figure 4.1 provides an overview of both the overall architecture of the simulator, in addition to the ways modules (written as Python classes) can be used in order to define custom outage scenarios and metrics. These are subsequently used to run custom simulations for which the impact of a natural or targeted disaster is quantified. More information about the implementation aspects can be found in Appendix A.

4.1.1. Terrestrial Grid

Discretizations are necessary in order to evaluate a metric over a continuous area of Earth. Global statistical and population data are generally provided with indexes using a standard method. Multiple discrete grid systems are commonly used and available, each with advantages and disadvantages. Some methods, such as Google's S2 and Uber H3 prioritize keeping the individual grids regularly shaped, but have variations in grid area depending on location on Earth. Other methods, such as rHEALPix and OpenEAGGR are better at preserving area, at the expense of distortions and grid shape variations. H3 and S2 are commonly used for statistical analysis, with many existing datasets and software tools being built on these systems, making them easy to adapt for new analyses [89].

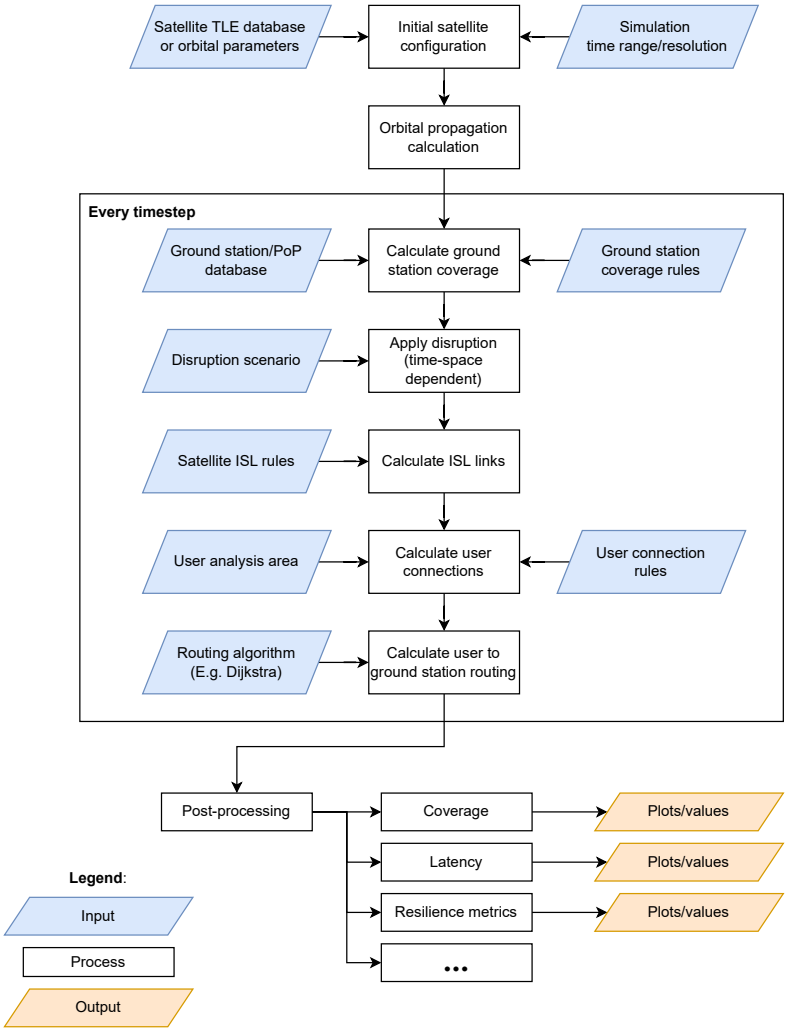

Figure 4.1: Overview of the resilience analysis simulation tool.

Grid systems are available different resolutions. For instance, the H3 grid is available in scales, corresponding to different hexagon dimensions. Each hexagonal cell consists of seven higher-resolution cells, which makes it possible to perform analyses at different granularity levels [90]. The H3 grids are widely used for geospatial analysis, thus making it a suitable candidate for analysis of location-dependent network performance. As an example, Kontur provides aggregated population statistics across different H3 resolutions [91].

Due to the combination of available statistical data and maturity of software tools, H3 is used as the terrestrial grid for this simulation. The resolutions primarily used in the resilience analysis are resolution 4, with an average hexagon area of 1770 square kilometer [92]. Comparisons have shown that the Starlink network likely uses H3 grids for the terrestrial mapping of users, which also makes it beneficial to analyze it and other networks using the same hexagonal grid system. The simulation program specifically uses `h3-py`, which provides Python bindings for the H3 grid. Within an area of interest, a dense grid is used, which is filtered to include the terrestrial area. Statistical metrics about the performance of the network are subsequently based on discrete analyses at each of the center coordinates of the hexagonal cells.

4.1.2. Latency, Coverage, and Capacity Estimation

The ground-to-ground latency of a connection is the time it takes for a signal to reach from a user terminal to one or more satellites, and back to a ground station. This latency is affected by two components, the propagation delay, and the processing delays. The propagation delay is the total distance divided by the speed of light, 299 792 458 m/s. Due to the lack of available data about the processing performance of commercial satellites, the processing delays are set to zero in the latency estimation, thus only considering the physical propagation delay. The minimum number of hops are determined, since this can be compared against different networks without network-specific performance parameters.

The shortest physical path is used for latency estimations during the analysis. One approach to finding the shortest path between points within a graph is Dijkstra's shortest path algorithm, which is available through implementations in the SciPy package. Within an ISL-enabled satellite network, this allows for the the theoretically fastest connection when only considering path delays. The latency is affected by the geographical position of users, the distribution of satellites, and the location of available ground stations. By sampling the latency at points corresponding to a hexagonal grid, latency statistics for an area of interest or the entire globe are found.

The coverage of a satellite network is assumed to be the regions covered by satellites with either a direct bent-pipe connection, or an indirect connection through ISLs. This represents the coverage area if the capacity of the network component do not limit the ability for users to connect to the network. The coverage area is found by determining whether the center of each evaluated terrestrial H3 grid position can connect to an internet-connected satellite. The fraction of the land area with connectivity is subsequently computed.

The operational status of a satellite network is not only determined by the coverage area, but also the number of users the satellite network is capable of serving. An approach is developed for estimating this service capacity, which can be applied to estimating the relative service capacity between the nominal constellation and a damaged constellation. The approach divides the surface of Earth into regular hexagonal cells, each assigned a certain number of users based on an estimated population adoption rate. The available capacity of the satellite is subsequently divided up into the visible cells. Each satellite is capable of serving a max number of users, which must be distributed within its visibility area. The mapping between the capacity of the overhead satellites to the users within a region is an allocation problem, which can be modeled as a graph between the satellites and the cells. A water-filling algorithm is used to determine the mapping, in which the available satellite capacity is evenly distributed across the visible cells, until the total capacity is depleted. Compared to a maxflow approach, this identifies areas where the user density exceeds the available capacity. Additional details about the capacity mapping process can be found in Appendix A. Estimating the service capacity can either be on a global scale, or a region of interest on Earth. The latter is the primarily use case for this metric in order to analyze the effect of a regional terrestrial disruption.

4.2. Model Inputs and Parameters

In order to model existing or upcoming satellite networks, sources of data are needed. This primarily involves information about the locations of the satellites over time, the locations of the ground stations.

4.2.1. Satellite Constellations and Maneuvering

The orbital information of objects around the Earth are closely tracked and published by the United States Space Command through Space-Track.org [93]. This makes it possible to gather snapshots of existing satellites and simulate their orbital propagation around Earth. The standard format for Earth satellites are in the form of the two-line element set (TLE), which contain identifying information about the satellite, and data required for computing the orbital propagation. Celestrak is an organization

that also publishes orbital data of Earth satellites for analysis purposes. The TLEs available through Celestrak are either derived from Space-Track data, or are aggregated directly from data provided by satellite operators. These are available for network operators such as Starlink, OneWeb, Amazon LEO, and GPS, and are more accurate than orbital elements derived from tracking data [94], since they are based on the internal data used for acquiring and tracking overhead satellites when connected to the network. For the analysis of OneWeb and Starlink constellations, the supplemental TLEs provided by the companies and retrieved through Celestrak are used. These are used as inputs to the Python Starfield library, which handles orbital propagation of the satellite constellation over time.

In addition to TLE data, a Keplerian orbital constellation model is also developed in order to generate and simulate the time-wise evolution of arbitrary regular constellations. Each constellation is defined as containing multiple orbital shells, where all satellites operate at a fixed altitude. Within the shell, the pattern of the constellation are determined by the number of orbital planes, the number of satellites in each plane, and the relative phase and position offsets between the planes. Although using a Keplerian orbital model gives similar short-term constellation shapes as using tracking data, it is useful for performing maneuvering simulations of individual planes. Tracking data contains noise due to tracking errors, station-keeping, and collision avoidance maneuvers, which limits the accuracy when propagated over a longer period of time compared to a idealized constellation model. In order to model the maneuvering of the satellites, the tracking data from the orbit-raising phase of the satellites are used as indicative of the maneuvering performance [36]. These are then used to determine how quickly a satellite is able to shift its relative phase within the orbit, which is subsequently used to move a satellite from an initial to a target position by varying the relative phase within an orbital plane.

The locations of ground stations and PoPs are derived from crowd-sourced datasets gathered from public domain regulatory information and measurements. For Starlink, the *Unofficial Starlink Global Gateways & PoPs* contain location information of known active and inactive Starlink ground stations and PoP locations [25, 24]. The ground station locations can subsequently be used for simulation purposes in order to determine whether a satellite is within view of a ground station. A similar unofficial crowd-sourced resource is available for OneWeb, which is used for the OneWeb specific simulations [95].

4.2.2. Up and Downlink Characteristics

The up and downlink characteristics of the satellite to user and the satellite to ground station connections have implications for performing resilience analysis. Although the up and downlink performances differ for a specific link, the capacity in the analyses is based on the user capacity, making it agnostic to the individual data rates of the connections. Still, it is necessary to determine whether it is possible for a satellite to form a functional connection to a terrestrial transceiver.

The most important factor is whether a satellite is in view of a user or a ground station, the visibility cone depends on the minimum elevation angle of the ground-based observer. The minium elevation, ϵ for a ground-based observer is influenced by the obstructions (buildings or terrain), the minimum tilt of the antenna. The elevation may further be limited by free space path loss of the signal path. This value is typically around 20 degrees or more for terminals located near the ground, but is also limited by beamforming or angle limits of the antenna.

In order to simplify the computation of the visibility cone for satellites in orbit around Earth, it is instead converted into an equivalent coverage radius, if the satellite and the ground observer are both projected onto the terrestrial coordinate system. The equivalent ground coverage radius is,

$$\alpha = \arcsin\left(\frac{R_{Earth}\sin(\pi/2+\epsilon)}{h_{sat}+R_{Earth}}\right) \tag{4.1}$$

$$\beta = \pi/2 - \epsilon - \alpha \tag{4.2}$$

$$r_{equiv} = \beta \cdot R_{Earth} \tag{4.3}$$

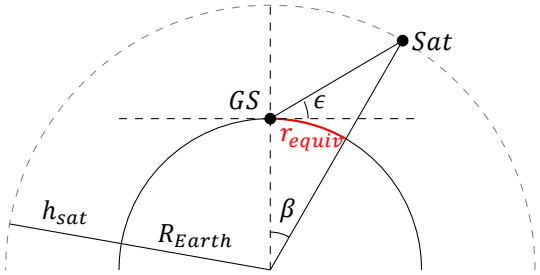

Figure 4.2: Illustration of the coverage area

Where R_{Earth} is the radius of Earth, assumed to be 6378 km, h_{sat} is the height of the satellite above Earth's surface, ϵ is the minimum elevation angle, and r_{equiv} is the equivalent coverage radius on the ground. This is illustrated in Figure 4.2. By determining whether a ground observer and a satellite are within this radius using terrestrial coordinates, the coverage can be determined efficiently. This estimate assumes that the Earth is spherical and does not take into account oblateness. Distances on the ground are computed as the great-circle distance using the haversine formula.

4.2.3. Inter-satellite Links

The connections between satellites are determined based on rules regarding the limit of the number of ISL links, rules regarding connections between nearby satellites. In the simplest case, a satellite may connect up to the maximum number of connections to nearby satellites with similar orbital characteristics.

The maximum possible distance for an ISL connection depends on the altitude of the satellites and the minimum altitude of the beam. At greater distances, the beam is either blocked by the Earth, or attenuated by the atmosphere. The maximum theoretical distance between two satellites limited by the atmosphere can be calculated with,

$$dist_{max} = 2 \cdot \sqrt{(R_{Earth} + h_{sat})^2 - (R_{Earth} + h_{atm})^2} \tag{4.4}$$

Where h_{atm} is the height of the atmosphere. This limitation due to the atmosphere is illustrated in Figure 4.3.

Along with the physical limit, the maximum distance is also limited by the link budget of the ISL transmitters and receivers of the satellites. Furthermore, the maximum number of ISL connections depends on the number of transceivers on each satellite. In the simulation, the ISL connections are in the form of a connectivity matrix, corresponding to the connections between every satellite. First, the distance between every satellite is found by generating a distance matrix using the Euclidian distance. The ISL connections subsequently are filtered based on a maximum distance and satellites within the same orbital shell, and further truncated based on the number of available transceivers (3 for Starlink). With a connectivity matrix, the path distances can then be computed. First, a virtual node is added to the connectivity matrix, representing a virtual ground station node, with connections to every satellite node with ground station visibility. The dense connectivity and distance matrices are subsequently converted to a sparse scipy array using `csr_array`. The path minimum path distances between every satellite and the virtual ground is then found using Dijstra's shortest path algorithm from SciPy, which simultaneously determines the satellites without the ability to connect to the ground through the ISL network. Finally, the hop count is determined by iterating through the results of the shortest path solution for each satellite.

The result of the ISL computation are matrices representing how the satellites are connected within the network at each timestep, and their minimum direct or indirect distance to a central ground station. These form the basis for coverage and latency calculations.

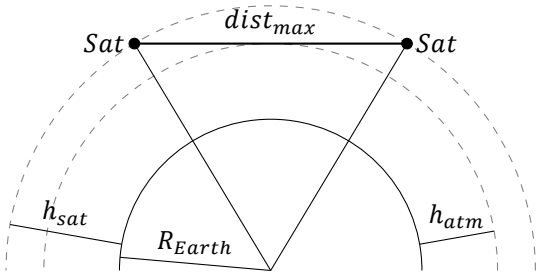

Figure 4.3: Illustration of the physical ISL distance limit

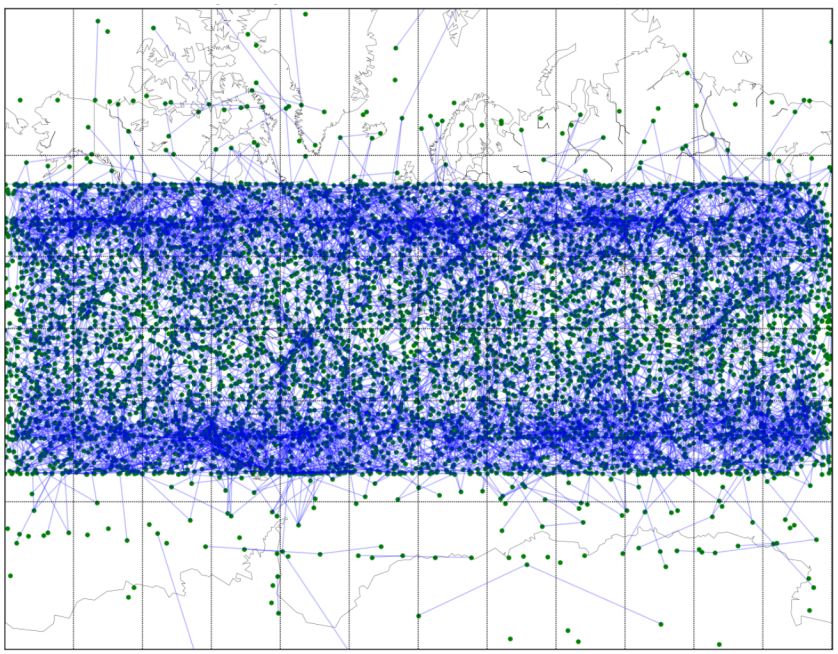

Figure 4.4: Visualization of a subset of possible Starlink ISL connections

4.2.4. Modeling Starlink

Starlink stands out in being the largest currently deployed LEO satellite network. As a result, significant amount of data is available for the physical structure of the network and how it operates, including satellite and ground station locations. For the simulation, the publicly available satellite ephemeris data is used in order to determine the satellite locations over time. Additionally, crowd-sourced ground station and PoP data is used in order to build a model of the locations of ground infrastructure [25]. The cell layout of Starlink follows a H3 grid, with the downlink signal structure having been previously analyzed and reverse-engineered [23].

The downlink availability modeled is based on the availability of ISL connections. ISLs were made available with the v1.5 satellites, allowing for expanded connectivity in areas without a nearby ground station. Based on the network formed by ISL links, the extended coverage area can be estimated, in addition to a calculation of the end-to-end latency through the ISL network. Each Starlink satellite can make three ISL connections based on information about the satellite systems [68]. Figure 4.4 shows a subset of possible ISL connections and the satellites nodes overlaid on map.

The distribution of Starlink ground stations are shown in Figure 4.5 (dated August 2025). Although the ground stations are associated with nearby PoPs, the analysis focuses on the ground stations themselves as the termination point of the connection. This allows for valid comparisons to networks without detailed PoP information.

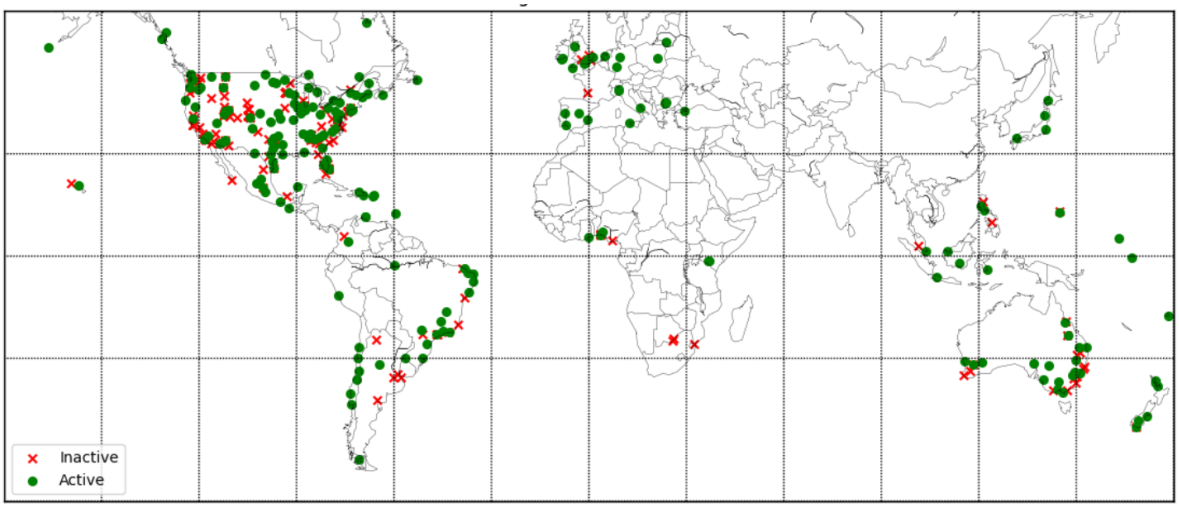

Figure 4.5: Starlink Ground Station Locations

The coverage analysis considers the satellites within view of a ground station at a certain point in time, and the cells which are within view of the satellites. The Starlink user terminals have a minimum elevation angle of approximately 20 degrees, a value used across the different simulations cases.

New Starlink satellites are continuously being deployed into orbit, this is illustrated in Figure 4.6, showing the rise in the number of active Starlink satellites over a period of 80 days. In mid-2025, an average of 215 additional satellites were added to the network each month. The figure also illustrates how the number of Starlink satellites decrease between launches due to deorbited satellites. Within the TLE-based simulation, a single TLE snapshot dated the 14th of April, 2025, is used as primary analysis point. Daily snapshots of Starlink TLEs were gathered in order to gather some information about the behavior of both the overall constellation and the maneuvering of individual satellites. Additionally, the final starlink constellation shapes often differ from the planned constellations, with variations in orbital altitude and the distribution of satellites. An overview of planned generation 1 and 2 constellations are shown in Table 4.1. The generation 1 constellation has been fully deployed, however, only around 3000 satellites out of the 4714 launched satellites remain operational as of the start of 2026 [35].

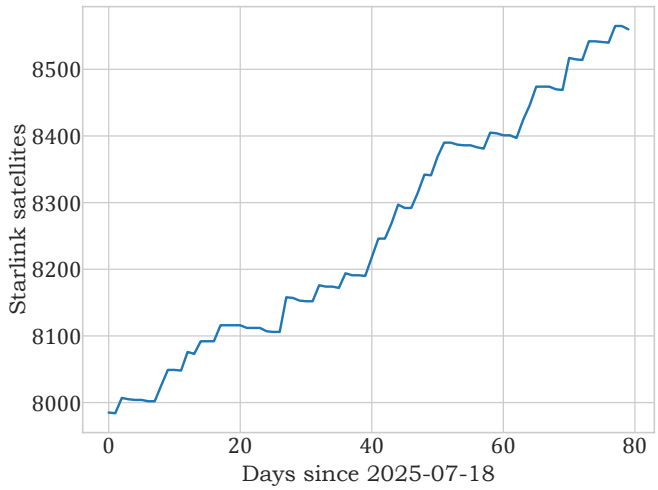

Figure 4.6: The number of Starlink satellites over time in 2025

Gen	Altitude (km)	Inclination (°)	Number of Planes	Satellites per Plane	Total Satellites
1	550	53	72	22	1584
1	570	70	36	20	720
1	560	97.6	6	58	348
1	540	53.2	72	22	1584
2	523	43	28	120	3360
2	525	53	28	120	3360

Table 4.1: Planned generation 1 (fully deployed) and generation 2 (partially deployed) Starlink constellations [35].

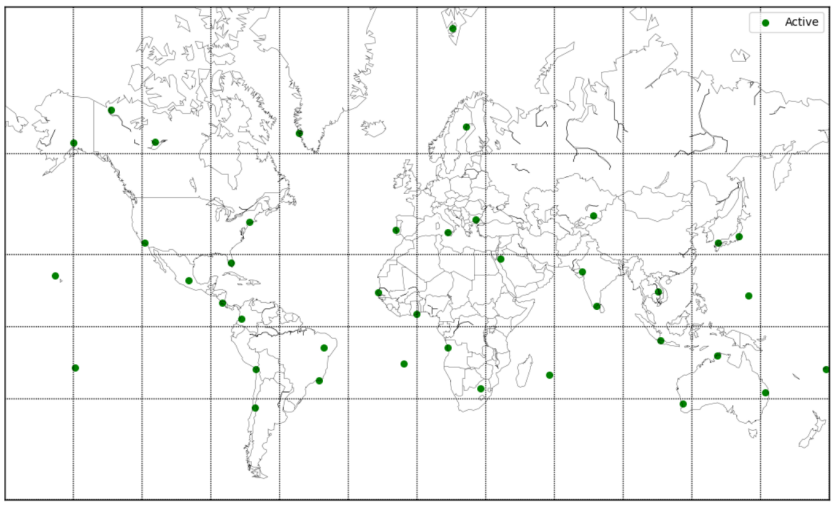

Figure 4.7: OneWeb Ground Station Locations

4.2.5. Modeling OneWeb

In many ways, the satellite network for OneWeb is similar to the Starlink model. The orbital information for the satellites are gathered from Celestrak, while the ground station locations are available in the form of crowd-sourced datasets. Figure 4.7 shows the distribution of 40 Oneweb ground stations around the world (As of August 2025). This distribution is sparser, but more evenly distributed globally compared to the Starlink ground stations.

OneWeb satellites have a few key differences compared to Starlink satellites. The orbital altitudes are 1200 km, resulting in a wider coverage area for both satellites and ground stations. Additionally, the operational OneWeb satellites do not use ISL connections, and rely on geographically distributed ground stations, which is evident when comparing Figure 4.7 and Figure 4.5. Starlink has many ground stations located in key regions such as North America and Europe, but also areas with few or no ground stations. With the exception of northern Asia, there are fewer OneWeb ground stations scattered evenly across the world.

Multiple OneWeb user terminals are available, with advertised download speed up to 195 Mbps. OneWeb user terminals are available in different form factors and designs, with some manufactured by third parties like Intellian. These range from portable phased array panels, parabolic dishes for fixed installations. Additionally, OneWeb are aimed at enterprise customers, and does not provide services to consumers. Within the simulation, a set of TLEs dated the 14th of April, 2025, is used. Additionally, for the maneuvering and recovery simulations, the OneWeb constellation is recreated mathematically using the parameters given in Table 4.2.

Altitude (km)	Inclination (°)	Number of Planes	Satellites per Plane	Total Satellites
1200	86.4	12	54	648

Table 4.2: Orbital data of OneWeb satellites

4.2.6. Modeling Amazon LEO

As of January 2026, Amazon LEO has launched over 100 operational satellites and aims to be a competitor to the Starlink network. This network was formerly known as 'Project Kuiper' until it was re-branded in November 2025. As such, many sources refer to this network by the Kuiper name. The satellites primarily operate at altitudes of 590, 610, and 630 km. As with OneWeb and Starlink, the orbital information of the operational satellites are available through Celestrak. The deployment of constellation is scheduled in multiple phases, with the first phase containing 578 satellites at an altitude of 630 km and an inclination of 51.9, this corresponds to the tracking data of the operational satellites. The original plan for the constellation proposed by Amazon LEO to the FCC in 2019 contained 1156 satellites in 34 orbital planes with 34 satellites in each plane at an altitude of 630 km with an inclination of 51.9 degrees. In 2024 and 2025, the constellation proposal was modified to only contain one to four satellites per orbital plane, with the 630 km orbits at 51.9 degree inclination containing 289 planes, each with four satellites [96]. With the orbital parameters known, a Walker-Delta constellation using the same orbital parameters allows for an approximation of the fully deployed satellite constellation. The 630 km orbits correspond to 51.9: 1156/289/f, where f is the relative spacing between adjacent planes. This constellation configuration is shown in Figure 4.8. Although the network is planned to be activated prior to the full deployment of the 1156 satellites, the analysis assumes that the initial Amazon LEO constellation contains the full shell of 1156 satellites.

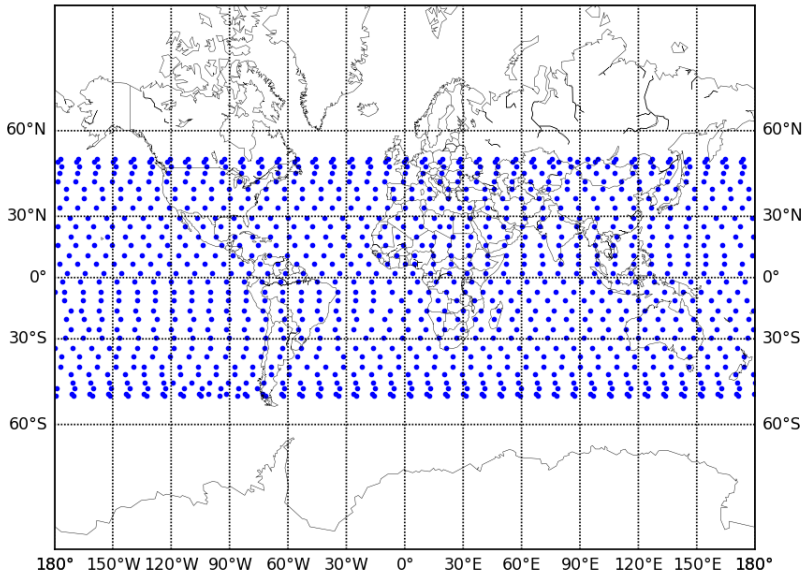

Figure 4.8: Visualization of possible distribution of planned Amazon LEO 51.9 degree satellites

In addition to the 51.9 degree satellites, four other orbital shells are included in the generation 1 proposal [96]. An overview of these orbits is given in Table 4.3. This indicates a total of 3232 planned satellites in the initial generation.

Instead of using the Skyfield library, the positions of the Walker-Delta constellation are computed using using Keplerian orbital elements. These consist of the the inclination, altitude, right ascension of the ascending node, and the true anomaly. Although the regulatory documentation provides information about the number of planes and satellites per plane, they do not indicate the offset between planes. As such, the offset is chosen such that satellites are evenly distributed within the shells, which is visualized in Figure 4.8. Note that the plan for the initial deployment of Amazon LEO has a limited latitude range

Altitude (km)	Inclination (°)	Number of Planes	Satellites per Plane	Total Satellites
590	30.0	1	2	2
590	33.0	782	1	782
610	42.0	1292	1	1292
630	51.9	289	4	1156

Table 4.3: Proposed satellite orbits in generation 1 of Amazon LEO

and doesn't cover the northern or southern regions of the world. An additional 1292 satellites located in three shells are planned to be deployed in high inclination orbits to serve these regions. Additionally, the constellation is planned to be expanded with the Generation 2 system in the future with an additional 3212 satellites located in three orbital shells. In total, recent regulatory documents indicate a total of 7736 satellites by the end of the deployment [96]. A possible configuration of all these satellites is shown in Figure 4.9. This shows that the polar regions have a lower density of satellites, similar to the distribution of satellites within the Starlink network.

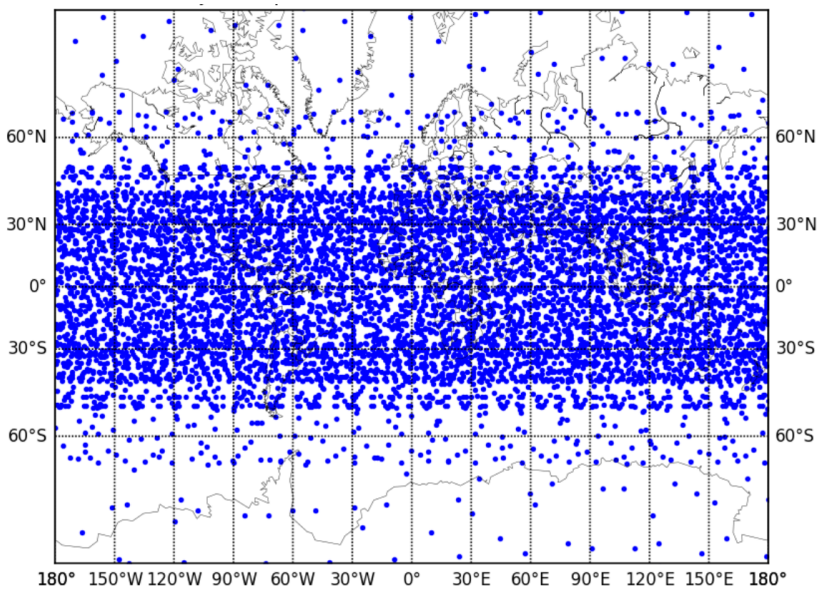

Figure 4.9: Visualization of all planned satellites for Project Kuiper, consisting of generations 1, generation 2, and polar satellites.

The AWS ground station network consists of geographically distributed ground stations which can be used as a service by satellite operators. As of mid 2025, the network lists 12 ground stations located around the world [97], but this may increase in the future as the capacity of the network grows. Due to the similar altitudes of Amazon LEO and Starlink satellites, their equivalent ground coverage areas are expected to be similar. The user terminals are planned to be available in both a compact 100 Mbps version, and a 400 Mbps version [98].

The Amazon LEO satellites are planned to use optical inter-satellite links, similar to Starlink satellites. Amazon has successfully tested 100 GBps links up to a distance of 1000 km [99]. Since Amazon LEO is expected to be deployed in multiple stages. This gives an opportunity to analyze how the different stages of the deployment affects the performance and resilience of the network.

4.3. Modeling Space and Terrestrial Disruptions

The goal of many satellite internet constellations is to provide increased internet access to more regions of the world, but as described in chapter 3, satellite networks can still be susceptible to various types of disruptions, such as space weather events, natural system degradation, natural or man-made disasters

impacting the ground station, targeted attacks to satellites, and more. Some of the disasters scenarios are localized to a region, while others have the possibility of extending to a wider-reaching area. In this section, the approach to simulating the different types of disruption events is discussed.

4.3.1. Disruption Events

A disruption to the satellite network can be modeled as one or more nodes being taken offline for some duration. This can either be the result of a targeted attack, or an unintentional outage. In the simulation, a generic disaster method is defined, which is able to pick which satellites or ground stations are disabled. These can be based on finding all nodes within a region, or targeting of individual nodes. The following describes how the different types of disruption scenarios are applied in the simulation.

Space weather events: Space weather disruptions are modeled as disruption areas in space. These may span over a wide region in which satellites are disabled in the simulation. Space weather events can have a specific start time, and can either be one-off or continuous disruptions to the satellites. For a continuous disruption, satellites entering the region are disabled following the initiation time of the event. Within the simulation, a baseline space disruption event consists of a defined circular area in space, in which satellites are disabled at a certain timestep. In the subsequent propagation of the constellation, the satellites remain disabled.

Natural disasters: Terrestrial disruptions can damage critical ground stations. Additionally, ground stations are connected to PoPs. This means that a natural or man-made disaster affecting a PoP can result in disruptions in multiple ground stations. This, however, did not affect the case studies due to the proximity of the PoPs to the ground stations within the affected region. Some areas are prone to earthquakes, while other areas may experience hurricanes or other extreme weather events, which can all be described in terms of a disaster area in which terrestrial infrastructure becomes in-operational.

The Global Earthquake Impact Database (GEID) contains a number of earthquake scenarios based on historical events. One example is the 1960 earthquake in Chile, the most powerful earthquake on record. This earthquake had an estimated magnitude of 9.4-9.6 and resulted in significant damage to the region. Using historical data, the impact of a similar earthquake on the ground station infrastructure can be estimated. For the analysis of a specific earthquake scenario, an impact region is defined based on the earthquake impact region from the GEID dataset. The infrastructure within this region is then disrupted in the simulated scenario.

The 1960 Chile earthquake is used as a disaster scenario for a natural disaster. Shown in Figure 4.10a is the polygon used to model the disaster area of the 1960 Earthquake. The region corresponds to a peak ground acceleration exceeding 0.3 g based on the GEID entry.

Power outages: In order to model a power outage, it is assumed that a geographical region loses access to electricity. As a result, the ground stations within the blackout region become inactive. Similar to the natural disasters, a total power outage is modeled as a region or polygon of disrupted service.

On the 28th of April, 2025, a large-scale power outage impacted the Iberian Peninsula, resulting in blackouts across Spain and Portugal. As a result, communication and internet connectivity was severely disrupted in the region, with internet traffic dropping to 17% of the expected usage. The 2025 power outage in the Iberian Peninsula is used as a disaster scenario in order to compare the effects of a recent large-scale blackout on various types of internet networks. Shown in Figure 4.10b is the disruption region polygon created based on the 2025 Iberian blackout.

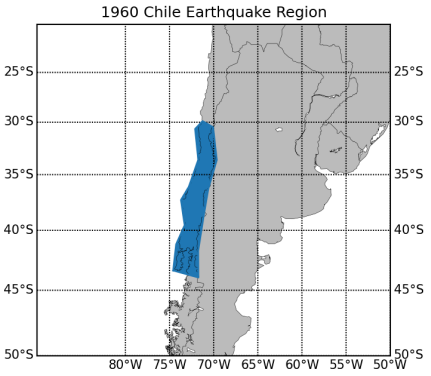

(a) Impact polygon for the 1960 Chile earthquake

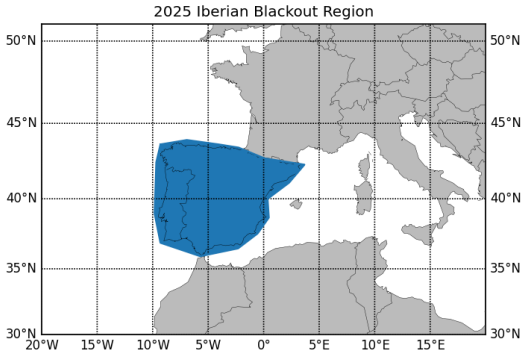

(b) Impact polygon for 2025 Iberian blackout

Figure 4.10: Disaster regions

4.3.2. Targeted Disruptions

The infrastructure can be susceptible to damage from targeted attacks. The purposes of this analysis is to identify whether a hostile actor could use targeted attacks in order to cause disruptions to the satellite network. Within the simulation framework, this is achieved by determining the most important satellites through centrality measures, which are then attacked. By comparing the effect of targeted attacks between different satellite networks, their relative resilience can be compared. This has a key limitation, since it only considers the structural aspects of the networks, but allows for comparisons between different constellation types without a packet-level simulation.

The relative importance of satellites operating within an ISL network depends on both the instantaneous orbital configuration, but also how the satellite constellation evolves over time. As a result, the importance of a satellite at any point in time might not be representative of the importance over a specific period of time. This necessitates an analysis that also considers changes over time.

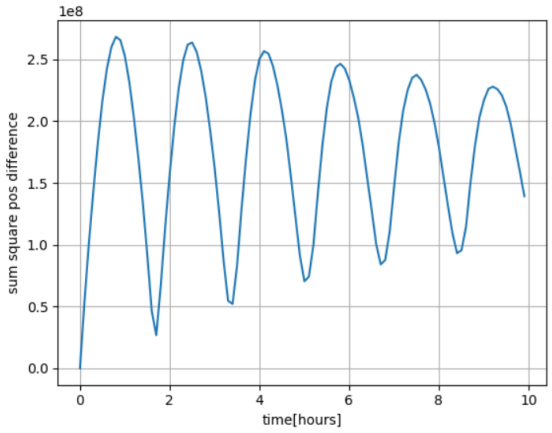

(a) The square of squares difference in satellite positions over time compared to the initial constellation shape

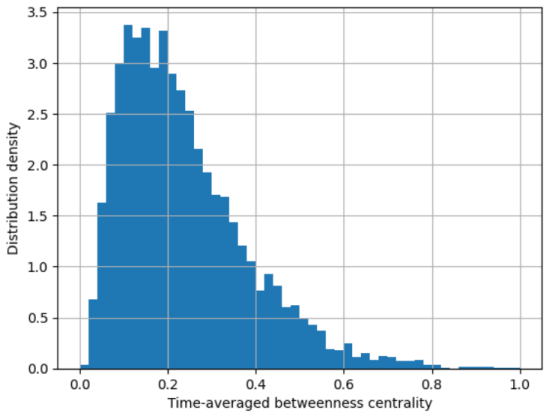

(b) Histogram showing the time-averaged centrality distribution of the Starlink ISL network

Figure 4.11: Analysis of the properties of the Starlink ISL network

A useful analysis interval should cover a period of time representative of the operational importance of a satellite. When considering the ISL network by itself without ground stations, the arrangement of satellite links are determined by their relative positions as a result of their orbital characteristics. These

relative positions evolve over time, but may repeat for regular orbits. In order to determine a suitable analysis interval, the relative positions of the Starlink satellites and the inter satellite connections are plotted over time as shown in Figure 4.11a. These reveal that the positions converge approximate every 95 minutes, or one orbit, and that inter satellite connections become more similar every half orbit. The same trend is found with the other considered satellite constellations, if the orbital periods of the shells are similar. Extending the time interval reveals that the relative satellite positions deviate over time. This is a result of the satellites orbiting at different altitudes, resulting in different orbital period.

Based on the interval after which the constellation becomes self-similar, the betweenness centrality of each satellite is taken to be the average across multiple samples taken within an interval of one nominal orbit. The approach of averaging the static betweenness centralities using snapshots across a time interval which gives similar results to temporal betweenness for datasets for which the temporal evolution has a smaller influence on network routing. This assumes that satellites can only forward packages using the ISL connections present at any snapshot, and cannot store packages for future ISL connections. This assumption is justified by the package routing latencies being two order of magnitude lower than the network reconfiguration intervals (this is 15 seconds for Starlink). The results of averaging the centrality measures are then used to target high priority satellites. Figure 4.11b shows a histogram of the normalized result of the normalized and time-averaged betweenness centrality for the Starlink ISL network. By targeting and taking down satellites, the level of performance degradation can be found as a function of how many satellites are attacked.

5

Results

This chapter contains the results of the resilience analysis of the different network providers and variants. An initial base resiliency analysis is conducted in order to determine the overall network without a specific disruption scenario. This is followed by the analysis of the impact of both terrestrial and space-based disaster scenarios for the purpose of a comparative analysis between the different network providers.

Section 5.1 gives an overview of the case studies to be considered, section 5.2 presents and discusses the results from the targeted space attack scenario, section 5.3 presents the results from the terrestrial disruption scenarios, and section 5.4 contains an analysis of the satellite maneuvering and recovery process. This is extended in section 5.5, where the results from a regional space disruption and subsequent recovery are discussed. Finally, section 5.6 discusses some of the key findings from the results, and provides some additional insight into how the services differ from a user-centric perspective.

5.1. Case studies

As discussed in the previous chapter, a number of specific networks and scenarios will be analyzed through a series of case studies. The networks being analyzed are Starlink, OneWeb, and Amazon LEO. Due to their current deployment status, Starlink and OneWeb are primarily analyzed based on tracking data, while the Amazon LEO constellation is based on the planned constellation parameters discussed in subsection 4.2.6. Considering the different operational phases of Amazon LEO allows for a comparison of how different stages in an emerging constellation contribute to the overall resilience of a satellite network. For Starlink and OneWeb, the tracking data is dated to 14th of April 2025, which serves as the starting point of the simulations. The Starlink dataset contains 7199 satellites, while the OneWeb dataset contains 651 satellites. Although the OneWeb constellation does not use ISLs, a modified simulated network assuming the use of ISLs is added in order to investigate how it affects the results. This results in six LEO satellite networks that form the basis of the results in this chapter. An overview of the overall parameters of these networks are given in Table 5.1.

Each of the networks will be subjected to four different case studies in order to investigate how they are impacted by disruptive scenarios. The first is an artificial attack scenario to investigate how the network performance degrades as satellites are removed, the satellites are attacked based on a relative importance measured by the centrality metric, while the latency, coverage, and hops are measured. The next two case studies investigate the regional impact of a terrestrial outage event, namely the 2025 Iberian Peninsula electrical blackout, and the 1960 Valdivia Earthquake in Chile as described in subsection 4.3.1. The regional impact on coverage and capacity are investigated. A final case study

investigates how a regional disruption in space affects performance, highlighting how the dynamic nature of the network may influence geographically distant regions, and how maneuvering can be applied as a response to satellite outages.

Name	ISLs?	Date	Satellites	Altitude [km]	Est. period [min]
Starlink	yes	April 2025	7199	530-580	95
OneWeb	no	April 2025	651	1200	109
OneWeb w/ISLs	yes	April 2025	651	1200	109
Amazon LEO Initial	yes	TBD	1156	590-630	97
Amazon LEO Gen 1	yes	TBD	3232	590-630	97
Amazon LEO Full	yes	TBD	7736	590-630	97

Table 5.1: Networks and variations to be analyzed

5.2. Targeted Space Attacks

The first scenario considers the impact of the attack ratio on the operation of a satellite network. The attack ratio is defined as the percentage of satellites taken offline using centrality-based targeting compared to the initial number of satellites. The impact on the operational performance of the satellite if subsequently plotted for analysis. For Starlink and Amazon LEO, a 95 minute analysis interval is used. For the OneWeb network, the measurements are determined over an interval of 109 minutes, corresponding to the orbital period of the higher altitudes satellites. Two different variants of the OneWeb network are considered. One is a hypothetical network using the OneWeb satellites, if they had the capability of using ISL links similar to Starlink, while the other is the baseline OneWeb network without the capability of inter-satellite communications.

Using the targeting based on betweenness centrality, the performance of the network is determined for multiple attack ratios, with the resulting graph shown in Figure 5.1a.

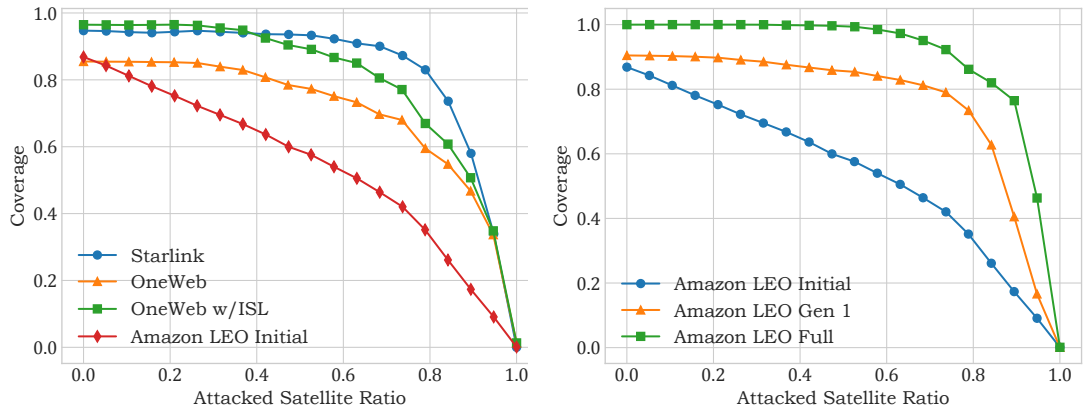

(a) Results for Starlink, OneWeb, Amazon LEO

(b) Results for different stages of Amazon LEO

Figure 5.1: Satellite coverage vs attack ratio

This comparison shows that both Starlink and OneWeb have a wide geographical coverage of more than 80% of terrestrial regions in normal operation, while the 51.9 degree shell of Amazon LEO has a lower coverage.

An additional comparison is made for the various projected phases of the Amazon LEO constellation as shown in Figure 5.1b. This comparison of the future evolution of the network illustrates how the deployment of additional satellites affects both the coverage resiliency and the initial coverage. When more satellites are added between the initial operational constellation and the entire generation 1 constella-

tion, the initial coverage remains the same, but it is significantly more resilient against partial outages. When additional polar satellites are added in the full constellation, the initial coverage is increased, with some effect on the coverage resiliency.

For each of the test cases, a total of 100 evenly spaced samples are taken across an entire orbital cycle of the constellation. In line plots, the average across the 100 samples are plotted. Additionally, box-plots reveal the spread of the metrics across the duration of the orbit. These are shown in Figure 5.2 and Figure 5.3. The height of the box-plots indicate that the coverage deviation increases as fewer satellites are present in the constellation. Based on these results, some observations can be made regarding how the constellation parameters affect the resilience against large-scale distributed satellite outages. As the number of satellites within the network increases, more satellites must be taken offline to disrupt the global coverage. This is due to the increased coverage redundancy, since more alternative satellites are able to serve the same geographical regions on the ground. The effect of ISL connections is also apparent when comparing the difference between the simulated OneWeb variants in Figure 5.3. With the addition of ISL connectivity, the baseline coverage increases from approximately 0.85 to 0.95. This illustrates that some terrestrial areas are not covered by the current distribution of ground stations, despite being being in view of the satellites. The addition of ISL connections increases the level of coverage throughout the entire disruption scenario as shown in Figure 5.1a.

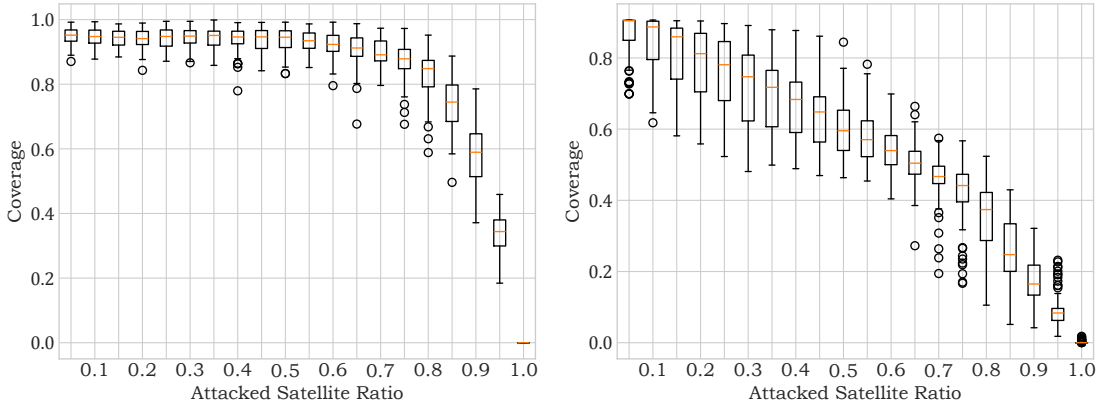

(a) Coverage box-plot for Starlink

(b) Coverage box-plot for Amazon LEO Initial

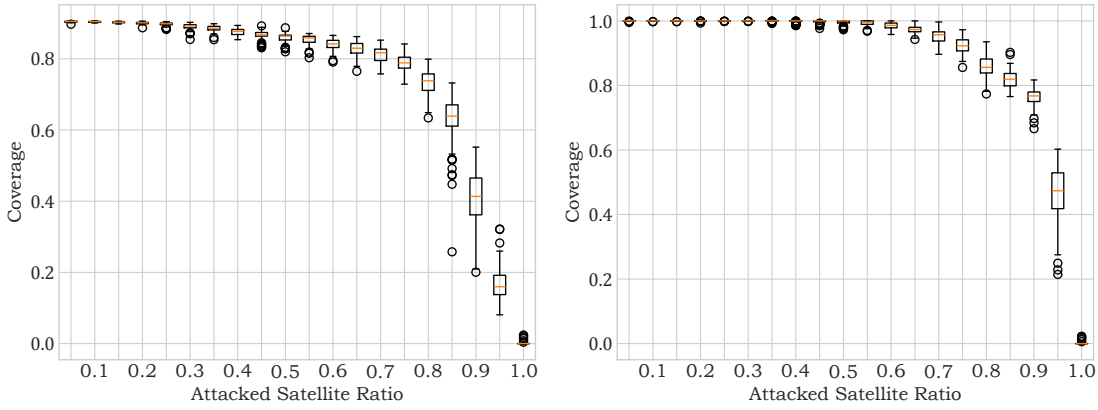

(c) Coverage box-plot for Amazon LEO Gen 1

(d) Coverage box-plot for Amazon LEO Full

Figure 5.2: Box-plots of satellite coverage vs attack ratio for Starlink and Amazon LEO

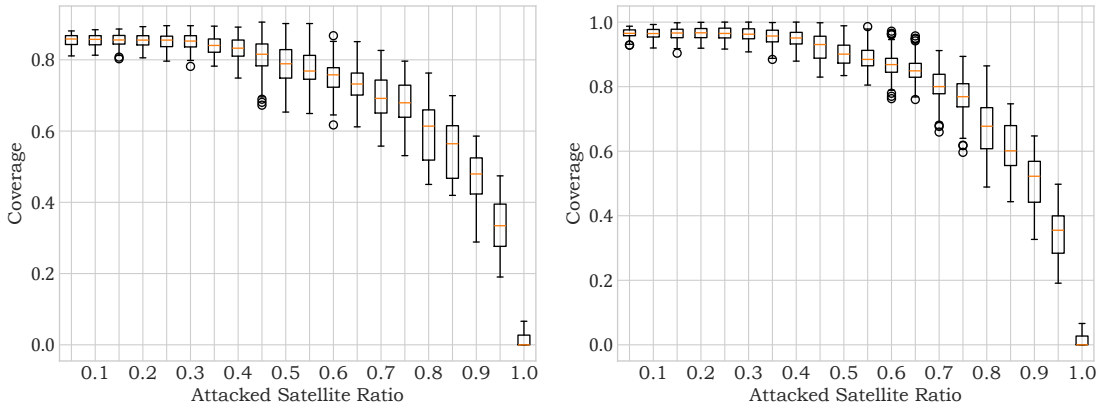

(a) Coverage box-plot for OneWeb

(b) Coverage box-plot for OneWeb with ISLs

Figure 5.3: Box-plots of satellite coverage vs attack ratio for OneWeb

5.2.1. Effect on Latency and Hops

In order to compare the latencies between the different systems, the physical propagation latency is considered. This is due to the lack of information about the processing and queuing delays on the satellites. Since this latency depends on the total path, it is highly dependent on the altitude of the orbiting satellites and the path through the ISL network. The mean latency of the connected regions are shown in Figure 5.4a. This indicates that the latencies derived from the signal propagation delay and excluding processing delays are in the range of 10-20 ms for Starlink, OneWeb, and Amazon LEO. As the number of operational satellites decrease, the latency change as a result of fewer satellites being available for connections. The simulated latencies need to be considered in combination with the coverage results, since the mean values are calculated based on regions within the coverage area. For instance, the Amazon LEO latency appears to decrease with fewer satellites, however, this is due to the loss of coverage in regions far from ground stations.

The OneWeb and Amazon LEO ground station networks have a wide geographical distribution, while the Starlink ground station are more clustered, resulting in changes in the latency of the connected regions when the number of satellites decrease.

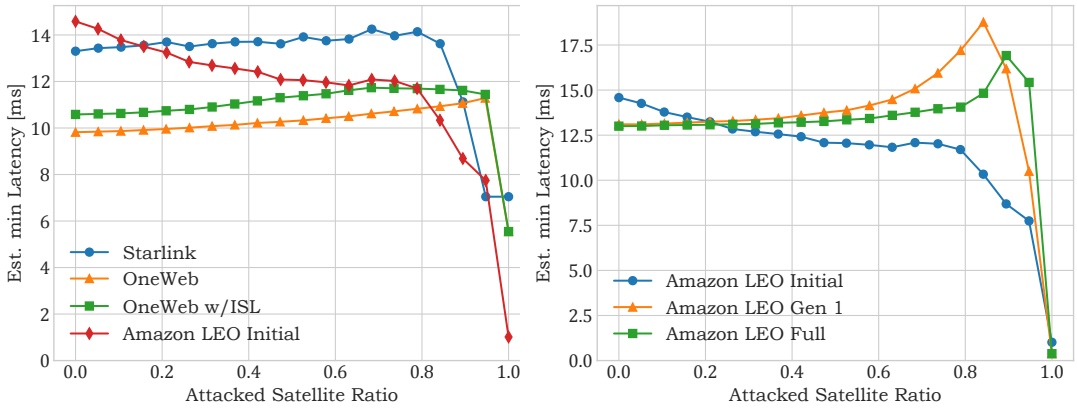

(a) Latencies for Starlink, OneWeb, and Amazon LEO based on shortest-path routing

(b) Latencies for different stages of Amazon LEO

Figure 5.4: Estimated mean propagation latencies vs attack ratio based on shortest-path routing

Similar to Figure 5.1b, the latency comparison of the various stages of the Amazon LEO constellation is shown in Figure 5.4b. This shows that the physical link latency of the connected regions is to an extent affected by the constellation deployment. The initial average latency remains constant, but when larger number of satellites are available for ISL connections after a disruption, the average latency increases. When considered in combination with the coverage graphs, it shows that the more densely connected network is better at remaining connected, but may rely on ISL connections for reaching remote regions where nearby ground stations are unavailable.

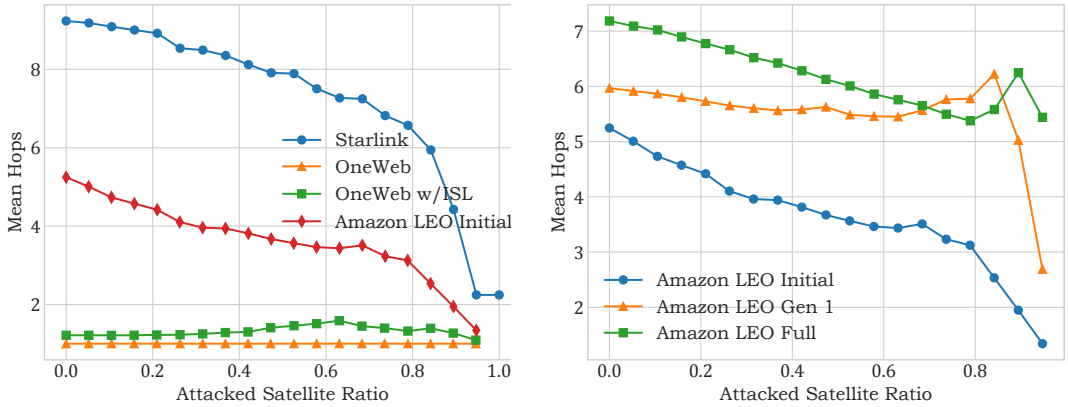

(a) Mean number of hops for Starlink, OneWeb, and Amazon LEO (b) Mean number of hops for stages of Amazon LEO

Figure 5.5: Average hops vs attack ratio

Another aspect to the latency effect is the effect on the average number of hops. With certain satellites are taken offline, it becomes more difficult to form a path through the ISL network between a cell and a ground station. The average hops as the network degrades is shown in Figure 5.5. This illustrates that the average hops, similar to the latency, is highly dependent on the state of the network. Since disrupting satellites leads to the inability of forming longer-distance connections, the average number of hops in the connected region of the world tends to decrease, as fewer satellites are present.

5.3. Ground Disruptions

While evaluating the effect of ground disruptions on the operation of the satellite network, a region of interest is defined around the disaster region in order to determine both the local and global impact on the network performance. In this section, the results of the simulations for the 1960 Chile Earthquake and the 2025 Iberian Blackout are discussed. Each of the scenarios will be evaluated in order to determine both the total estimated capacity and the change in capacity within a region. For the capacity estimates, it is assumed that the regional user density is the same as the population density. Additionally, it is assumed that each Starlink user corresponds to the population with a ratio of 1:20000 (including oversubscription ratio). Each satellite with a direct or indirect connection to a ground station is given a capacity of 960 users, each with a required capacity of 100 Mbps. Note that the primary metric is the relative difference before and after an outage as opposed to the absolute estimated number of users. Comparisons showed that the ratio is not sensitive to changes in the assumed user ratio. The population density map is derived from the 2023 Kontur population density dataset with a granularity of 22 km [91], corresponding to the H3 hexagonal grid with a resolution of 4.

5.3.1. 1960 Chile Earthquake

As described in section 4.3, the 1960 Chile earthquake is used as an analysis scenario. Starlink has five ground stations and one PoP located within this impact region, while OneWeb has just one ground station and one PoP. The Amazon ground station network used by Amazon LEO does not contain ground stations in this region, but does have a location in the south of Chile in Punta Arenas. The locations of the AWS service areas give indications for potential locations of future ground stations, while Chile being a new region in 2026. Additionally, 2022 reports indicate that ground stations will be built in Longovilo, which is within the 1960 Chile Earthquake disaster area. In order to allow for a direct comparison on the impact between the different networks, this hypothetical ground station is added in the disruption analysis.

Figure 5.6 shows the effect of such a disruption on the regional latency with the Starlink network. With the nearby ground stations unavailable, the local latency increases as further ground stations are used. As the local ground stations become unavailable, the propagation latency increases as alternative ground stations must be used.

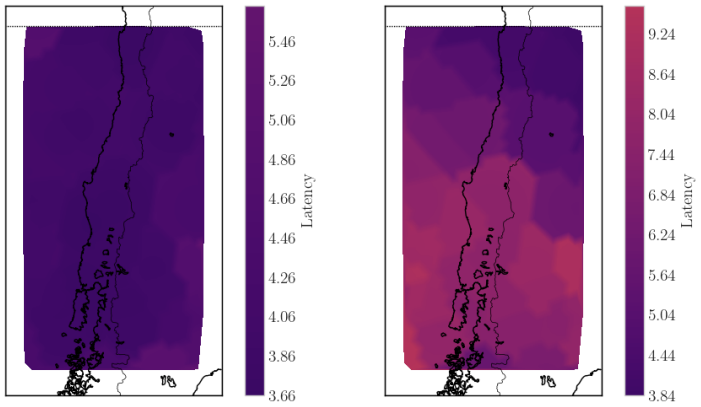

(a) Before outage (b) After outage

Figure 5.6: The regional propagation latency of Starlink during the Chile earthquake scenario

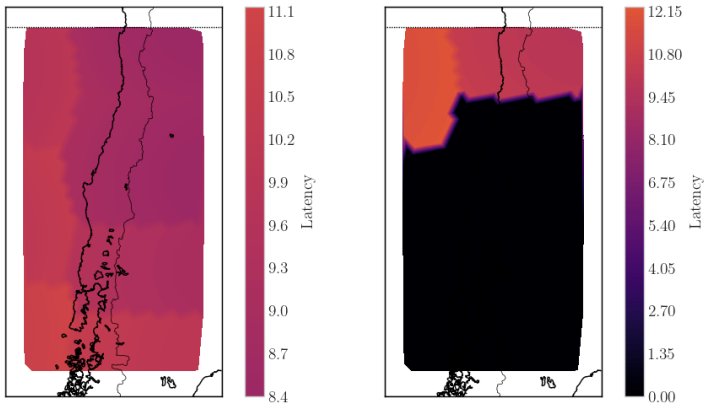

(a) Before outage (b) After outage

Figure 5.7: The regional propagation latency of OneWeb during the Chile earthquake scenario. Black areas indicate regions with no coverage.

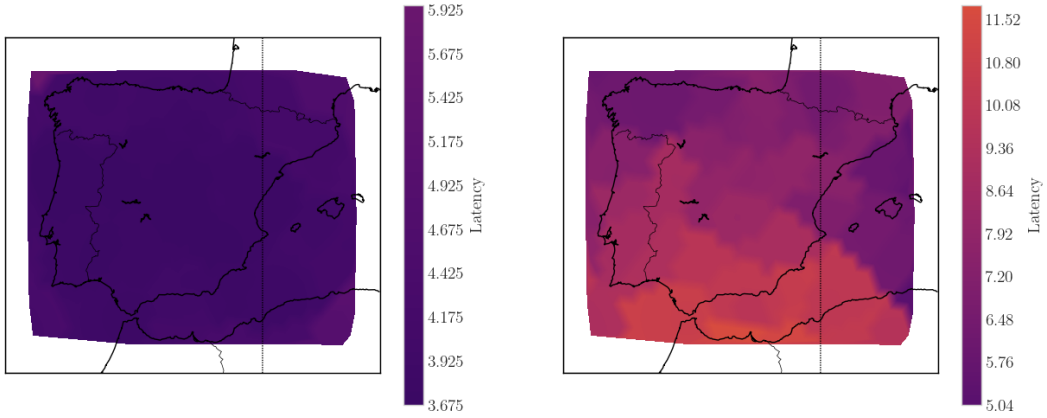

(a) Before outage (b) After outage

Figure 5.8: The effect of the Iberian blackout on the regional latency for Starlink

An overview of the key results from the disruption scenario is shown Table 5.2. The values show that both the capacity and coverage remains identical for the networks with ISL connectivity, while the capacity and coverage is significantly lowered within the OneWeb network without ISL connections. Additionally, the mean latency within the analysis area is increased in every scenario, with the ISL-enabled networks suffering an a larger latency increase compared to OneWeb without ISLs. Regions retaining OneWeb connectivity still use a single satellite with a direct ground station connection, which explains the smaller change in latency compared to the other networks. The heatmaps showing the regional latencies and capacities for every network can be found in Appendix B. These results indicate that the OneWeb ground station located in Chile is critical for service in the region, and constitutes a single point of failure for regional OneWeb users. If this ground station is taken offline, a the majority of the analysis region loses coverage as shown in Figure 5.7.

Network	Capacity ratio	Coverage ratio	Latency ratio
Starlink	1	1	1.67
OneWeb	0.67	0.243	1.15
OneWeb w/ISLs	1	1	1.48
Amazon LEO Initial	1	1	2.177
Amazon LEO Gen 1	1	1	2.70
Amazon LEO full	1	1	4.06759

Table 5.2: Overview of normalized effects of the Chile earthquake scenario

5.3.2. 2025 Iberian Peninsula Blackout

The impact region of the 2025 Iberian blackout contains 4 Starlink ground stations and 1 PoP used by Starlink. The same region contains a single OneWeb ground station. As of the end of 2025, Amazon has deployed a new ground station in Santander within the blackout region [100]. An Amazon LEO ground station is thus placed here for the disruption simulation.

These results mirror the Chile earthquake scenario. They indicate that a network with ISL connections suffering a localized disruption to the ground sector results in an increased latency in the disrupted region, due to signal having to take a longer path to reach a ground station. With enough ISL connections, this does not have a significant effect on the coverage area. For a network without ISL connections, the faults in the ground sector result in regions without connectivity, however the connected regions retain a consistent ground-to-ground connection latency. This effect is illustrated for the Starlink scenario in Figure 5.8, with the regional ground station outages resulting in an increased latency within the region.

The effect on the relative service capacity within the region are also analyzed. This is the reduction in the network capacity within the vicinity of the disruption region, and depends on the ability for the network to fall back on alternative ground stations. The heatmaps on Figure 5.9 show the effect of the Iberian blackout on the distributed capacity of the OneWeb network. The heatmap shows that high density regions can be affected, since insufficient capacity is available to serve the entire population of users.

Similarly, the effect of the regional disruptions for Amazon LEO with ISL is analyzed, indicating that the capacity and coverage remains unchanged, with an increase in regional latency for each variant of the constellations of approximately 1.8 to 2. The difference in the effect between the constellations with and without ISL connections indicate that inter-satellite connectivity has a significant impact of regional ground-based disasters. This is a result of the ability for satellites to switch ground stations in the event of a regional disruption. An overview of the results from the disruption scenario is shown Table 5.3 and the heatmaps for every evaluated network can be found in Appendix B.

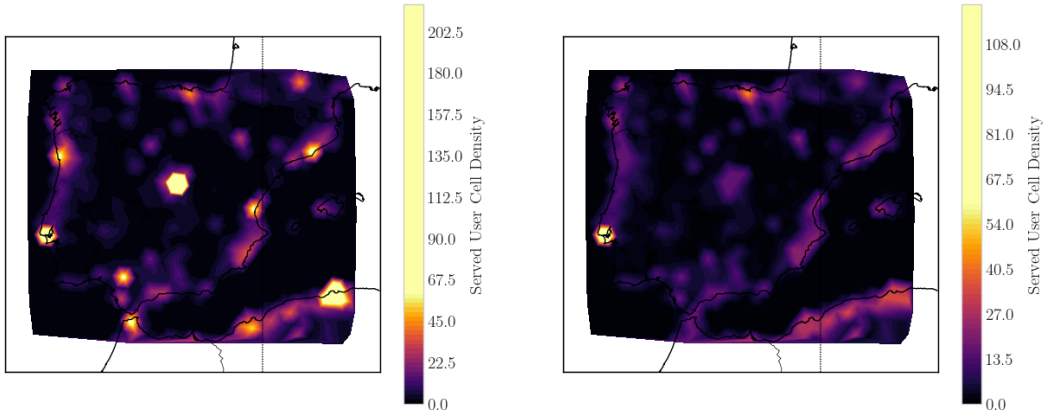

(a) Before outage (b) After outage

Figure 5.9: The effect of the Iberian blackout on OneWeb cell capacity showing regions with higher user densities.

Network	Capacity ratio	Coverage ratio	Latency ratio
Starlink	1	1	2.07
OneWeb	0.796	0.881	1.25
OneWeb w/ISLs	1	1	1.27
Amazon LEO Initial	1	1	1.79
Amazon LEO Gen 1	1	1	1.95
Amazon LEO full	1	1	1.84

Table 5.3: Overview of normalized effects of the Iberian Peninsula blackout scenario. The ratios are the metric after the disruption compared to the initial value.

5.4. Space Disruptions and Recovery

Up to this point, the main consideration has been disruptions to components of a satellite network and their subsequent service impact rather than the recovery process. In this section, the possibility for a satellite network to restore operation is explored by analyzing how the Starlink, Amazon LEO, and OneWeb networks are able to adapt in response to an outage scenario. This analysis focuses on the recovery from disasters impacting the satellites rather than the terrestrial infrastructure.

5.4.1. Deployment of New Satellites

Due to the regular launches and operational data of Starlink satellites, it is possible to estimate the period of time necessary for new Starlink satellites to replace the damaged ones. This assumes that all new satellites deployed after an outage event are used to replace the nonfunctional satellites. Additionally, this analysis will focus on the satellites in the 53 and 43 degree orbits described in subsection 4.2.4 rather than the polar orbits. The v2 mini satellites that are actively being deployed in 2025 are launches in groups of 28 satellites. This, however, is insufficient to determine the full recovery rate. Once the satellites are deployed in orbit, they are grouped in a cluster and must maneuver and raise their orbits to the final locations. This process can take over a month, which limits the rate at which a disruption can be repaired. Shown in Figure 5.10a is an example of the orbit-raising process of a newly launched Starlink satellite, which took approximately 45 days to reach its final orbit [36]. Figure 5.10b shows the aggregated post-launch behavior of 120 Starlink satellites, showing that the fastest satellite can reach their target orbit in 10-20 days after launch. Using new launches in order to replace satellites would be subject to this delay.

Another consideration is the affected orbital plane. Based on historical data, each launch targets a specific orbital plane (and in rare cases, two orbital planes at different altitudes), with the satellites being capable of shifting their phase within the plane. Assuming the same approach is used for a recovery process, multiple launches would be required to replace non-operational satellites in multiple planes.

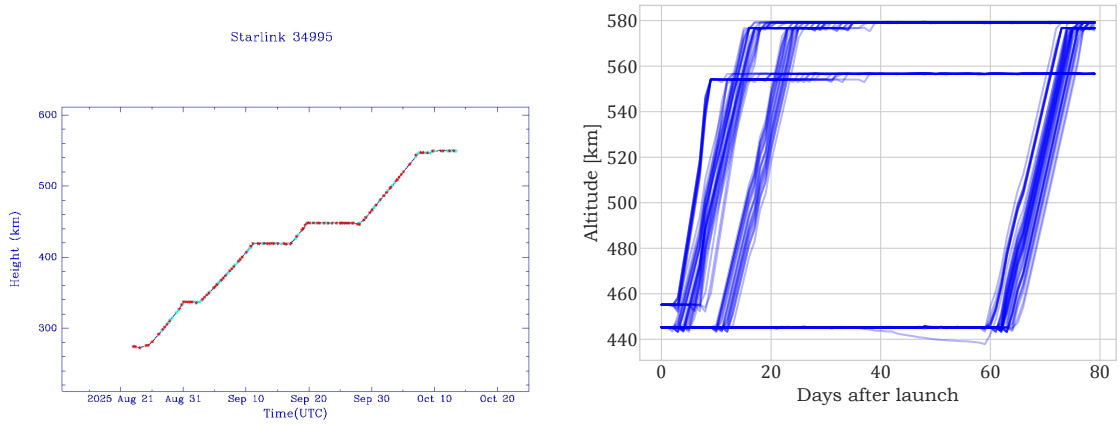

(a) Orbit-raising of a Starlink satellite [101].

(b) Aggregated post-launch altitudes of 120 Starlink satellites launched in 2025

Figure 5.10: Starlink post-launch orbit-raising

5.4.2. Redistribution of Satellites

One alternative to launching new replacement satellites is to maneuver existing orbital satellites in order to cover the disrupted regions. Existing satellites in the same orbital plane can maneuver themselves to replace damaged satellites. Satellites in front and behind damaged satellites can shift their phase, which reduces the recovery time compared to launching new satellites. The required time for a phase shift depends on the available propellant that can be consumed by the maneuver, however, the shortest possible maneuver can be considered in order to model a rapid effort to restore disrupted service. This can be derived based on orbital maneuver data for satellites of interest.

Studies of the Starlink orbital data indicate the frequent use of maneuvering for collision avoidance, which is indicated by growing discrepancies between the orbital prediction and the satellite positions over time. Position predictions of V2 mini satellites can have errors of tens of kilometers as a result [102]. These discrepancies have been used to detect orbital maneuvers, revealing that Starlink satel-

lites occasionally maneuver between different orbital shells [19]. While the thrusters are active during the initial orbit-raising seen in Figure 5.10a, the climb rate is approximately constant. This can be used to estimate the minimum required time for a phase shift maneuver. The final orbit-raising maneuver lasted for 9 days, and raised the orbit from 452 to 550 km, or approximately 10.9 km per day. Analyzing a set of 120 recently launched satellites (Figure 5.10b) shows that the orbit-raising speed generally falls in the range 10.4 ± 0.6 km/day. This information can be used in order to estimate the maneuvering capabilities of the satellite within the orbit. Since higher orbits have longer orbital periods, a satellite can shift its phase by temporarily changing its orbit as described in subsection 2.1.4. By simulating the relative phase difference when maneuvering up and down within a time period, an approximate lower bound for the maneuvering speed is found. The estimate indicates that any Starlink satellite within an orbital plane is capable of being positioned at any other point on the plane in approximately 8 days, which is lower than the required time for deploying new satellites into orbit. If a small portion of an orbital plane needs to be replaced, the smaller phase shift allows for a replacement time of less than 8 days.

A similar analysis can be done using the available data for Amazon LEO satellites. Evaluating the orbital changes of an Amazon LEO satellites, Kuiper-00105 gives an estimated orbit changing speed of 2.77 ± 0.16 km per day. Amazon LEO satellites are generally launched to altitudes closer to their operating altitude, and the slower orbit raising indicates a lower thrust during maneuvering. The orbital history of the satellites from the Amazon LEO KF-2 launch are shown in Figure 5.11, indicating a relatively constant rate of orbit raising across different satellites within the group. Comparing the rate at which Amazon LEO and Starlink satellites are able to change their phase shows that Starlink can maneuver approximately three times faster than Amazon LEO, assuming the same rate of orbit change is used for both maneuvering and initial orbit-raising.

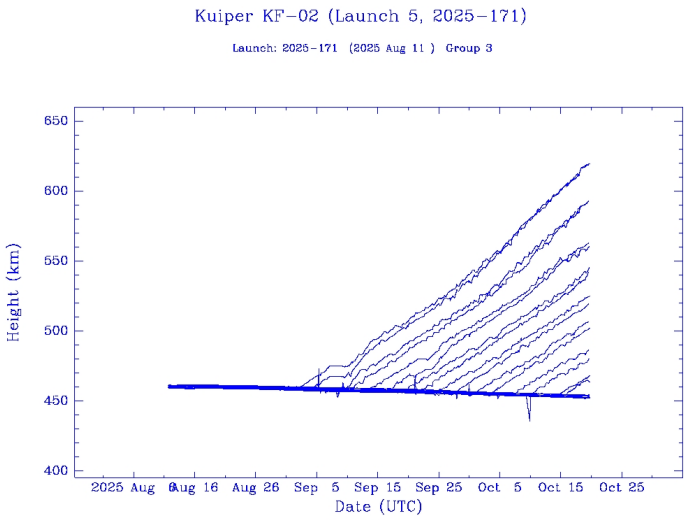

Figure 5.11: Orbit-raising of an Amazon LEO satellites from the KF-2 launch in 2025 [40].

Conducting a similar analysis for the orbit-raising phase of OneWeb satellites show an orbit-raising speed of 6.7 ± 0.4 km/day. The target orbit of OneWeb satellites are at 1200 km, which has a slight influence on the effect on the orbital period. The estimated phase shifts for Starlink, OneWeb, and Amazon LEO satellites over time are shown in Figure 5.12a. This assuming the thrusters are burning continuously during the phase shift in order to raise and lower the orbits. The comparison indicates that Starlink satellites have the highest orbital mobility, followed by OneWeb and Amazon LEO. Additionally, it shows that the satellites are capable of significant position shifts within the orbital plane in less than 10 days. By inverting this data, it is also possible to determine how long it would take for a satellite to shift some amount relative to the surrounding satellites, as measured by the projected ground distance. This is illustrated in Figure 5.12b. If a region of satellites with a certain radius is taken offline, this indicates how quickly the surrounding satellites would be able to shift by that radius. For a distance of 2000 km, this is approximately 2 days for Starlink, 3 days for OneWeb, and 5 days for Amazon LEO. This will be

further expanded in the maneuvering analysis for a full constellation.

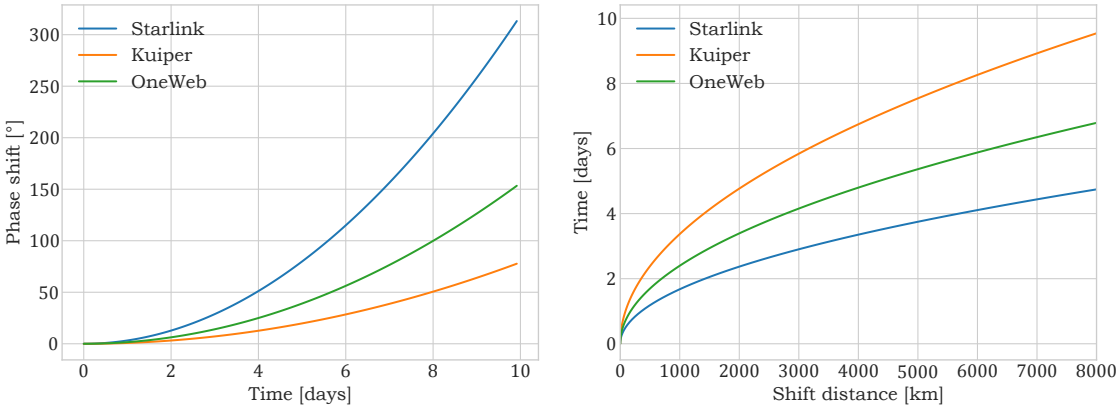

(a) Estimated fastest phase shift of different satellite types

(b) Estimated shift distance of different satellites

Figure 5.12: Estimated maneuvering capabilities of satellites

An additional consideration is how quickly a satellite network is capable of recovering the density when a part of the satellite network is disrupted. Figure 5.13 shows how a region of satellites are disabled within the orbit. Note that only half the the orbit is shown here, and that the other half can be assumed to be mirrored on the x-axis.

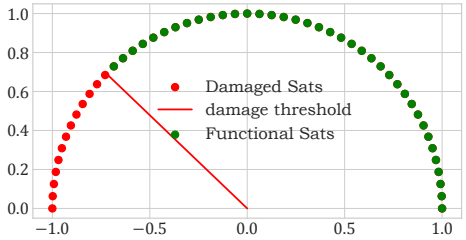

Figure 5.13: illustration of disabled satellites within an orbital plane

Figure 5.14 shows the recovery of the local satellite density of a Starlink and Amazon LEO plane as a result of a localized plane disruption. Satellites within a region covering a phase angle of 90 degrees are disabled, and the remaining satellites are maneuvered to be equally distributed over the entire plane. This shows that the Starlink constellation is capable of fully covering up the area in under 4 days, while Amazon LEO is capable of doing so in approximately 7 days. These plots are related to the resilience triangle, and will be further extended to consider the entire constellation.

5.5. Space Disruptions and Resilience Triangle

In this section, the results from the analysis of the space disruptions are presented. Figure 5.15 shows an example of how a cluster of satellites modeled as damaged is propagated over time. It can be seen that the initial disruption is localized, but the satellites scatter. The damaged cluster converge every half orbit, migrating westward. This results in a periodic capacity decrease around the world. Similar latitudes in each hemisphere are most affected. The westward motion is due to the relative position of

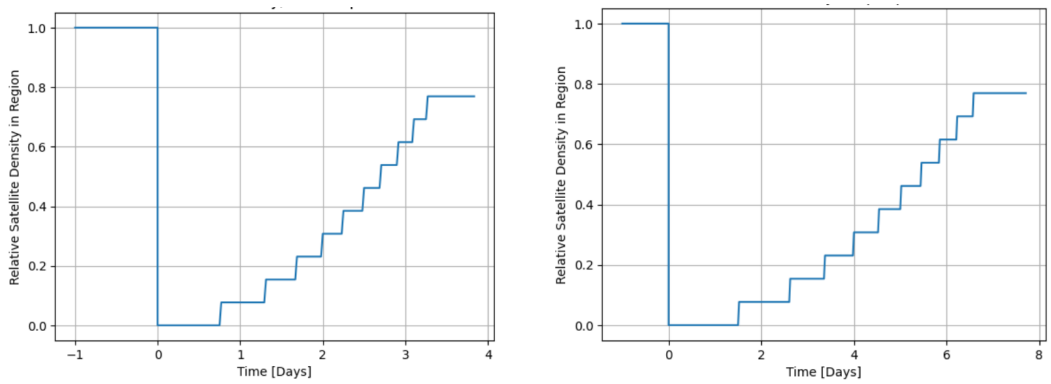

(a) Recovery of satellite density within a Starlink plane

(b) Recovery of satellite density within an Amazon LEO plane

Figure 5.14: Estimated recovery of satellite density

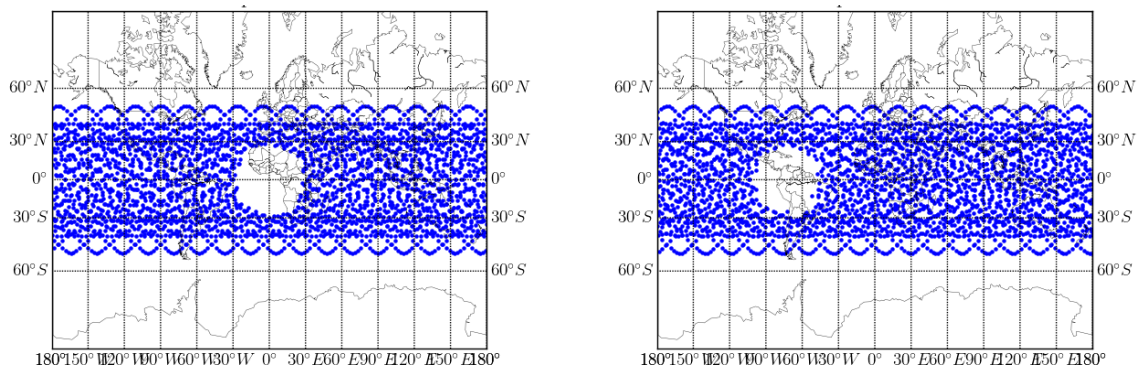

(a) A snapshot of the constellation after the simulation disruption

(b) A snapshot of the constellation after three orbital periods

Figure 5.15: Propagation of a satellite cluster over time for Amazon LEO (generation 1)

the satellites as the Earth rotates. After each orbit, the change in longitude corresponds approximately to the ratio between one orbital period and one sidereal day. Due to this orbital propagation, the effect of a disaster is dynamic, and the local impact changes as the satellite positions evolve. In order to compare how the different constellations react to localized space disruptions, a region of damaged satellites are simulated, and the effect on the network performance analyzed over time. The simulated disruption region is centered at coordinates 0.0°, 0.0° N with a radius of 3000 km. This initial simulated disruption region is visible in Figure 5.15.

When satellites are in a global constellation, redistribution also occurs as a result of differing orbits. Due to the different orbital periods, a disrupted section of the constellation can scatter over time, resulting in a more even distribution of coverage. Global redistribution of satellites can also occur as deliberate maneuvering of satellites. Orbital planes with irregular satellite distributions due to disrupted satellites can use maneuvering in order to close gaps in the constellation. Although each individual satellite maneuvers within its own plane, the overlapping orbital planes result in a more even redistribution.

Satellite redistribution are a result of two separate factors. First is the natural distribution due to the different orbital shells have very different orbital periods. This results in a spatial scattering of the satellites over time which can hate in recovering from a spatial disruption area. Separately, the maneuvering of the satellites can also be used to recover from my fault by moving his existing satellites to locations with a lower density due to the disruption.

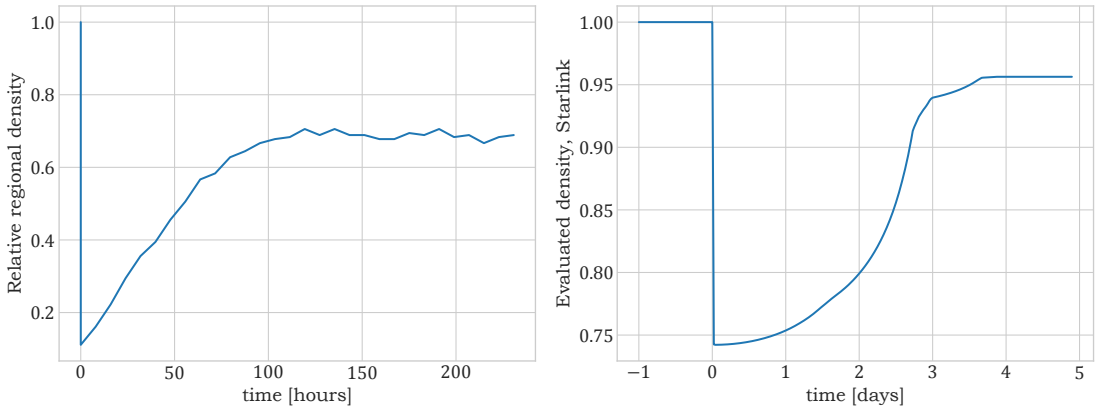

(a) Starlink relative regional density over time

(b) Starlink normalized structural density over time

Figure 5.16: Density recovery of Starlink satellites

5.5.1. Starlink

The first example is the effect on the Starlink constellation. This is considering the generation 1 deployment of Starlink satellites. The high density of Starlink satellites mean that a localized impact region may contain many tens or hundreds of satellites. First the natural distribution of the satellites is considered. Starlink satellites orbit at different altitudes, resulting in a dispersion of the damage area over time. This is illustrated in Figure 5.16a, which shows that the whole left by the damage scenario gradually closes over time. This is a density computed within a region surrounding the ”hole” in the constellation, with the evaluation region following the disrupted region over time. This occurs over a time frame of approximately 4 days.

The other example is structural recovery from maneuvering as shown in Figure 5.16b. Here, the considered metric is the cumulative lowest density across the orbital planes. The shows that the maneuverability of the Starlink satellites allow for structural recovery within the time frame of 3-4 days. This is faster than the natural redistribution of the satellites, and shows that deliberate repair of the constellation can aid in the rapid recovery of service. These results indicate that the Starlink network can recover from regional satellite disruptions in the matter of days.

5.5.2. OneWeb

The next example is the OneWeb constellation. The lower density of OneWeb satellites means that a region of damage results in a lower number of affected satellites. OneWeb satellites are located at a single orbital altitude. This means that the satellites do not naturally scatter over time, and the disrupted area in this satellite constellation therefore remains unless the satellites maneuver. This is illustrated in Figure 5.17a, which shows that the regional satellite density never fully recovers without satellite maneuvering. If maneuvering is used, the hole in the constellation can be repaired, which is shown in Figure 5.17b. By moving the remaining satellites, the regional density can be recovered in approximately 4 days. This analysis scenario illustrates that a satellite constellation consisting of a single orbital shell requires an active response in order to replace inoperative satellites following a regional satellite disruption.

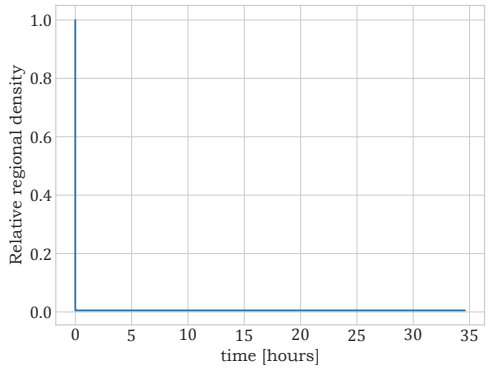

(a) OneWeb regional density over time. The density drops to zero instantly and never recovers.

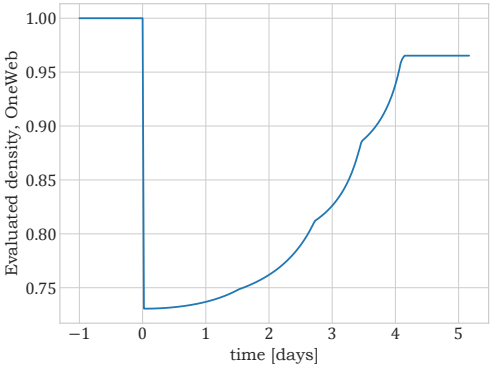

(b) OneWeb normalized structural density over time

Figure 5.17: Density recovery of OneWeb satellites

5.5.3. Amazon LEO

The 630 km shell of the Amazon LEO satellites have a higher density compared to OneWeb, but lower compared to Starlink. Additionally, the 51.9 degree inclination does not cover the northern and southern latitudes. Although the fully deployed mega-constellation is structurally similar to Starlink, the effects when disrupted by a space region are quite different. This is due to the different orbital altitudes, and the different maneuvering abilities of the satellites.

The initial deployment of 1156 satellites are all at the same altitude and inclination, forming a single shell. This means that no natural redistribution of satellites occur following a disruption event, similar to the single shell OneWeb constellation. This starts to change as more phases are added. Figure 5.18a shows that the localized density recovers in approximately 50 hours as a result of the natural distribution of the satellite orbits when considering all generation 1 satellites. The faster natural redistribution compared to Starlink is due to the greater altitude difference in the constituent orbital shells. Structural recovery, however, takes up to seven days as shown in Figure 5.19. This is caused by the weaker thrusters used in Amazon LEO satellites. After the maneuvering of the satellites, the average density across the entire constellation recovers.

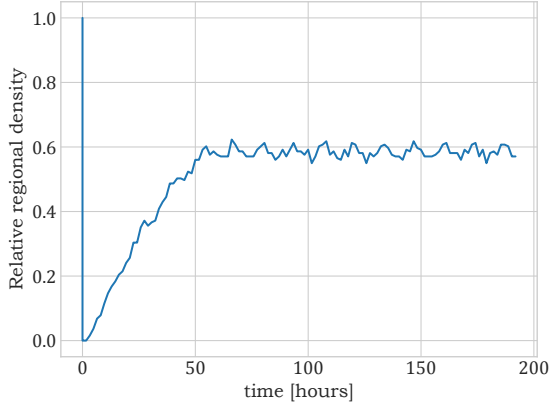

(a) Amazon LEO regional density over time

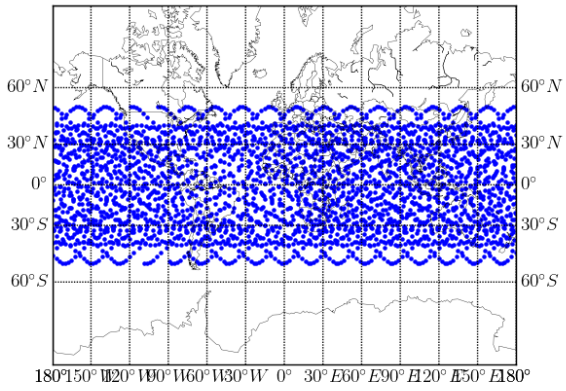

(b) Amazon LEO constellation snapshot after redistribution

Figure 5.18: Amazon LEO Gen 1 after natural redistribution

	Structural recovery time [days]	Density recovery [days]	Mean resilience loss [density-days]
Starlink	4 ± 0.5	4 ± 0.5	0.66
OneWeb	4 ± 0.5	N/A	0.85
Amazon LEO Initial	7 ± 1	N/A	1.57
Amazon LEO Gen 1	7 ± 1	4 ± 0.5	1.89
Amazon LEO Full	7.5 ± 1	2.5 ± 0.5	1.41

Table 5.4: Structural resilience overview

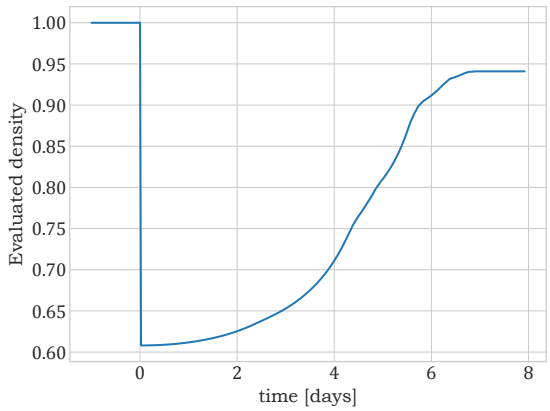

Figure 5.19: Amazon LEO structural density over time

A number of differences are found when comparing the constellation types. When considering the maneuvering of the satellites, Starlink and OneWeb are able to recover in 4 days. Amazon LEO, on the other hand, requires up to seven days. When considering the natural redistribution of the satellites, Starlink recovers in the approximately 4 days While Amazon LEO recovers in just two days. Due to the single shell of OneWeb the constellation never recovers without intervention. An overview of the computed resilience and recovery times is available in Table 5.4.

5.6. Key Findings and Insight

The results of the terrestrial disruption scenarios show that the impact of disaster scenarios have significant differences between Starlink, Amazon LEO, and OneWeb. One key differentiating factor is the ability for the networks to use inter-satellite links. Out of the three, OneWeb is the only network that relies solely on a simple bent-pipe connection and a wide distribution of ground stations. When subjected to terrestrial ground station outages, this can result in a regional disruption in OneWeb connectivity, since the satellites can no longer connect to a ground station. Meanwhile, Starlink can utilize their ISL connections in order to reroute their connections to alternative ground stations, which has previously been demonstrated during the 2025 Iberian Peninsula outage. Similarly, Amazon LEO satellites include the ability to use ISL links, which make it possible to reroute their connections similar to Starlink. This finding demonstrates that ISL connections are crucial in constructing a satellite internet network that is resilient against terrestrial disasters.

An additional consideration is the effect of the constellation size. Although Starlink has global coverage, the deployment of additional satellites provides redundancy when the satellites experience a geographically distributed disruption based on the betweenness centrality. This confirms that expanding the number of active satellites improves resilience against satellite disruptions, while also increasing the network capacity.

Another key finding is the effect of satellite maneuvering and orbital distribution on the recovery process following a regional disruption in space. Although the disruption may initially be localized, the effect spreads across the world as the satellites orbit and the planet revolves. This highlights the global and dynamic aspect of satellite internet networks, and also raises the concern of how hostile attacks against satellites may impact different regions of the world. The recovery process following an orbital disruption can involve the maneuvering of surrounding operational satellites, which make it possible to ”patch” faulty regions within the orbit. The recovery time primarily depends on the maneuvering capabilities of the satellites, and how the satellites are distributed in different orbits.

6

Discussion and Conclusion

The results in chapter 5 have shown how different parameters of a satellite internet network affects the resilience again disaster scenarios. The most important factor affecting the resilience against ground station outages appear to be the presence of inter-satellite links, allowing for traffic to be routed to alternative ground stations. Additionally, the number of satellites and their distribution affects the resilience against satellite disruptions in space, with larger and more diverse orbital configurations contributing to the resilience against satellite outages and the recovery process. This chapter will discuss the limitations of the work and areas that warrant further studies. Section 6.1 discusses some of the main limitations with the simulation and results, while section 6.2 discusses how future work can contribute to satellite resilience analysis. Finally, section 6.3 provides a conclusion to the thesis.

6.1. Limitations

In this thesis, the primary goal has been to develop a framework to analyze the resiliency aspects of LEO satellite internet networks from a structural perspective by considering specific simulated case studies. As such, an intrinsic limitation is in the choice of the case studies, which may not generalize to other disruption scenarios. The terrestrial case studies considered consists of an south-American earthquake and an European Power outage, and does not include case studies in other continents such as Africa, North America, and Asia. Additionally, the in-space disaster events are based on a synthetic area in order to allow for simple comparisons, but thus may not follow the distribution of possible hazards around the world, such as radiation belts or countries with anti-satellite technology. Additionally, the simulated disruption in space are only applied once. A radiation or space debris hazard may pose a persistent threat which continuous to disrupt satellite service over an extended period of time, which is expected to influence the outcome of of a simulation. Additionally, such a persistent hazard may only damage some of the satellites within a region, which may be below the threshold for creating significant low-density region with the constellation.

Another limitation is in the comparative analysis between the different satellite network providers. Although the goal is to conduct a comparative analysis between their resiliency, they do not all have the same target market. OneWeb is primarily used by enterprise customers, whereas Starlink and the Amazon LEO are primarily aimed at the consumer market. Additionally, although they provide similar services, the deployed networks as of January 2026 differ in multiple ways, including the number of users and current service availability, which affects the direct comparisons between the networks. Amazon LEO is planning to deploy additional ground stations in addition to the existing AWS locations, which will also affect the results, primarily relating to latency estimations.

The analysis conducted in this thesis uses the shortest-path routing and primarily a structural consideration of the network. A separate aspect is the routing of packages through the network, which is affected by factors such as the user density, user activity, and the exact routing parameters. This is information which is not publicly available, which limits the accuracy of some of the estimations such as the capacity and latency. Additionally, the considered latency is the physical light-speed latency, which does not consider the effects of queuing delays and network congestion.

6.2. Future Work

Satellite internet networks are actively evolving. New Starlink satellites are regularly being deployed in orbit, and Amazon LEO is in the process of forming an initial functional network. Mega-constellations have the ability to transform the way we communicate, but also introduces a new network infrastructure with its own challenges. While this thesis aimed to provide some insight into the resilience aspects with a focus on case studies using existing constellations, future work can investigate the resilience aspects from a more generic perspective. The availability of additional data about the routing and capacity allocation methods used by satellite internet providers would make it possible to perform higher fidelity resilience analyses. This thesis has primarily focused on structural resilience aspects, but attacks can also occur to the routing as opposed to physical infrastructure elements. Such an attack or overload scenario carries the risk of becoming a cascading failure.

In this thesis, some of the risk factors involved with orbital debris have been discussed. Additional research can be conducted to determine and simulate the in-orbit effects of a satellite debris, how it affects LEO satellites, and how long it would take for the debris to de-orbit. Such an analysis might reveal how the resilience of satellite networks are affected by a heightened collision risks in orbit. Additionally, the regional space disruptions can be modeled from a adversarial perspective. As previously highlighted, satellite outages are unique compared to terrestrial infrastructure outages, since each satellite can have a global influence. This can be investigated in order to determine whether a hostile attack against the network can target certain regions of the world.

6.3. Conclusion

In recent years, companies have been building and deploying expansive orbital and ground infrastructure with the goal of providing global satellite internet connectivity. In order to provide a robust alternative to terrestrial internet networks, these LEO satellite networks must be resilient against an array of possible threats. A literature study indicated that, although existing work has extensively analyzed how network routing affects resilience, limited work has focused on the impact of the terrestrial component and how the motion of satellites affects the recovery from space disasters. Additionally, the literature study investigated how space weather events such as extreme solar flares can disrupt the operation of satellites through energetic particles and radiation from the Sun.

As a result, this thesis explored the resilience of both the structure and the performance with a focus on terrestrial disasters, such as power outages and earthquakes. Additionally, regional and distributed satellite outages were analyzed, representing the impact of energetic events in space. The goal is to assess how different disaster cases impact the service of major existing and emerging providers, namely OneWeb, Starlink, and Amazon LEO (formerly known as Project Kuiper). Each of these networks has significant differences in the number of satellites, orbital structure, and the availability of inter-satellite communication links.

A simulation framework has been developed based on publicly accessible satellite and ground station data. The service impact was quantified by analyzing how the network coverage and minimum propagation latency change as critical components of the network become unavailable. This simulation framework was developed in Python, using a combination of publicly available satellite tracking data and planned constellation parameters.

The first analysis investigated how a satellite network degrades. The results indicate that the most significant contribution is the satellite density. A denser satellite constellation results in greater overlap and redundancy in coverage, which in turn allows for continued service as satellites become unavailable. This was illustrated by the increased tolerance to satellite outages as additional satellites were added based on the future plans of the Amazon LEO constellation.

An additional analysis investigated the impact of regional outages in space. A regional outage may be the result of an extreme space weather event, or it may be the result of anti-satellite weaponry. Here, the results indicate that outages in space propagate over time as the satellites orbit. A regional outage in one area can thus result in disrupted service in other areas around the world as the satellites orbit. Additionally, it was found that the layout of the satellite constellation contributes to a natural redistribution of satellites over time, which results in a recovery of satellite density within the disrupted region of space. The recovery can be further aided by deliberate satellite maneuvering, with the recovery time primarily depending on the maneuvering capabilities of the nearby satellites. The results indicate that, even a large-scale outage of satellites has potential to recover some global service in days or weeks, assuming the satellites can safely operate within the region following a disaster.

For terrestrial disruptions, the analysis has focused on two case studies representing large-scale disaster and outage events. The first case study is the 2025 electrical blackout that impacted the Iberian Peninsula, while the second case study focused on the potential impact of a large-scale earthquake in Chile, with the disruption region based on the 1960 Valdivia earthquake. In both of these scenarios, OneWeb experienced decreased capacity and coverage, while Kuiper and Starlink experienced a regional increase in latency while retaining the same coverage and capacity. Both of these case studies highlight that the impact is primarily regional. Satellite networks with deployed inter-satellite links are significantly less impacted by regional ground station outages, since they can fall back to alternative ground stations, at the expense of increased connection latency.

The results of this thesis indicate that the resilience of a satellite network is dependent on multiple interrelated factors, with the service impact being influenced by the presence of inter-satellite links, the orbital satellite density, the maneuvering rate of the satellites, and the distribution of orbital altitudes within the satellite constellation. In general, Starlink is found to be more resilient to terrestrial and space-based disasters compared to OneWeb, due to the large number of operational satellites and availability of inter-satellite links. Starlink and the expected Amazon LEO constellation are similar, with Starlink satellites able to maneuver more rapidly, and the Amazon LEO constellation experiencing a faster passive redistribution of satellites.

This work contributes to the knowledge on how satellite networks can be impacted by external threats, and assesses how the currently deployed technologies may be impacted by terrestrial and in-space disaster events. With the expected future expansion of satellite constellations and the increased adoption of satellite internet in the consumer market, this knowledge provides insight into how suitable these systems are as a disaster-resilient alternative to terrestrial broadband internet. One key result is that ISL-connected networks are highly resilient against regional terrestrial disruptions, but are susceptible to attacks or disasters in space. The limitations in the analysis and simulation lie in a lack of knowledge about the details of inter-satellite connections and primarily analyzing the physical network without considering routing aspects. These factors may be the subject of future research into this rapidly expanding technology.

Bibliography

[1] Wikideas1 - CC BY 4.0. *File:Starlink 01.webp*. 2025. URL: https://commons.wikimedia.org/wiki/File:Starlink_01.webp.

[2] Nils Pachler et al. “An Updated Comparison of Four Low Earth Orbit Satellite Constellation Systems to Provide Global Broadband”. In: *2021 IEEE International Conference on Communications Workshops, ICC Workshops 2021 - Proceedings*. 2021. DOI: 10.1109/ICCWorkshops50388.2021.9473799.

[3] Ogutu B. Osoro and Edward J. Oughton. “A Techno-Economic Framework for Satellite Networks Applied to Low Earth Orbit Constellations: Assessing Starlink, OneWeb and Kuiper”. In: *IEEE Access* 9 (2021). ISSN: 21693536. DOI: 10.1109/ACCESS.2021.3119634.

[4] Hidetaka Uramoto et al. “Initial response to the 2024 Noto earthquake by the university hospital closest to the disaster area”. In: *Scientific Reports* 14.1 (2024). ISSN: 20452322. DOI: 10.1038/s41598-024-75844-w.

[5] Doug Madory. *Lunes Sin Luz: Spain and Portugal’s Historic Outage*. 2025. URL: https://www.kentik.com/blog/lunes-sin-luz-spain-and-portugals-historic-outage/.

[6] Vaibhav Bhosale et al. “Are Leo Networks the Future of National Emergency Failover? – a Quantitative Study and Policy Blueprint”. In: *SSRN Electronic Journal* (2025). ISSN: 1556-5068. DOI: 10.2139/ssrn.5337566.

[7] Starlink. *Starlink on X: Starlink is connecting more than 8M active customers*. 2025. URL: https://x.com/Starlink/status/1986168985453490449.

[8] Joscha Abels. “Private infrastructure in geopolitical conflicts: the case of Starlink and the war in Ukraine”. In: *European Journal of International Relations* 30.4 (2024). ISSN: 14603713. DOI: 10.1177/13540661241260653.

[9] Jessie Hamill-Stewart and Awais Rashid. “Threats Against Satellite Ground Infrastructure: A retrospective analysis of sophisticated attacks”. In: *Proceedings 2024 Workshop on Security of Space and Satellite Systems*. Reston, VA: Internet Society, 2024. ISBN: 979-8-9894372-1-4. DOI: 10.14722/spacesec.2024.23087.

[10] Giuseppe Aceto et al. *A comprehensive survey on internet outages*. 2018. DOI: 10.1016/j.jnca.2018.03.026.

[11] Hitoshi Yamamura, Kazuhisa Kaneda, and Yasumitsu Mizobata. “Communication Problems After the Great East Japan Earthquake of 2011”. In: *Disaster Medicine and Public Health Preparedness* 8.4 (Aug. 2014), pp. 293–296. ISSN: 1935-7893. DOI: 10.1017/dmp.2014.49.

[12] Saeed Fadaei et al. “A Comprehensive Study of Satellite Network Performance During 1.5 years of Solar Storm Activity”. In: *ACM SIGMETRICS*. 2026.

[13] H.□L. Lam et al. “Anik□E1 and E2 satellite failures of January 1994 revisited”. In: *Space Weather* 10.10 (Oct. 2012). ISSN: 1542-7390. DOI: 10.1029/2012SW000811.

[14] Alagappan Ramanathan and Sangeetha Abdu Jyothi. “Weathering a Solar Superstorm: Starlink Performance during the May 2024 Storm”. In: *Proceedings of the 2nd International Workshop on LEO Networking and Communication*. New York, NY, USA: ACM, Nov. 2024, pp. 31–36. ISBN: 9798400712807. DOI: 10.1145/3697253.3697270.

[15] ESA. *Space debris by the numbers*. 2025. URL: https://www.esa.int/Space_Safety/Space_Debris/Space_debris_by_the_numbers.

[16] Anelí Bongers and José L. Torres. “Star Wars: Anti-Satellite Weapons and Orbital Debris”. In: *Defence and Peace Economics* 35.7 (Oct. 2024), pp. 826–845. ISSN: 1024-2694. DOI: 10.1080/10242694.2023.2208020.

[17] Sangeetha Abdu Jyothi. “Solar superstorms: Planning for an internet apocalypse”. In: *SIGCOMM 2021 - Proceedings of the ACM SIGCOMM 2021 Conference*. 2021. DOI: 10.1145/3452296.3472916.

[18] Xin Xu, Zhixiang Gao, and Aijun Liu. “Robustness of satellite constellation networks”. In: *Computer Communications* 210 (2023). ISSN: 1873703X. DOI: 10.1016/j.comcom.2023.07.036.

[19] Yuanjie Li et al. “A Networking Perspective on Starlink’s Self-Driving LEO Mega-Constellation”. In: *Proceedings of the 29th Annual International Conference on Mobile Computing and Networking*. New York, NY, USA: ACM, July 2023, pp. 1–16. ISBN: 9781450399906. DOI: 10.1145/3570361.3592519.

[20] Zeqi Lai et al. “STARRYNET: Empowering Researchers to Evaluate Futuristic Integrated Space and Terrestrial Networks”. In: *Proceedings of the 20th USENIX Symposium on Networked Systems Design and Implementation, NSDI 2023*. 2023.

[21] Wei Huang et al. “A Preliminary Availability Assessment of A LEO Satellite Constellation”. In: *2024 Annual Reliability and Maintainability Symposium (RAMS)*. IEEE, Jan. 2024, pp. 1–6. ISBN: 979-8-3503-0769-6. DOI: 10.1109/RAMS51492.2024.10457737.

[22] Ricardo Correia et al. “User Terminal Segments for Low-Earth Orbit Satellite Constellations: Commercial Systems and Innovative Research Ideas”. In: *IEEE Microwave Magazine* 23.10 (2022). ISSN: 15579581. DOI: 10.1109/MMM.2022.3188124.

[23] Todd E. Humphreys et al. “Signal Structure of the Starlink Ku-Band Downlink”. In: *IEEE Transactions on Aerospace and Electronic Systems* 59.5 (2023). ISSN: 15579603. DOI: 10.1109/TAES.2023.3268610.

[24] Nitinder Mohan et al. “A Multifaceted Look at Starlink Performance”. In: *Proceedings of the ACM Web Conference 2024*. New York, NY, USA: ACM, May 2024, pp. 2723–2734. ISBN: 9798400701719. DOI: 10.1145/3589334.3645328.

[25] *Unofficial Starlink Global Gateways & PoPs*. 2025. URL: www.google.com/maps/d/viewer?mid=1805q6rlePY4WZd8QMOaNe2BqAgFkYBY.

[26] Roger. Bate, Donald D.. Mueller, and Jerry E.. White. *Fundamentals of astrodynamics*. Dover Publications, Inc., 1971, p. 455. ISBN: 0486600610.

[27] Gregory Stock, Juan A. Fraire, and Holger Hermanns. “Distributed On-Demand Routing for LEO Mega-Constellations: A Starlink Case Study”. In: *2022 11th Advanced Satellite Multimedia Systems Conference and the 17th Signal Processing for Space Communications Workshop, ASMS/SPSC 2022*. 2022. DOI: 10.1109/ASMS/SPSC55670.2022.9914716.

[28] Debopam Bhattacherjee and Ankit Singla. “Network topology design at 27,000 km/hour”. In: *CoNEXT 2019 - Proceedings of the 15th International Conference on Emerging Networking Experiments and Technologies*. 2019. DOI: 10.1145/3359989.3365407.

[29] Morio Toyoshima. “Recent Trends in Space Laser Communications for Small Satellites and Constellations”. In: *Journal of Lightwave Technology* 39.3 (2021). ISSN: 15582213. DOI: 10.1109/JLT.2020.3009505.

[30] Starlink. *Satellite Technology*. 2025. URL: https://starlink.com/technology.

[31] Huang Pu, Wen Guangwei, and Wang Zhaokui. “Simultaneously Adjusting Deployment Strategies for Mega-Constellations Using Low-Thrust Maneuvers”. In: *Journal of Spacecraft and Rockets* 62.1 (Jan. 2025), pp. 196–205. ISSN: 0022-4650. DOI: 10.2514/1.A36007.

[32] Rachit Bhatia et al. “The Operational Realities of Electric Propulsion”. In: *Proceedings of the International Astronautical Congress, IAC*. Vol. 2022-September. 2022.

[33] Wei Zhao et al. “A First Look at Networking-Aware LEO Maneuvers”. In: *Proceedings of the 1st ACM Workshop on LEO Networking and Communication*. New York, NY, USA: ACM, Oct. 2023, pp. 25–30. ISBN: 9798400703324. DOI: 10.1145/3614204.3616107.

[34] Leafnode. *Illustration of Hohmann transfer orbit*. 2007. URL: https://commons.wikimedia.org/wiki/File:Hohmann_transfer_orbit.svg.

[35] Jonathan McDowell. *Enormous ('Mega') Satellite Constellations*. 2025. URL: https://planet4589.org/space/con/conlist.html.

[36] Jonathan McDowell. *Starlink Statistics*. 2025. URL: https://planet4589.org/space/con/star/stats.html.

[37] Jonathan C. McDowell. "The Low Earth Orbit Satellite Population and Impacts of the SpaceX Starlink Constellation". In: *The Astrophysical Journal Letters* 892.2 (Apr. 2020), p. L36. ISSN: 2041-8205. DOI: 10.3847/2041-8213/ab8016.

[38] Polly Thompson. *Elon Musk's Starlink is adding 20,000 new users a day as it hits 9 million customers*. Dec. 2025.

[39] Mike Wall. *Amazon launches 27 satellites to begin building huge 'Project Kuiper' internet constellation*. Apr. 2025.

[40] Jonathan McDowell. *Kuiper Statistics*. 2025. URL: https://www.planet4589.org/space/con/kp/stats.html.

[41] Andrew Williams et al. "Analysing the Impact of Satellite Constellations and ESO's Role in Supporting the Astronomy Community". In: *Published in The Messenger vol. 184* pp. 3-7 (2021). ISSN: 0722-6691.

[42] Muhammad T. Chaudhary and Awais Piracha. "Natural Disasters—Origins, Impacts, Management". In: *Encyclopedia* 1.4 (Oct. 2021), pp. 1101–1131. ISSN: 2673-8392. DOI: 10.3390/encyclopedia1040084.

[43] Zayan EL Khaled and Hamid Mcheick. "Case studies of communications systems during harsh environments: A review of approaches, weaknesses, and limitations to improve quality of service". In: *International Journal of Distributed Sensor Networks* 15.2 (Feb. 2019), p. 155014771982996. ISSN: 1550-1477. DOI: 10.1177/1550147719829960.

[44] Teresa Gomes et al. "A survey of strategies for communication networks to protect against large-scale natural disasters". In: *2016 8th International Workshop on Resilient Networks Design and Modeling (RNDM)*. IEEE, Sept. 2016, pp. 11–22. ISBN: 978-1-4673-9023-1. DOI: 10.1109/RNDM.2016.7608263.

[45] D. Giardini and P. Basham. "The Global Seismic Hazard Assessment Program (GSHAP)". In: *Annals of Geophysics* 36.3-4 (Dec. 1993). ISSN: 2037416X. DOI: 10.4401/ag-4256.

[46] M. Pagani et al. "OpenQuake Engine: An Open Hazard (and Risk) Software for the Global Earthquake Model". In: *Seismological Research Letters* 85.3 (May 2014), pp. 692–702. ISSN: 0895-0695. DOI: 10.1785/0220130087.

[47] Hassan Haes Alhelou et al. "A Survey on Power System Blackout and Cascading Events: Research Motivations and Challenges". In: *Energies* 12.4 (Feb. 2019), p. 682. ISSN: 1996-1073. DOI: 10.3390/en12040682.

[48] Marcin Nawrocki et al. "The far side of DNS amplification: Tracing the DDoS attack ecosystem from the internet core". In: *Proceedings of the ACM SIGCOMM Internet Measurement Conference, IMC*. 2021. DOI: 10.1145/3487552.3487835.

[49] Raul Pedrozo. "Safeguarding Submarine Cables and Pipelines in Times of Peace and War". In: *International Law Studies* (2025). ISSN: 2375-2831. URL: https://gcaptain.com/russian-navy-vessels-seen-near-nord-stream-before-.

[50] Rositsa Miteva, Susan W. Samwel, and Stela Tkatchova. "Space Weather Effects on Satellites". In: *Astronomy* 2.3 (Aug. 2023), pp. 165–179. ISSN: 2674-0346. DOI: 10.3390/astronomy2030012.

[51] Kirolosse M. Girgis, Tohru Hada, and Shuichi Matsukiyo. "Estimation of Single Event Upset (SEU) rates inside the SAA during the geomagnetic storm event of 15 May 2005". In: *2021 IEEE International Conference on Wireless for Space and Extreme Environments (WiSEE)*. IEEE, Oct. 2021, pp. 27–30. ISBN: 978-1-6654-0371-9. DOI: 10.1109/WiSEE50203.2021.9613828.

[52] Joe Allen et al. “Effects of the March 1989 solar activity”. In: *Eos, Transactions American Geophysical Union* 70.46 (1989). ISSN: 23249250. DOI: 10.1029/89EO00409.

[53] William E. Parker and Richard Linares. “Satellite Drag Analysis During the May 2024 Gannon Geomagnetic Storm”. In: *Journal of Spacecraft and Rockets* 61.5 (Sept. 2024), pp. 1412–1416. ISSN: 0022-4650. DOI: 10.2514/1.A36164.

[54] ESA. *Flying through the biggest solar storm ever recorded*. Oct. 2025. URL: https://www.esa.int/Space_Safety/Space_weather/Flying_through_the_biggest_solar_storm_ever_recorded.

[55] U.S.-China Economic and Security Review Commission. *2011 Annual Report to Congress*. Tech. rep. 2000. URL: https://www.uscc.gov/sites/default/files/annual_reports/annual_report_full_11.pdf.

[56] Paweł Bernat. “ORBITAL SATELLITE CONSTELLATIONS AND THE GROWING THREAT OF KESSLER SYNDROME IN THE LOWER EARTH ORBIT”. In: *Inżynieria Bezpieczeństwa Obiektów Antropogenicznych* 4 (Dec. 2020). ISSN: 2450-1859. DOI: 10.37105/iboa.94.

[57] Mak Tafazoli. “A study of on-orbit spacecraft failures”. In: *Acta Astronautica* 64.2-3 (Jan. 2009), pp. 195–205. ISSN: 00945765. DOI: 10.1016/j.actaastro.2008.07.019.

[58] Jonathan McDowell. *Reentry data - Starlinks*. Oct. 2025. URL: https://planet4589.org/space/stats/restar.html.

[59] Kelly Kizer Whitt. *1 to 2 Starlink satellites are falling back to Earth each day*. 2025. URL: https://earthsky.org/human-world/1-to-2-starlink-satellites-falling-back-to-earth-each-day/.

[60] Zelin Wan et al. “A Survey on Centrality Metrics and Their Network Resilience Analysis”. In: *IEEE Access* 9 (2021). ISSN: 21693536. DOI: 10.1109/ACCESS.2021.3094196.

[61] Abdul Jabbar, Hemanth Narra, and James P.G. Sterbenz. “An approach to quantifying resilience in mobile ad hoc networks”. In: *2011 8th International Workshop on the Design of Reliable Communication Networks (DRCN)*. IEEE, Oct. 2011, pp. 140–147. ISBN: 978-1-61284-125-0. DOI: 10.1109/DRCN.2011.6076896.

[62] Jorik Oostenbrink and Fernando A. Kuipers. “A Moment of Weakness: Protecting Against Targeted Attacks Following a Natural Disaster”. In: *ACM SIGMETRICS Performance Evaluation Review* 47.4 (Apr. 2020), pp. 12–15. ISSN: 0163-5999. DOI: 10.1145/3397776.3397780.

[63] Christopher W. Zobel. “Comparative visualization of predicted disaster resilience”. In: *ISCRAM 2010 - 7th International Conference on Information Systems for Crisis Response and Management: Defining Crisis Management 3.0, Proceedings*. 2010.

[64] Michel Bruneau et al. “A Framework to Quantitatively Assess and Enhance the Seismic Resilience of Communities”. In: *Earthquake Spectra* 19.4 (Nov. 2003), pp. 733–752. ISSN: 8755-2930. DOI: 10.1193/1.1623497.

[65] Chia-Wei Hsu and Ali Mostafavi. “Dissecting resilience curve archetypes and properties in human systems facing weather hazards”. In: *Scientific Reports* 15.1 (Apr. 2025), p. 11897. ISSN: 2045-2322. DOI: 10.1038/s41598-025-95909-8.

[66] Xiaogang Qi et al. “A survey of routing techniques for satellite networks”. In: *Journal of Communications and Information Networks* 1.4 (2016). ISSN: 2096-1081. DOI: 10.1007/bf03391581.

[67] Ryutaro Suzuki and Yasuhiko Yasuda. “Study on ISL network structure in LEO satellite communication systems”. In: *Acta Astronautica* 61.7-8 (Oct. 2007), pp. 648–658. ISSN: 00945765. DOI: 10.1016/j.actaastro.2006.11.015.

[68] Quan Chen et al. “3-ISL Topology: Routing Properties and Performance in LEO Megaconstellation Networks”. In: *IEEE Transactions on Aerospace and Electronic Systems* 61.2 (Apr. 2025), pp. 4961–4972. ISSN: 0018-9251. DOI: 10.1109/TAES.2024.3512535.

[69] Giacomo Giuliari et al. “Internet backbones in space”. In: *ACM SIGCOMM Computer Communication Review* 50.1 (Mar. 2020), pp. 25–37. ISSN: 0146-4833. DOI: 10.1145/3390251.3390256.

[70] Zhijun Guo et al. “Resilience Analysis of Cooperative Mission Based on Spatio–Temporal Network Dynamics for Flying Ad Hoc Network”. In: *IEEE Transactions on Reliability* 73.2 (June 2024), pp. 1034–1043. ISSN: 0018-9529. DOI: 10.1109/TR.2023.3344726.

[71] M. Kretschmer et al. “WiBACK: a back-haul network architecture for 5G networks”. In: *International Conference on Frontiers of Communications, Networks and Applications (ICFCNA 2014 - Malaysia)*. Institution of Engineering and Technology, 2014, 11 (6 .)–11 (6 .) ISBN: 978-1-78561-072-1. DOI: 10.1049/cp.2014.1403.

[72] Jacek Rak. “A new approach to design of weather disruption-tolerant wireless mesh networks”. In: *Telecommunication Systems* 61.2 (Feb. 2016), pp. 311–323. ISSN: 1018-4864. DOI: 10.1007/s11235-015-0003-z.

[73] SWPC. *Space Weather Prediction Center*. 2025. URL: https://www.swpc.noaa.gov/.

[74] Brian Eriksson, Ramakrishnan Durairajan, and Paul Barford. “RiskRoute: A framework for mitigating network outage threats”. In: *CoNEXT 2013 - Proceedings of the 2013 ACM International Conference on Emerging Networking Experiments and Technologies*. 2013. DOI: 10.1145/2535372.2535385.

[75] Jian Wu et al. “Proceedings of the 2007 ACM CoNEXT conference”. In: ACM Digital Library, 2013. ISBN: 9781595937704.

[76] Jorik Oostenbrink and Fernando Kuipers. “A Global Study of the Risk of Earthquakes to IXPs”. In: *2022 IFIP Networking Conference, IFIP Networking 2022*. 2022. DOI: 10.23919/IFIPNetworking55013.2022.9829785.

[77] Alagappan Ramanathan and Sangeetha Abdu Jyothi. “Nautilus: A Framework for Cross-Layer Cartography of Submarine Cables and IP Links”. In: *Proceedings of the ACM on Measurement and Analysis of Computing Systems* 7.3 (2023). ISSN: 24761249. DOI: 10.1145/3626777.

[78] Alagappan Ramanathan, Rishika Sankaran, and Sangeetha Abdu Jyothi. “Xaminer: An internet cross-layer resilience analysis tool”. In: *Proceedings of the ACM on Measurement and Analysis of Computing Systems* 8.1 (2024). ISSN: 24761249. DOI: 10.1145/3639042.

[79] Aleksandr Stevens et al. “Can LEO Satellites Enhance the Resilience of Internet to Multi-hazard Risks?” In: 2024, pp. 170–195. DOI: 10.1007/978-3-031-56252-5{_}9.

[80] Zhuoyuan Li et al. “LEO Satellite Network Resilience Analysis: A Focus on Critical Satellites”. In: *LEONET 2024 - Proceedings of the 2nd ACM Workshop on LEO Networking and Communication, Part of: ACM MobiCom 2024*. Association for Computing Machinery, Inc, Nov. 2024, pp. 13–18. ISBN: 9798400712807. DOI: 10.1145/3697253.3697267.

[81] Alexander Kedrowitsch, Jonathan Black, and Danfeng Yao. “Resilient routing for low Earth orbit mega-constellation networks”. In: *Proceedings of the NDSS Workshop on Space Security*. 2024.

[82] Federica Paganelli Azza et al. “ Low-Thrust Reconfiguration Strategy for Flexible Satellite Constellations”. In: *Small Satellite Conference*. Aug. 2022. URL: https://digitalcommons.usu.edu/smallsat/2022/all2022/107/.

[83] Chris Stephens. *Renesas Powers a New Space Race*. Aug. 2023. URL: https://www.renesas.com/en/blogs/renesas-powers-new-space-race.

[84] Claudio Rocchini. *File:Graph betweenness.svg*. 2007. URL: https://commons.wikimedia.org/wiki/File:Graph_betweenness.svg.

[85] Ioanna Tsalouchidou et al. “Temporal betweenness centrality in dynamic graphs”. In: *International Journal of Data Science and Analytics* 9.3 (2020). ISSN: 23644168. DOI: 10.1007/s41060-019-00189-x.

[86] Simon Kassing et al. “Exploring the ”internet from space” with Hypatia”. In: *Proceedings of the ACM SIGCOMM Internet Measurement Conference, IMC*. 2020. DOI: 10.1145/3419394.3423635.

[87] Tobias Pfandzelter and David Bermbach. “Celestial: Virtual Software System Testbeds for the LEO Edge”. In: *Middleware 2022 - Proceedings of the 23rd ACM/IFIP International Middleware Conference*. 2022. DOI: 10.1145/3528535.3531517.

[88] Mohamed M. Kassem and Nishanth Sastry. “xeoverse: A Real-time Simulation Platform for Large LEO Satellite Mega-Constellations”. In: *2024 IFIP Networking Conference (IFIP Networking)*. IEEE, June 2024, pp. 1–9. ISBN: 978-3-903176-63-8. DOI: 10.23919/IFIPNetworking62109.2024.10619898.

[89] Alexander Kmoch et al. “Area and shape distortions in open-source discrete global grid systems”. In: *Big Earth Data* 6.3 (July 2022), pp. 256–275. ISSN: 2096-4471. DOI: 10.1080/20964471.2022.2094926.

[90] H3. *H3 indexes points and shapes into a hexagonal grid*. URL: https://h3geo.org/.

[91] Kontur. *Kontur Population: Global Population Density for 22km H3 Hexagons*. 2023. URL: https://data.humdata.org/dataset/kontur-population-dataset-22km.

[92] H3. *Tables of Cell Statistics Across Resolutions*. URL: https://h3geo.org/docs/core-library/restable.

[93] Kel Elkins. *Tracking Satellites and Space Debris in Earth Orbit (Feb 2024)*. June 2025. URL: https://svs.gsfc.nasa.gov/5258/.

[94] celestrak. *Supplemental GP Element Sets*. 2025. URL: https://www.celestrak.org/NORAD/elements/supplemental/.

[95] “Unofficial OneWeb SNP/PoP Map”. In: (2025). URL: https://www.google.com/maps/d/viewer?mid=1myyEQLtT1Dk1vYFoR3LlsrDs-U223tQ.

[96] FCC. *Report No. SAT-01931, RE: Applications Accepted for Filing*. Tech. rep. Washington: FCC, July 2025. URL: https://docs.fcc.gov/public/attachments/DOC-412671A2.pdf.

[97] Amazon. *AWS Ground Station Locations*. 2025. URL: https://docs.aws.amazon.com/ground-station/latest/ug/aws-ground-station-antenna-locations.html.

[98] Amazon Staff. *Here’s your first look at Project Kuiper’s low-cost customer terminals*. 2023. URL: https://www.aboutamazon.com/news/innovation-at-amazon/heres-your-first-look-at-project-kuipers-low-cost-customer-terminals.

[99] Amazon Staff. *Amazon’s Project Kuiper completes successful tests of optical mesh network in low Earth orbit*. Dec. 2023. URL: https://www.aboutamazon.com/news/innovation-at-amazon/amazon-project-kuiper-oisl-space-laser-december-2023-update.

[100] Jesús Lastra. *Amazon ya tiene lista en Santander la estructura para su internet por satélite*. Nov. 2025. URL: https://www.eldiariomontanes.es/economia/amazon-lista-santander-estructura-internet-satelite-20251107071753-nt.html#vca=fixed-btn&vso=rrss&vmc=cp&vli=economia.

[101] Jonathan McDowell. *Starlink Group 17-6 (Launch 298, 2025-184)*. 2025. URL: https://planet4589.org/space/con/star/sg298/index.html.

[102] Anqi Lang and Yu Jiang. “Orbit Determination for Continuously Maneuvering Starlink Satellites Based on an Unscented Batch Filtering Method”. In: *Sensors* 25.13 (June 2025), p. 4079. ISSN: 1424-8220. DOI: 10.3390/s25134079.

A

Implementation details

In order to conduct the analysis discussed in this thesis, a program was developed for setting up a virtual satellite network and estimate the parameters within it.

A.1. Capacity mapping

The population of each cell is estimated based on a combination of the population density and published estimates of the number of Starlink subscribers. Although the density of Starlink users differ from the population density across countries and regions, this estimate serves primarily to model the local local densities for the purpose of modeling the resource allocation of satellites within a region.

Each cell can either be fully, partially, or not served by the satellites. For the estimation, a water-filling algorithm is used, which models the cells as buckets with a max capacity. The satellites can then use their capacity to ”fill” these buckets, starting from the lowest density regions. An unoptimized pseudocode representation of the capacity distribution is as follows:

```
for satellite in satellites:
    covered_cells = []
    for cell in cells:
        if distance(cell, satellite) < MAX_COVERAGE_DISTANCE:
        covered_cells.append(cell)

    while satellite.capacity > 0 and missing_capacity(covered_cells) > 0:
      delta = calculate_minimum_increment(covered_cells, satellite.capacity)
        for cell in covered_cells:
            if cell.missing_capacity > 0:
                cell.missing_capacity - delta
                satellite.capacity - delta
```

The purpose of this greedy algorithm is to provide an estimate for how the satellite capacity is distributed among the users, through an indirect mapping to the cell populations. This allows for estimation of areas where the number of users are limited by the capacity of the system, while keeping a wider geographical distribution compared to a maxflow approach.

B

Terrestrial Disaster Heatmaps

This appendix contains all the terrestrial disaster heatmaps for the Iberian Peninsula blackout and the Chile earthquake scenarios. Note that black regions in the latency heatmaps represent areas with no coverage.

B.1. Chile Earthquake Capacity

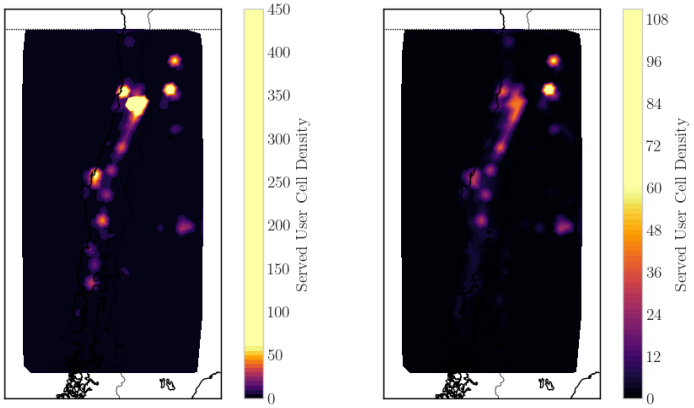

(a) Before outage (b) After outage

Figure B.1: The effect of the Chile earthquake on the regional capacity for OneWeb

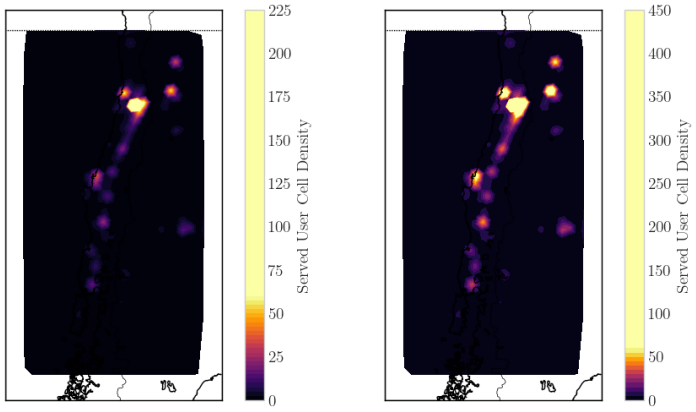

(a) Starlink (b) OneWeb w/ISLs

Figure B.2: The regional capacity in Chile for Starlink and OneWeb w/ISLs, these remain identical after the disruption.

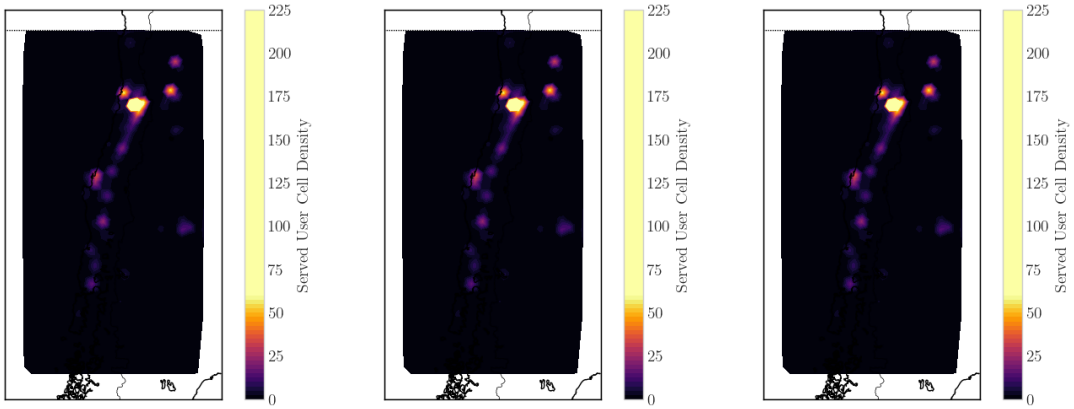

(a) Amazon LEO Initial (b) Amazon LEO Generation 1 (c) Amazon LEO Full

Figure B.3: The regional capacity in Chile for stages of Amazon LEO, these remain identical after the disruption.

B.2. Chile Earthquake Latency/Coverage

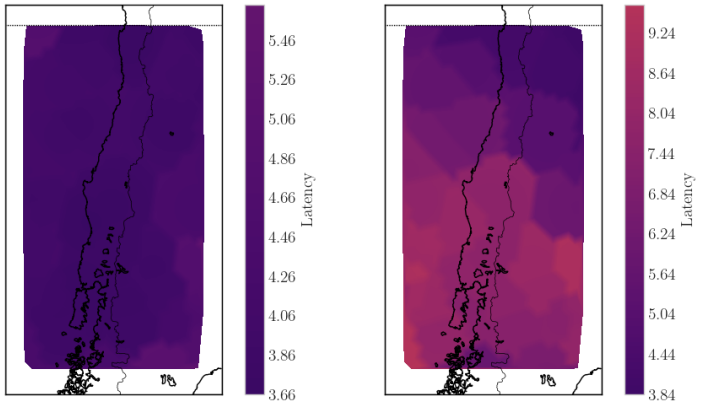

(a) Before outage (b) After outage

Figure B.4: The effect of the Chile earthquake on the regional capacity for Starlink

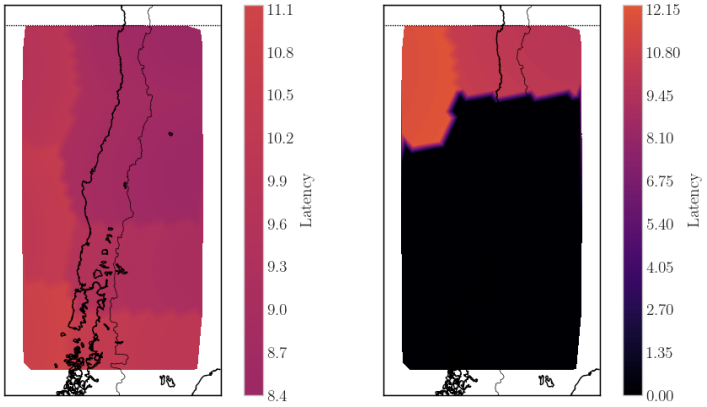

(a) Before outage (b) After outage

Figure B.5: The effect of the Chile earthquake on the regional capacity for OneWeb

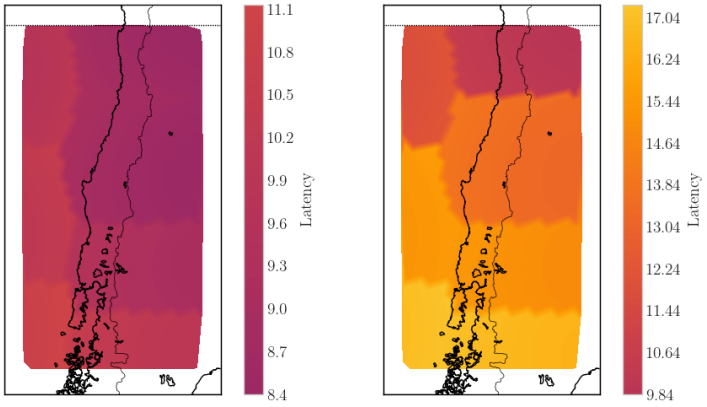

(a) Before outage (b) After outage

Figure B.6: The effect of the Chile earthquake on the regional capacity for OneWeb w/ISLs

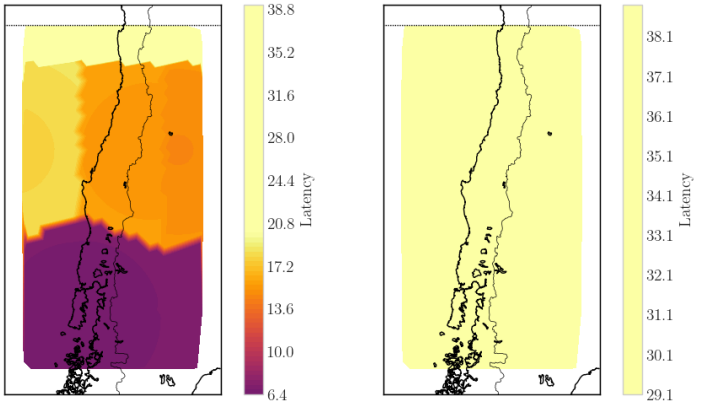

(a) Before outage (b) After outage

Figure B.7: The effect of the Chile earthquake on the regional capacity for Amazon LEO Initial

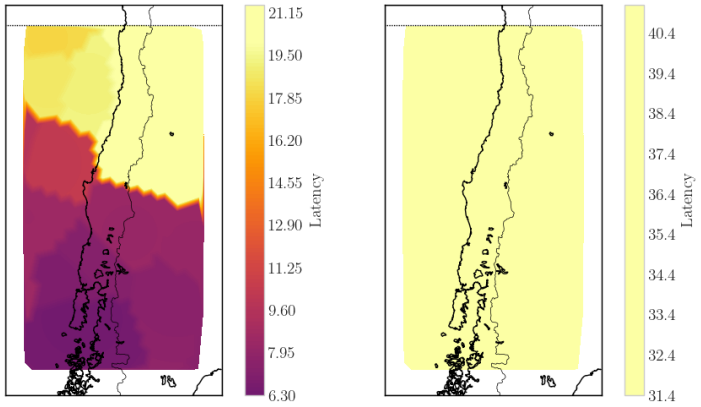

(a) Before outage (b) After outage

Figure B.8: The effect of the Chile earthquake on the regional capacity for Amazon LEO Generation 1

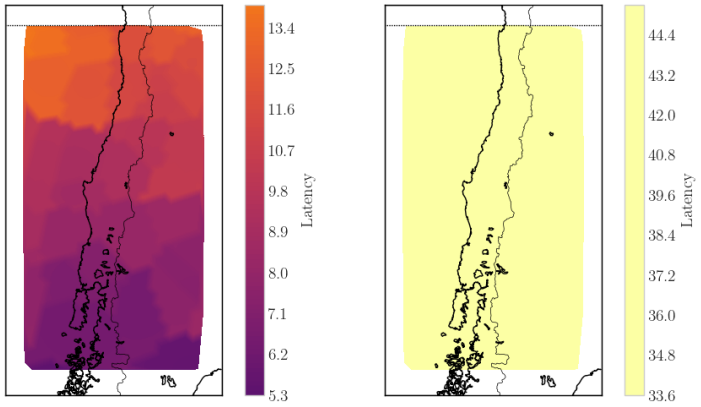

(a) Before outage (b) After outage

Figure B.9: The effect of the Chile earthquake on the regional capacity for Amazon LEO Full

B.3. Iberian Blackout Capacity

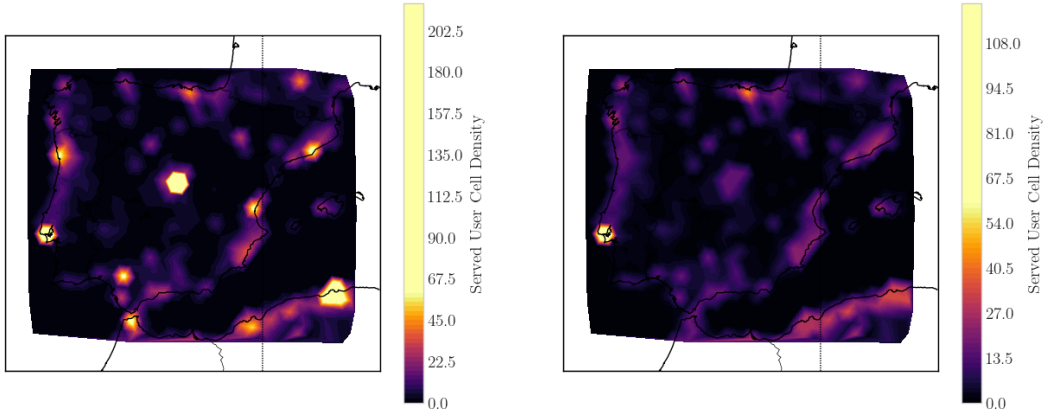

(a) Before outage (b) After outage

Figure B.10: The effect of the Iberian blackout on the regional capacity for OneWeb

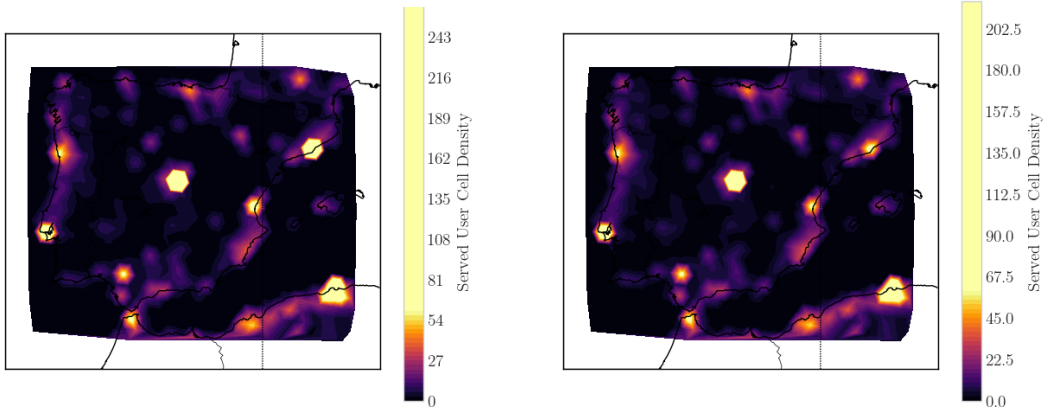

(a) Starlink capacity

(b) OneWeb w/ISLs capacity

Figure B.11: The regional capacity for Starlink and OneWeb w/ISLs. These remain identical after the disruption.

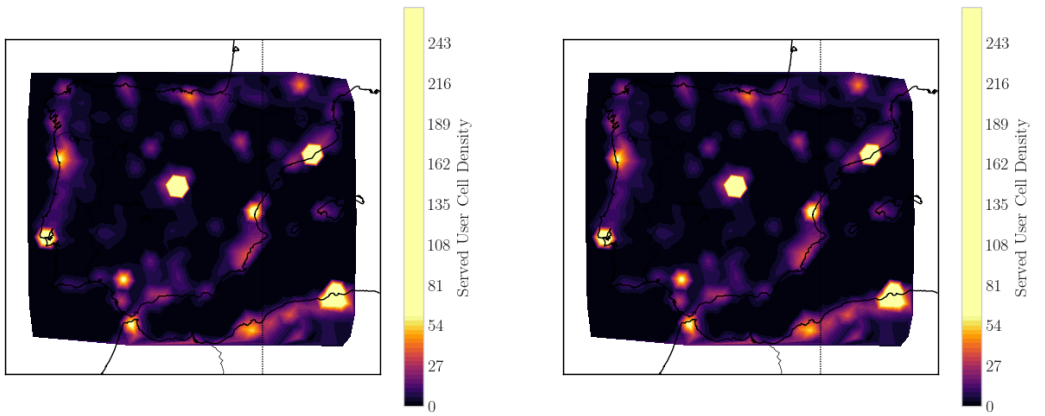

(a) Amazon LEO Initial

(b) Amazon LEO Generation 1

Figure B.12: The regional capacity for stages of Amazon LEO. These remain identical after the disruption.

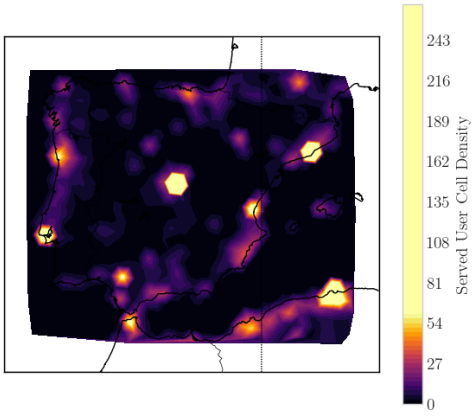

Figure B.13: The regional capacity for the full Amazon LEO constellation. This remains identical after the disruption.

B.4. Iberian Blackout Latency/Coverage

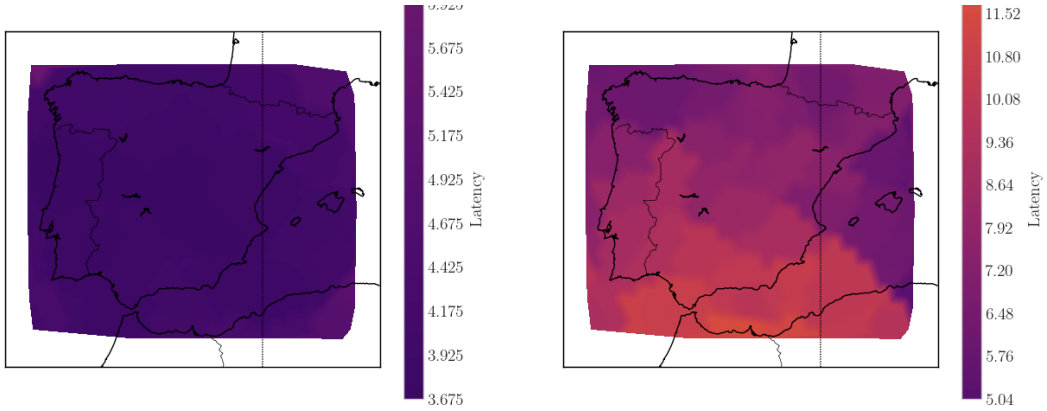

(a) Before outage (b) After outage

Figure B.14: The effect of the Iberian blackout on the regional capacity for Starlink

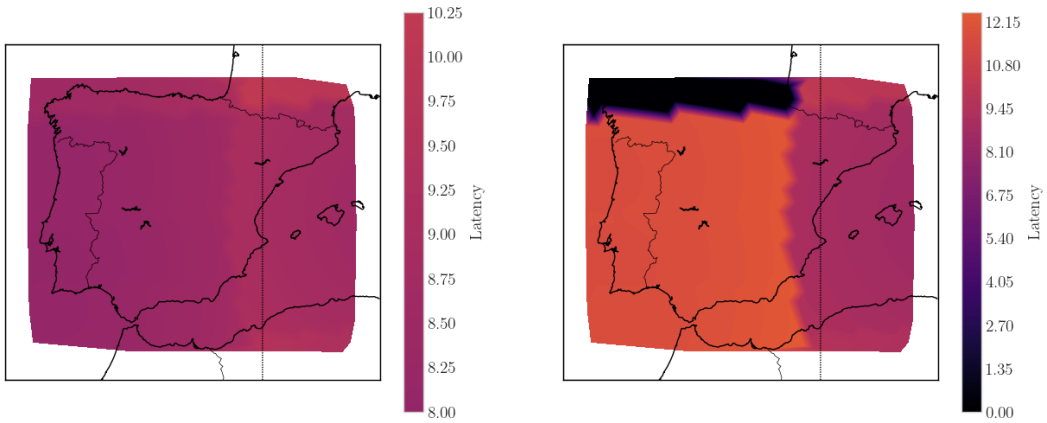

(a) Before outage (b) After outage

Figure B.15: The effect of the Iberian blackout on the regional capacity for OneWeb

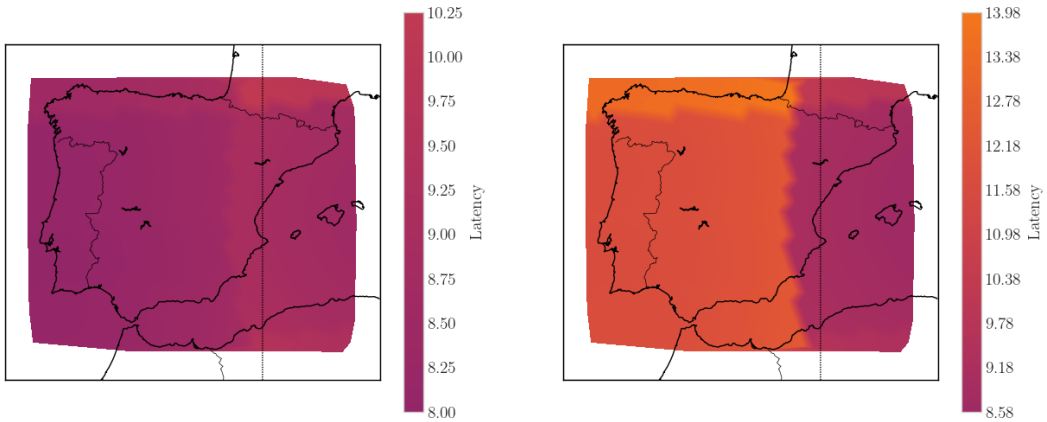

(a) Before outage (b) After outage

Figure B.16: The effect of the Iberian blackout on the regional capacity for OneWeb w/ISLs

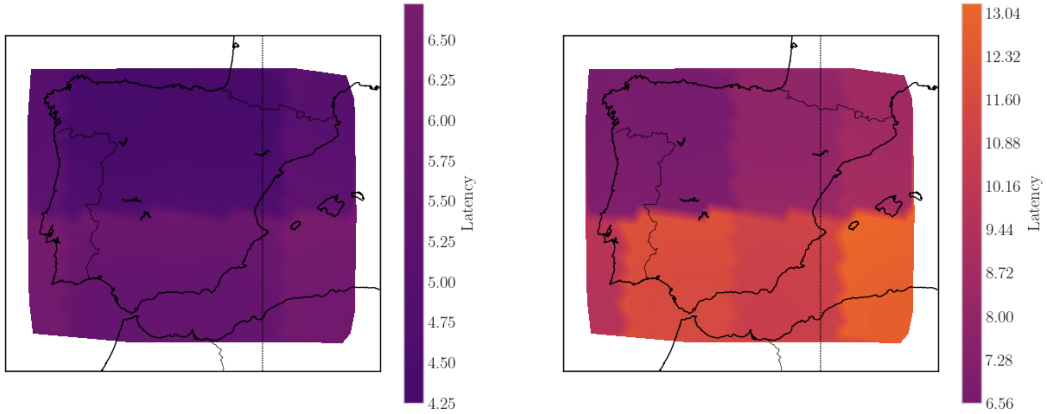

(a) Before outage (b) After outage

Figure B.17: The effect of the Iberian blackout on the regional capacity for Amazon LEO Initial

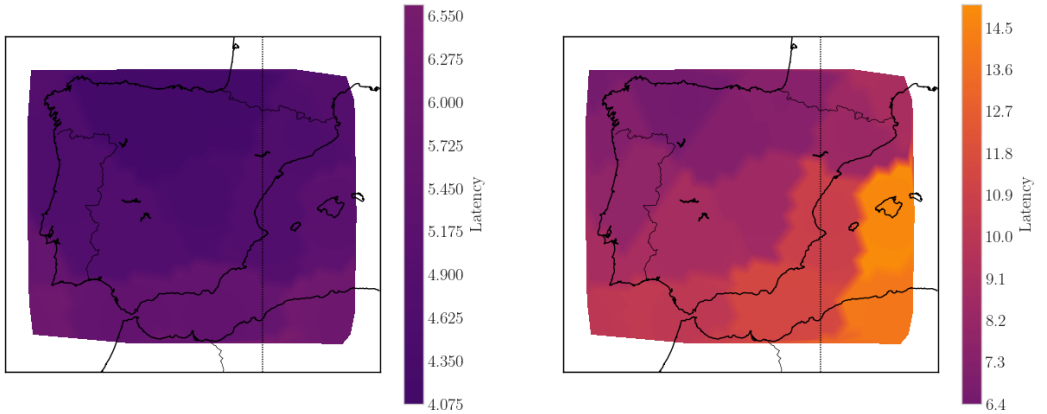

(a) Before outage (b) After outage

Figure B.18: The effect of the Iberian blackout on the regional capacity for Amazon LEO Generation 1

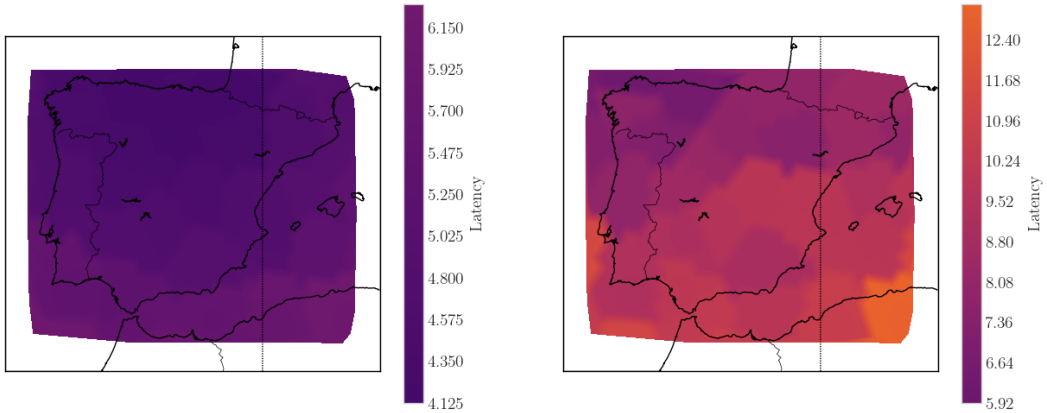

(a) Before outage (b) After outage

Figure B.19: The effect of the Iberian blackout on the regional capacity for Amazon LEO Full